NACA

RESEARCH MEMORANDUM

THE ORIGIN OF AERODYNAMIC INSTABILITY OF SUPERSONIC INLETS AT SUBCRITICAL CONDITIONS

By Antonio Ferri and Louis M. Nucci

Langley Aeronautical Laboratory
Langley Field, Va.

NATIONAL ADVISORY COMMITTEE
FOR AERONAUTICS

WASHINGTON

January 26, 1951

NATIONAL ADVISORY COMMITTEE FOR AERONAUTICS

RESEARCH MEMORANDUM

THE ORIGIN OF AERODYNAMIC INSTABILITY OF SUPERSONIC INLETS AT SUBCRITICAL CONDITIONS

By Antonio Ferri and Louis M. Nucci

SUMMARY

The phenomenon of the starting of aerodynamic instability or "buzz" in supersonic inlets having external compression has been investigated. The starting of the buzz has been related to the existence in the flow field of a velocity discontinuity across a vortex sheet which originates at a shock intersection. It has been confirmed by tests of a number of inlet configurations that the buzz starts when this vortex sheet is at the lip of the cowling. An analysis of the flow for this condition showed that separation will occur on the inner surface of the cowling with consequent choking in the subsonic diffuser.

When the flow on the central body is unseparated, the vortex sheet moves from outside the cowling inward as the entering flow is reduced, and the fluctuations start when the sheet enters the inlet. When the flow separates from the central body, a lambda shock forms and gives rise to another vortex sheet inside the inlet. In this case the sheet moves outward as the flow is reduced, and fluctuations start when it approaches the inner surface of the cowling.

Performance data for the inlets are presented for a range of Mach number up to 2.7, and it is shown that freedom from buzz can be obtained for inlet designs suitable for application to aircraft.

INTRODUCTION

The majority of inlets now proposed for supersonic ram-jet and turbojet airplanes and missiles have all or a large part of the supersonic compression occurring outside the inlet, so that the Mach number at the entrance of the inlet has a low-supersonic value close to 1. In this way, the limitations due to the starting problem are eliminated, and high pressure recovery can be obtained. Extensive experimental data at the design condition are available for inlets of this type.

In practical problems, the inlet is designed for the cruising speed of the airplane or missile, which often is near to, or is, the maximum speed of the vehicle, but for lower flight speeds it is required that the inlet be able to operate at a rate of entering volume flow usually less than the maximum entering volume flow permitted by the inlet. Now, in many of the inlets having external compression it has been found that, when a reduction of volume flow is attempted, a phenomenon of aerodynamic instability that has been termed "buzz" occurs which causes the inlet to operate inefficiently.

The buzz consists of an oscillatory phenomenon of the stream entering the inlet which produces pulsations of the static and total pressure, of the entering volume flow, of the shock-wave pattern at the entrance of the inlet, and, therefore, of the aerodynamic forces on the inlet. Because of the large amplitude of these fluctuations, operation of the inlet is not feasible in the vibrating phase.

The phenomenon of buzz was first encountered by Oswatitsch (reference 1). The inlets were tested in a Mach number range between 2.5 and 3.0, and in all cases no regulation of volume flow was possible due to the presence of buzz. Inlets designed with external compression were also tested at the Langley Aeronautical Laboratory (reference 2). These inlets were designed for a lower Mach number range without internal compression, and no buzz phenomena were encountered until a large reduction of volume flow was obtained. However, regulation of volume flow was attempted only at Mach numbers lower than the design Mach numbers, so that the conical shock from the central body was ahead of the cowling lip.

Similar tests performed later in the same Mach number range (reference 3) showed the presence of buzz when the reduction in volume flow was relatively small, apparently contradicting the test results obtained in reference 2. However, the regulation of volume flow attempted in reference 3 was at the design condition.

Later, the tests of reference 2 were extended to higher Mach numbers (reference 4). Here, when regulation of mass flow was attempted, the buzz phenomena were encountered in all the tests performed. All the inlets tested had small central-body cone angles, and when subcritical conditions were tested (reduced volume flow) a flow separation on the central body was found. The vibrations were considered to be related to the upstream travel of the separation on the surface of the central body as the volume flow was reduced. However, no clear explanation of the relation between the separation and the buzz was advanced at that time.

Many other tests performed later by different investigators have confirmed the presence in many cases of the fluctuation phenomena; however, no satisfactory explanation of the starting of buzz has been given.

Because of the importance of the problem, and in order to clarify the process involved, the origin of these flow fluctuations has recently been considered in detail at the Langley Aeronautical Laboratory. A physical explanation has been found and is presented in this paper. Several tests performed to check experimentally the soundness of the physical explanation are also discussed. The requirements for flow stability have been established and experimental data necessary for the design of a number of supersonic inlets capable of subcritical operation without buzz are presented in this paper.

The present results agree with those presented in reference 2 and show that, in practical applications, stable flow conditions can be obtained at Mach numbers lower than the design Mach number where flow regulation is needed.

SYMBOLS

A_1	area of stream tube entering inlet at free-stream conditions
A_2	cowling-entrance area
A_m	minimum area of exhaust nozzle
a and b	cross sections of stream tubes before and after diffusion in figure 5
M_1	free-stream Mach number
M_2	Mach number just behind conical shock (fig. 4)
M_3	Mach number at point A for high-velocity stream (fig. 4)
M_4	Mach number at point A for low-velocity stream (fig. 4)
M_5	Mach number of low-velocity stream after diffusion (fig. 5)
M_6	Mach number of high-velocity stream after diffusion (fig. 5)
p_a, p_b	static pressures over cross sections S_a, S_b of diffuser before and after diffusion (fig. 5)
p_o	total pressure of free stream
p_{o_3}	total pressure at condition M_3
p_{o_4}	total pressure at condition M_4

p_f total pressure inside inlet after diffusion (at survey plane, see fig. 6)

r fuel-air ratio referred to the stoichiometric mixture corresponding to $r = 1$

S_a, S_b cross section of diffuser before and after diffusion (fig. 5)

V_e velocity at entrance of burner or compressor

α angle of attack

θ_c semiapex cone angle of central body, also called cone angle

θ_l cowling-position parameter (angle between axis of inlet and a line to cowling lip from apex of cone)

ANALYSIS OF THE PROBLEM

Variation of Entering Volume Flow with Mach Number and Engine Requirements

In order to appreciate the problem and the significance of the results obtained, it seems appropriate here to review briefly the reasons why a regulation of entering volume flow is required at flight speeds lower than the design value and to establish roughly the range of volume-flow regulation required as a function of Mach number.

Let us consider a ram-jet or turbojet engine. The volume of air entering the engine is a function of the engine configuration and operating conditions as well as of the free-stream Mach number. In the case of an engine having a variable-minimum-area exhaust nozzle, the volume flow is determined by the consideration that the velocity in front of the burner or of the axial-flow compressor is held constant if the burner or compressor is operated at the design point. The minimum area of the nozzle must then be increased when the flight Mach number decreases. However, especially in ram jets, the exhaust nozzle usually has fixed geometry. In this case, the Mach number after combustion is constant, and for a given fuel-air ratio and combustion efficiency the speed in front of the burner varies approximately as the square root of the stagnation temperature of the entering stream. The required variation of entering volume flow as a function of Mach number for the two cases is quite different.

In figure 1, examples are presented of the variation of the area of the entering-free-stream tube with free-stream Mach number for the condition of constant velocity V_e at the entrance of the burner or compressor and for the condition of constant-geometry exhaust nozzle (A_m constant). In both cases the pressure recovery has been assumed to be the maximum for the Mach number and configuration considered and varies from $\frac{p_f}{p_o} = 0.7$ at $M = 3.0$ to $\frac{p_f}{p_o} = 0.92$ at $M = 1.5$.

In the example presented, design Mach numbers equal to 2 and 3 have been assumed. The velocity in front of the burner for the design conditions, V_e, has been chosen equal to 260 feet per second. (Other values of V_e varying from 160 to 360 ft/sec were also used, and no appreciable change of the constant-velocity curve was found.) The calculations were made for an altitude where the temperature becomes constant with height. For the case of the engine with a constant-geometry exhaust nozzle, additional assumptions are required. The fuel-air ratio was chosen equal to 30 and 50 percent of the stoichiometric value ($r = 0.3$ and $r = 0.5$) and the combustion efficiency was taken as 100 percent. It can be seen that, for the condition of fixed-nozzle geometry, a much larger regulation of volume flow is required at Mach numbers lower than the design Mach number.

For comparison, the variation of the maximum possible entering volume flow as a function of Mach number for inlets designed for $M = 2$ and $M = 3$ is also presented in figure 1. This maximum occurs for supersonic flow at the entrance. The inlets considered have 25° and 30° conical central bodies. The comparison shows that while the curve of entering volume flow for constant V_e is closer to the curve of the maximum volume possible for the inlets and in this example coincides with the curve of the 30° cone designed for $M = 2$, a large regulation of entering volume flow with respect to the maximum possible may be required, especially for the case of constant minimum nozzle area A_m, if the inlet is to operate at the condition of maximum pressure recovery.

These data are only illustrative, but they show the need for regulating the entering volume flow for vehicles having fixed-geometry exhaust nozzles such as are presently used to a great extent.

A possible scheme for avoiding subcritical operation is to design the inlet for a speed well below the maximum flight speed. Between these two speeds the inlet will operate with supersonic entrance flow and a strong shock in the subsonic diffuser. In figure 1 the variation of entering volume flow obtainable with this type of operation is shown by the dashed curve. The inlet was proportioned for maximum pressure recovery at $M = 2.0$ assuming the same volume-flow requirements as for the constant-area exhaust nozzle case. The resulting entrance area

was 55 percent of that of the inlet designed for $M = 3.0$. At $M = 3.0$, therefore, this inlet has only 55 percent of the entering flow volume of the larger inlet. The pressure recovery at $M = 3.0$ must be less than that of the larger inlet in proportion to the ratio of entering volume flows in order to obtain the same velocity in front of the burner or compressor. These losses in both mass flow and pressure recovery combine to make this method of obtaining flow regulation inefficient.

From this simple analysis it appears that regulation of the volume flow is necessary for efficient operation over a range of flight speeds. In the case of missiles, such regulation is especially important because of the desirability of producing thrust at the lowest possible speed in order to simplify the launching problem.

Flow Phenomena Associated with Throttling of a Supersonic Inlet

In order to discuss the problems related to the regulation of entering volume flow in supersonic inlets, consider for simplicity an inlet having a central body with a conical tip and a cowling of circular cross section. Assume that the cone angle is sufficiently small and that the lip of the cowling is thin and sharp and approximately alined with the local flow direction so that the flow at the entrance of the inlet can be supersonic for conveniently low values of the back pressure. For this condition, a transition from supersonic to subsonic flow occurs inside the inlet with a strong shock (fig. 2(a)) and the diameter of the entering stream tube for a given flight Mach number and angle of attack is fixed by the geometry of the inlet and is the maximum possible for the Mach number considered.

A decrease in back pressure (or increase of throttling area A_m) moves the strong shock downstream without changing the entering volume flow; while if the throttling area A_m is decreased, the strong shock moves upstream until it reaches the entrance of the cowling A_2 and then moves outside the cowling (fig. 2(b)). For this condition some spillage occurs around the cowling, and the entering stream tube decreases with respect to the maximum. When the velocity at the entrance of the cowling and everywhere inside the diffuser is subsonic, this flow configuration is usually called "subcritical" in opposition to the "supercritical" configuration which defines the condition of maximum entering volume flow and requires the existence of a supersonic region inside the diffuser.

Although for supercritical conditions the flow in front of the inlet is stable, in many cases when subcritical conditions are reached, a buzz phenomenon is encountered and a fluctuation of the stream entering

the inlet occurs. The fluctuation phenomenon as observed experimentally appears to occur essentially in the following way, as illustrated by a section of motion-picture film in figure 3: A pressure disturbance coming from inside the inlet pushes the strong shock upstream along the cone (frames 1 to 4), decreasing the entering volume flow by a large amount; the shock then moves back to a position near the lip of the cowling for which the entering volume flow is larger than the volume flow before the fluctuation began (frames 4 to 11). Then the shock again moves gradually upstream (frames 12 to 18) until the position (1) is reached which was mentioned at the beginning of the description. The process is then repeated cyclically. The exact behavior of the fluctuation phenomena depends on many different parameters, such as the external configuration of the inlet, subsonic diffuser, and the throttling system, and, therefore, can be easily changed in tests by altering the experimental apparatus. In the example presented in figure 3, the frequency of the fluctuations, which is also a function of the parameters just listed, was reduced to a low value by attaching a long pipe to the inlet so that motion pictures of the fluctuation could easily be taken. The motion picture was taken at 64 frames per second.

From the tests reported in references 1 to 4, it appears that stable subcritical conditions were obtained only for very small entering-flow reductions when separation was present on the central body, while a larger reduction of entering volume flow without buzz was measured for some configurations when separation on the central body could be avoided. Therefore, tests over a wide range of Mach numbers of inlets without separation were made in order to find the parameters involved with the onset of the buzz.

The tests were conducted on a number of central bodies and cowlings for various cowling-position parameters. The experimental results of the tests are presented and analyzed in the section of this paper entitled "Results and Discussion;" however, the essential findings can be stated as follows:

1. Some stable volume-flow regulation was possible in the Mach number range investigated (1.9 to 2.7) if separation was avoided on the surface of the cone.

2. The amount of stable volume-flow regulation possible for a given central-body-cowling combination at a given Mach number was a function of the cowling-position parameter and was a minimum (zero) when the conical shock was at the lip of the cowling. The possible volume-flow regulation increased as θ_l decreased, that is, as the conical shock became farther removed from the cowling lip.

3. The relative size of the central body and the shape of the internal diffuser were not important parameters in the starting of

fluctuations, as the buzz started at the same value of the entering volume flow, being independent of the internal configuration, if the external configuration did not change.

4. The buzz phenomenon started abruptly, and not gradually, as would occur for a resonance phenomenon, and the starting of the buzz was independent of the means by which the system was throttled.

5. For some inlet configurations, stable flow conditions were obtained even when the pressure recovery decreased as the volume flow was reduced.

From the preceding observations, the conclusion was reached that some abrupt change of the flow phenomenon in front of the inlet must act as a trigger for the buzz. The existence of such a change can be illustrated in the following manner: Consider, for example, an inlet having a central body with a 30° semiapex cone angle at a free-stream Mach number of 1.9 as shown in figure 4. The flow behind the conical shock is supersonic with a Mach number of 1.30. For subcritical inlet-flow conditions a strong shock wave exists ahead of the entrance. From the intersection of the conical shock with the strong shock (point A in the following discussion) a vortex sheet originates, across which the static pressure is constant. However, across this discontinuity, differences of entropy, velocity, and, therefore, total pressure exist. For the flow condition shown in figure 4, the discontinuity is outside the inlet and, therefore, does not affect the flow entering the inlet. However, when the entering volume flow is reduced, the discontinuity moves closer to the lip of the cowling; that is, the point A moves along the conical shock wave until the vortex sheet reaches the lip of the cowling.

When the vortex sheet enters the cowling, the internal flow changes abruptly inside the inlet. The vortex sheet on the inside surface of the cowling represents an infinitesimal layer of flow having a much smaller stagnation pressure. Because of the presence of this thin layer, separation can be expected to occur in a region of high average velocity and tends to choke the inlet, as illustrated in the following example: Consider a subsonic diffuser in which a stream consisting of two layers of flow having different values of entropy exists (fig. 5). The line AB corresponds to a discontinuity of velocity or a vortex sheet; however, the static pressure across the vortex sheet does not change. Let S_a and S_b correspond to areas of the two end sections of the stream tube under consideration. Assume that M_3 is equal to 0.83, as for the inlet with a 30° cone shown in figure 4 at a free-stream Mach number of 1.9, and M_4 is equal to 0.63. Assume that the relations between M_3 and M_6 and between M_4 and M_5 are given by one-dimensional theory. As a first case, let $a_1 = 0$ and $M_6 = 0.52$; then $\frac{S_b}{S_a} = 1.27$, and the

static-pressure ratio $\frac{p_b}{p_a} = 1.31$. As a second case, let $a_1 = a_2 = \frac{1}{2}S_a$; for the same ratio S_b/S_a, since the pressure over the area S_b must be constant, it is found that $M_5 = 0.38$ and $M_6 = 0.65$, while the pressure ratio becomes 1.18. As a third case, let $a_2 = 0$; then for the same ratio S_b/S_a, $M_5 = 0.44$ and $\frac{p_b}{p_a} = 1.14$.

Therefore, for a given diffuser $\left(\frac{S_a}{S_b} = \text{Constant}\right)$, the Mach number M_5 decreases if a_1 decreases while the pressure p_b increases. Now, when the vortex sheet tends to go inside, the value of a_1 is infinitesimal and $b_1 = 0$; therefore, the conditions are the same as for $a_1 = 0$ as in the example considered. In this case, for $\frac{p_b}{p_a} = 1.31$, M_5 becomes zero and separation occurs at a station of the diffuser where the average Mach number is high ($M_6 = 0.52$). Since the separation in an actual diffuser occurs on the cowling surface, it causes a large reduction of effective area. Because this area is near the critical value (area for $M = 1$) the reduction chokes the inlet, producing a strong wave which moves upstream and starts the fluctuations.

When the wave moves upstream, the strong shock moves toward the apex of the cone, causing a decrease in entering volume flow, which decreases the back pressure, and, therefore, the shock moves back toward the cowling, passing the position for steady operation and causing the vortex sheet to move outside, after which the process repeats periodically and buzz occurs. If the explanation given is correct, the minimum stable volume flow must occur for the condition when the vortex sheet reaches the cowling.

In the following table are given some of the results of analysis for inlets having semiapex cone angles of 25°, 30°, 35°, and 40° at free-stream Mach numbers of 1.9, 2.46, and 2.7. In the table, M_1 is the free-stream Mach number, M_2 is the Mach number behind the conical shock, M_3 is the Mach number near the point A (fig. 4) in the high-velocity stream, and M_4 is the Mach number near A in the low-velocity stream. The values of M_3 and M_4 have been calculated from M_1 and M_2 from the consideration that across the streamline through A a finite variation of entropy and velocity occurs, but total energy, static pressure, and stream direction do not change. The value of M_6 given in the table corresponds to the Mach number of the high-velocity stream for the condition of zero velocity ($M_5 = 0$) in the low-velocity stream for the same static pressure.

Cone angle (deg)	M_1	M_2	M_3	M_4	M_6
25	1.90	1.46	0.82	0.60	0.54
	2.46	1.83	1.02	.53	.85
	2.70	2.00	1.16	.50	1.02
30	1.90	1.30	.83	.63	.52
	2.46	1.63	1.01	.53	.84
	2.70	1.76	1.10	.50	.96
35	1.90	1.10	.94	.89	.28
	2.46	1.42	.97	.56	.74
	2.70	1.53	1.08	.53	.91
40	1.90	1.00	----	----	----
	2.46	1.20	.92	.66	.61
	2.70	1.30	.95	.51	.78

As is shown in the table, for the cases when M_2 is somewhat larger than 1, separation of the low-velocity stream can be expected in a zone where the velocity of the high-velocity stream is high, and, therefore, choking effects can be expected if the low-velocity stream tube is small. When the stream Mach number M_1 decreases or the angle of the cone increases, M_2 decreases and the magnitude of the discontinuity across the vortex sheet from A decreases or disappears ($M_2 < 1$). In this case, M_6 becomes small (see, for example, 35° cone at $M = 1.90$) and the separation cannot produce choking and originate the buzz.

In the following sections, tests conducted to verify this explanation are discussed.

APPARATUS AND TESTS

Tests were performed in one of the blowdown jets of the Langley Gas Dynamics Branch using low-humidity air from large, pressurized tanks. Closed test sections approximately 3 inches by 5 inches for $M = 2.7$ and 4 inches by 5 inches for $M = 2.46$ were used. For $M = 1.9$ an open test section 4 inches by 5 inches was used.

A typical model arrangement is shown in figure 6. The inlet model configuration was altered by changing the cowling, central body, and relative position of the central body (cowling-position parameter) with respect to the cowling. The different cowling and central-body shapes

used in the tests are shown in figures 7 and 8, respectively. The internal coordinates of the cowlings are given in table I. In referring to the inlet configurations the cowlings will be distinguished by the letters of figure 7, while the central bodies will be distinguished by two numbers, the first corresponding to the semiapex cone angle and the second to the maximum diameter in inches.

During each test, spark shadowgraphs and shadow motion pictures were taken. The inlet entering mass flow was measured by a calibrated orifice. The pressure recovery, which was measured by means of two rakes, located as shown in figure 6, was obtained from a mass-flow-weighted average as discussed in reference 4.

The motion pictures were taken with a 16-millimeter camera. The camera was focused on a piece of ground glass on which the shadow image of the shock-wave phenomena appeared. The intensity of the available light source limited the film speed to 64 frames per second. In order to obtain enough details for the analysis from the relatively slow film speed, the frequency of the fluctuations was reduced by inserting a long pipe between the throttling valve and the inlet model. Some models were tested with pipes of different lengths and diameters. All the models tested had a maximum diameter of approximately 1.8 inches, and the corresponding test Reynolds numbers referred to the maximum diameter varied between 3.5×10^6 and 4.3×10^6.

In all the experimental data, experimental errors exist which are difficult to evaluate.

Precise determination of the throttle setting for minimum stable entering volume flow depends on the rapidity of the variation of throttle position. In all tests the inlet was throttled slowly by means of a manually operated valve.

The entering volume flow was measured by a calibrated orifice. The error expected in this measurement is about 2 percent.

The most difficult parameter to determine was the cowling-position parameter. This value has been determined optically from a "no flow" shadowgraph of the inlet configuration by extending the outlines of the cone to the point of intersection, thus establishing the location of the apex and the corresponding value of the cowling-position parameter. The errors expected in this parameter are approximately 20 to 30 minutes. The same precision was obtained for central-body cone angles.

The pressure recovery is accurate within 1 percent.

RESULTS AND DISCUSSION

Inlets without Separation on the Central Body

The proposed explanantion for the starting of the fluctuations was verified by all the tests performed. Some typical results obtained for inlets without separation on the central body are discussed in this section.

In figures 9 to 14, data are presented on inlet configurations tested at Mach numbers of 1.9, 2.46, and 2.7, for which regulation of volume flow was performed.

In figure 9 are shown shadowgraphs at a free-stream Mach number of 1.90 of an inlet having the 30°-1.10 central body located at an angle $\theta_l = 43^{\circ}54'$ with respect to cowling D for three values of entering volume flow. The "no flow" shadowgraph is also shown for comparison. The last shadowgraph (fig. 9(d)) corresponds to the condition of minimum entering volume flow with stable conditions. From figure 9(c) the strong curvature of the vortex sheet in front of the cowling lip can be seen, together with the formation of a strong zone of expansion on the outside surface of the cowling. Both phenomena tend to make the determination of the condition when the vortex sheet is at the lip of the cowling difficult; therefore, for all tests this position was checked by measuring optically the diameter of the entering-free-stream tube defined by the vortex sheet for the condition of minimum stable mass flow and comparing this value with the diameter of the free-stream tube determined by the flowmeter. In figure 10, shadowgraphs are presented of an inlet having a 30°-0.907 central body and cowling D for the condition of minimum stable entering volume flow at each of the values of the cowling-position parameter shown. In all cases the fluctuations started when the vortex sheet reached the lip of the cowling, as indicated from the shadowgraphs and from the measurements described previously.

These configurations correspond to those analyzed in the previous example in which it was shown that separation must occur at a station in the subsonic diffuser where $M = 0.52$ or higher as soon as the vortex sheet enters.

In figure 11 other inlets having different central bodies, subsonic diffusers, and cowling shapes are shown. For these inlets the cowling-position parameter was about the same. The phenomena were similar for all configurations tested. If the value of the minimum volume-flow ratio for steady conditions is plotted as a function of the cowling-position parameter, it is found that for a given cone angle and Mach number the value of the volume flow before pulsations is constant and independent of the shape of the cowling or of the size of the internal body and is, therefore, only a function of the external configuration.

Results of tests made at Mach numbers of 2.46 and 2.70 are shown in figures 12 and 13, respectively. The cone angles are 35° for a Mach number of 2.46 and 40° for a Mach number of 2.70. The shadowgraphs presented show the condition of minimum stable entering flow. For these cone angles, the table presented previously indicates separation at a station where the average Mach number is of the order of 0.75, when the vortex sheet entered the cowling. The tests confirmed that this was the last stable position of the vortex sheet.

In figure 14 two sections of motion-picture film showing the starting of the fluctuation in an inlet having 30°-1.10 central body and cowling B for $\theta_l = 42°$ at $M = 1.90$ are shown. The inlet configuration was identical in both tests; however, the throttling system was different. In the tests corresponding to figure 14(a), a 1-foot-long pipe of 2-inch inside diameter was inserted between the hand valve and the flange at the end of the model (fig. 6). In the tests corresponding to figure 14(b), a 25-foot-long pipe of 4-inch inside diameter was inserted between the hand valve and the model. The pipe was attached to the model with a 1-foot-long transition piece. In figure 14(a) the frames from 1 to 13 correspond to constant throttling conditions and to the minimum steady entering volume flow. After frame 13 regulation was performed; the throttling was increased a very small amount and then kept constant. The fluctuations started immediately (frame 16 and following frames of fig. 14(a)). The frequency was so high that different phases of the fluctuations appear superimposed in each frame of the film. In figure 14(b) the results for a similar test when the long pipe was attached to the model are presented. The frames from 1 to 16 correspond to the minimum steady entering volume flow and are identical to the pictures presented in frames 1 to 13 of figure 14(a). After frame 16 the throttling was increased a very small amount and then kept constant. The fluctuations started as in figure 14(a) but proceeded much more slowly. The complete cycle ends at frame 40. In the two cases the cycles are different, but fluctuations started in both cases when the vortex sheet was at the lip of the cowling.

All of the foregoing tests indicated that the explanation offered was satisfactory. However, other possibilities still existed; for example, the slope of the pressure-recovery curve as a function of the entering volume flow might be a factor in the onset of buzz. In the tests previously discussed the pressure recovery remained constant or increased slightly as the entering volume flow decreased, until the buzz started, because as the volume flow is being reduced the supersonic pressure recovery does not change noticeably when the vortex sheet is outside the cowling, whereas the subsonic recovery increases because the velocity in the subsonic diffuser decreases. When the vortex sheet goes inside the cowling, it could be expected that if buzz did not occur the pressure recovery would tend to decrease because the supersonic pressure recovery decreases. The change, however, would be gradual, and the value of the

slope of the pressure-recovery curve, if buzz did not originate, would change only slightly. Naturally, when the buzz starts, an abrupt change in the pressure-recovery curve will immediately follow.

In order to determine whether buzz can be originated only by a change in sign of the slope of the pressure-recovery curve, independently of the position of the vortex sheet, the following test was performed: An inlet having a 30°-0.907 central body and cowling C was tested at a Mach number of 1.9. The inlet configuration was tested at a cowling-position parameter $\theta_l = 51^\circ 55'$. Shadowgraphs of this inlet are shown in figure 15. For this configuration, the internal contraction was too large to permit supersonic flow at the entrance, and, therefore, a strong shock occurred in front of the inlet even for the condition of maximum entering volume flow. For the cowling-position parameter selected, the vortex sheet was well inside the inlet (fig. 15(a)). For this case the Mach numbers of the two layers entering the cowling are the same as for the other inlets having 30° cones for the same free-stream Mach number; however, the ratio of the sizes of the stream tubes of high-velocity and low-velocity air is quite different. Therefore, as was shown in the preceding analysis, the cross section where the low-velocity stream can produce separation is much larger than the critical section. For the condition presented in figure 15(a), when the high-velocity stream has a Mach number $M_3 = 0.83$, the low-velocity stream at the same static pressure has a Mach number of 0.63. The ratio a_2/a_1 of the two streams as determined from measurements is 3.3. The low-velocity stream is small but not infinitesimal, and, therefore, the increase in pressure along the diffuser is more gradual. For example, when the Mach number of the low-velocity stream M_5 is equal to 0.20, corresponding to a compression ratio (without losses) of 1.27, the Mach number of the high-velocity stream M_6 is equal to 0.56. At this station, the area of the diffuser is equal to 1.52 times the area of the stream tube behind the shock as compared to an area ratio of 1.21 for the condition of the vortex sheet at the lip of the cowling; therefore, it is unlikely that separation would produce choking, and regulation of entering volume flow with stable conditions should, therefore, be possible. At the same time, the supersonic pressure recovery should decrease noticeably as the entering volume flow is decreased. Tests showed that stable regulation of entering volume flow was possible in spite of the positive slope of the pressure-recovery curve. Some shadowgraphs for different values of entering volume flow are shown in figures 15(b) and 15(c). All the shadowgraphs correspond to steady-flow conditions. The measured value of the pressure recovery at each condition is also given in figure 15.

In order to verify further the proposed mechanism of buzz and at the same time to obtain some indication of the possibility of obtaining larger stable entering-volume-flow regulation, another test was performed with a special inlet design. In the explanation given, it was assumed

that the two layers of different-entropy air did not mix and, therefore, that the vortex sheet could be considered as a dividing line. However, in reality, turbulent mixing must occur in a region near the discontinuity, which will tend to increase locally the velocity of the layer having lower velocity. Significant mixing of the two layers would be expected only if the mixing region were of appreciable length and the thickness of the low-velocity layer small. Based on these considerations, an inlet was designed with the following characteristics:

In order to obtain mixing before separation, a long channel with a very low diffusion angle was inserted upstream of the station where separation was expected. The diffuser design used is shown in figure 16. For this inlet design at a free-stream Mach number of 1.9, when the vortex sheet meets the lip of the cowling, the area ratio of the diffuser between the station at the lip of the cowling and the station 3 inlet diameters downstream corresponded to an isentropic compression ratio of only 1.02. Because of the presence of boundary layer, the pressure gradient along the diffuser must be less than the calculated value; therefore, separation was not expected to occur in this part of the diffuser. At the same time, because of the long mixing region, it was expected that the velocities of the two layers would tend to become more uniform, increasing the stability of the low-velocity layer.

The effect of mixing, however, will be effective only for a relatively thin low-velocity layer and will be limited to the region near the vortex sheet. When the thickness of the low-velocity layer increases, mixing will not change the velocity in the flow near the surface of the cowling, and separation will still occur.

Tests were performed on the inlet described, and it was found that the vortex sheet could enter the cowling without fluctuations (fig. 17). As the volume flow was further reduced, however, a point was reached where fluctuations start. Figure 17(c) shows the minimum stable volume flow for this configuration before fluctuations. For the configuration presented in figure 16, a reduction of minimum stable volume flow of about 16 percent, as compared with the minimum stable value measured for the condition of the vortex at the lip, was measured. A similar result was obtained for the same cone and cowling and $\theta_l = 48^\circ 12'$.

Inlets with Separation on the Central Body

In the tests previously discussed, no separation was present at the surface of the central body. When the cone angle of the central body was decreased sufficiently for separation to occur on the central body, the starting condition of the fluctuation phenomenon appeared to be different, as buzz started before the vortex sheet previously considered entered the lip of the cowling. Tests of this type of inlet

showed that the process of starting the fluctuations was different. However, the immediate cause of the onset of fluctuations was again related to the presence of a velocity discontinuity near the lip of the cowling which produced separation at the inside surface of the cowling in a station of the diffuser where separation can produce choking.

Consider, for example, an inlet as shown in figure 18 having a cowling F and 25°-1.1 central body. This inlet was tested at a free-stream Mach number of 2.70 at $\theta_l = 34°32'$. For this condition the inlet had no internal contraction and started as shown in the shadow photograph (fig. 18(a)). When the inlet was throttled in order to reduce the entering volume flow, the strong shock moved toward the cowling entrance and separation on the central body moved upstream, producing a lambda shock as shown in figure 18(b). Because of the formation of the lambda shock, the pressure recovery increased with respect to the pressure recovery for the condition of figure 18(a) (reference 4). The pressure recovery corresponding to the shock configuration in figure 18(b) was 0.53. As the throttling process was increased still further, the lambda shock continued to move forward as shown in figure 18(c), and the pressure recovery increased to a value of 0.55. Figure 18(c) corresponds to the condition of minimum stable volume flow. If the throttling process was continued beyond the value corresponding to the shock pattern shown in figure 18(c), fluctuations started. The possible reduction of stable flow in the presence of separation was much less than for the condition in which separation did not exist on the surface of the central body. The vortex sheet from the intersection of the conical shock with the strong shock was still outside the entrance of the cowling; however, the reason for the start of fluctuations was the same as for the case without separation on the surface of the central body. A vortex sheet originates at the intersection of the two legs of the lambda shock, producing two layers having different stagnation pressures inside the inlet.

The aerodynamic phenomena of figure 18(c) are presented schematically in figure 19. At the point A a vortex sheet arises from the intersection of the two legs AB and AC of the lambda shock. The shock AB is generated by the separation (δ) at the point B. The point D is the intersection of the strong shock from A with the stagnation streamline of the cowling. The total pressure in the stream tube through AC is different from the total pressure in the stream tube through AD; therefore, two layers of fluid having different Mach numbers but the same static pressure enter the cowling. For the shock pattern shown in figure 18(b), the Mach number behind AD is about 0.58, whereas behind AC the Mach number is 0.82; therefore, when a compression ratio of about 1.26 occurs, neglecting mixing and viscous effects, the stream tube downstream of AD is at rest, while the stream tube AC has a Mach number of 0.55. Now, if the stream tube AD is large, as for the case shown in figures 18(a) and 18(b), a large pressure rise

along the diffuser is obtained only with a large increase of the stream-tube area; therefore, separation occurs far downstream in the diffuser at a station where the cross-sectional area EF of the stream tube CD = AD + AC is much larger than the critical area. In this case, separation cannot produce choking. When the stream tube AD tends to zero, however, a large pressure rise along the diffuser can be obtained with much less increase of the stream-tube area, and, therefore, the area EF where separation occurs decreases and approaches the critical area. Then the separation, producing a large reduction of effective area, produces choking and can start the fluctuations.

In this example, when the stream tube AD approaches zero, the Mach number at GF for a pressure rise along the diffuser corresponding to zero velocity at EG is equal to 0.55. For the condition being considered, the area EF is only 25 percent above critical, so that the separation at E can choke the inlet and start the fluctuations. The viscous effects raise the Mach number in GF corresponding to zero velocity in EG, increasing the likelihood of choking. The lower limit for stable conditions occurs when the vortex sheet produced by the lambda shock at A moves from well inside the cowling, as in figure 18(b), to a position near the lip of the cowling, as in figure 18(c), reducing the size of the stream tube AD to values approaching zero.

It thus appears that the separation from the central body is not the direct cause of the fluctuations, but the separation does initiate the process which produces buzz. The separation on the central body depends somewhat on the internal configuration of the inlet; therefore, the starting of buzz is affected by the shape of the subsonic diffuser. In these tests, however, such an effect seemed small, and the most important parameters still appeared to be the cone angle and the cowling-position parameter.

In figure 20 another inlet configuration having separation on the central body is shown. The inlet consisted of cowling C and central body 25°-1.1 located at an angle $\theta_l = 33^\circ 14'$ with respect to the lip of the cowling. The vortex from the lambda shock may be seen in figure 20(b).

If separation from the surface of the central body were eliminated by removal of the boundary layer, the fluctuation phenomenon would start as discussed for the case of no separation. In order to find the effect of boundary-layer removal, inlets were tested with and without a boundary-layer removal slot on the central body. A result of such tests is presented in figure 21. The inlets consisted of cowling E and central bodies 30°-1.10 and 30°-30°-1.10 suction (without and with boundary-layer removal, respectively), which were located at $\theta_l = 38^\circ 40'$. Figure 21(a) corresponds to the minimum volume-flow condition for the inlet without boundary-layer removal. The separation from the central

body, which was unstable, did not permit volume-flow regulation. When boundary-layer removal was introduced, as shown in figures 21(b) and 21(c), the separation from the central body was eliminated, and regulation of volume flow was possible. The shadowgraph in figure 21(c) corresponds to the condition of minimum entering volume flow before fluctuations. For this case the vortex sheet produced by the intersection of strong shock and the conical shock is at the lip of the cowling.

The Regulation of Entering Volume Flow at Angles of Attack

In the preceding sections, the minimum stable entering volume flow as a function of the inlet configuration has been discussed for inlets at zero angle of attack. In flight, however, a large angle-of-attack range may be required, and a few tests were, therefore, made on four configurations at Mach numbers of 1.9 and 2.7 to study the effect of angle of attack on the value of the minimum stable entering volume flow.

When an inlet is operating at an angle of attack, the boundary layer tends to collect on the upper side of the central body; separation also tends to occur there because of the cross-flow component normal to the axis of the inlet. Separation is thus especially likely on the upper surface. In addition, the conical field about the central body is distorted, so that it is not alined with the axis of the inlet. These effects change the amount of minimum entering volume flow with respect to zero angle of attack because the position of the vortex sheet changes relative to the lip of the cowling, and the lack of axial symmetry makes analysis more difficult. However, the results of the few tests performed indicate that the effect of the angle of attack tends to reduce both maximum and minimum values of entering volume flow, so that the angle-of-attack condition seems less critical with respect to the possibility of obtaining the volume flow required by the engine without buzz than does the case of zero angle of attack.

Some of the angle-of-attack results are shown in figures 22 to 24 for Mach numbers of 1.90 and 2.70. In figure 22 shadowgraphs are shown for an inlet having cowling D and central body 30°-0.907 located at an angle $\theta_l = 45^\circ 46'$ with respect to the cowling lip. The tests were performed at a Mach number of 1.9 for an angle of attack of 9°. For comparison, shadow pictures for zero angle of attack at the condition of minimum entering volume flow are also presented. Figure 22(a) shows a shadowgraph of the inlet for the condition of maximum entering volume flow which was reduced from 0.87 for the zero-angle-of-attack case to 0.85 for $\alpha = 9^\circ$. Figure 22(b) shows an intermediate volume-flow condition and figure 22(c), the condition of minimum steady entering

volume flow. Figure 22(d) presents the condition of minimum volume flow at zero angle of attack. As it appears from the shadowgraphs, the angle of attack produced a strong dissymmetry of the flow field around the cowling, and regulation was possible until the vortex sheet on the upper side entered the cowling. The value of the minimum volume flow for an angle of attack of 9° was 0.71, while for an angle of attack of zero it was 0.78.

Results of tests of another inlet at $M = 1.9$ and $\alpha = 8^\circ 30'$ are shown in figure 23. The inlet consisted of cowling E and central body 30°-0.8 at $\theta_l = 46^\circ 14'$. Figure 23(a) shows the condition of maximum entering volume flow. The minimum stable entering volume flow for an angle of attack of $8^\circ 30'$ is shown in figure 23(b), while the minimum stable volume flow for an angle of attack of 0° is shown in figure 23(c). In this case, as in the preceding one, the minimum-volume-flow condition corresponds to the position of the upper vortex sheet at the lip. The values of entering volume flow change similarly with angle of attack. Design data for other cases with different cowling-position parameters are presented subsequently.

Figure 24 shows a shadowgraph of an inlet having 22°-1.20 central body and cowling B at angles of attack of 4° and 6° for the condition of minimum steady volume flow. The minimum entering volume flow is 95 percent of the value at an angle of attack of 0°. Both pictures show that when separation occurs on the central body, the lambda-shock position is the determining factor in the starting of the fluctuations.

Experimental Performance of Various Inlets

From the preceding discussion, it appears that the minimum steady entering volume flow is essentially a function of the external geometry of the inlet upstream of the entrance and is practically independent of the cowling shape, internal contraction, and subsonic diffuser, unless special diffusers having great mixing lengths are used. However, an analytical determination of the minimum steady volume flow is difficult because it would be necessary to determine the subsonic flow behind the strong shock in order to find the condition at which the vortex sheet enters the cowling. Since the minimum steady volume flow entering an inlet is an important parameter in estimating the performance of supersonic vehicles and selecting the inlet design, detailed test data at Mach numbers of 1.90, 2.46, and 2.70 are shown for several inlet configurations. These inlets had various cowling shapes and central bodies located at various positions with respect to the cowling entrance.

The data are presented in figures 25 to 62. From the explanation given for the starting of the buzz, it can be seen that for a given cone angle, Mach number, and angle of attack, the minimum stable entering

volume flow is a function only of the cowling-position parameter and is independent of the other geometrical parameters; therefore, all the experimental values of the minimum stable flow for a particular central body, cone angle, and Mach number have been presented in the same figure plotted as a function of the cowling-position parameter. In all the figures presented, a unique curve can be obtained from the experimental points, and the scatter is of the order of the precision of the measurements, as expected. The maximum entering volume flow for supersonic velocity at the entrance of the inlet for a given cone angle, Mach number, and angle of attack is also a function only of the cowling-position parameter. This value can be determined theoretically and is given in the figures by the upper solid curve. The maximum actually attainable is less than the theoretical when the inlet is choked or has a detached shock at the lip of the cowling. The values of maximum volume flow measured under such conditions (determined from shadowgraphs) are denoted by flagged symbols, to distinguish them from the values measured with supersonic velocity at the entrance. For a given θ_l and inlet configuration, the open symbol corresponds to the maximum measured entering volume flow and the solid symbol corresponds to the minimum measured stable entering volume flow. The minimum stable volume flow for inlets having separation on the central body is less than for inlets without separation having the same geometry; therefore, the curve of entering volume flow as a function of the cowling-position parameter changes slope when separation on the central body starts.

In figures 25 to 62 the variation of entering volume flow as a function of the cowling-position parameter for the configurations having minimum stable entering volume flow determined by the presence of separation on the central body is represented by a dashed curve that starts from the lower solid curve, which represents the variation when separation does not exist. The experimental points also follow this curve closely. All the volume-flow values given have been referred to the volume flow of the free-stream tube entering a diameter equal to the cowling-entrance diameter at the stream Mach number under consideration; therefore, the volume flow is given as the ratio of the area of the entering free-stream tube to the area of the entrance of the cowling A_1/A_2.

Another parameter of importance for supersonic-inlet design at reduced mass flow is pressure recovery; therefore, the measured pressure recovery at minimum stable volume flow is also plotted on a separate figure following the volume-flow data. Inasmuch as pressure recovery is somewhat sensitive to cowling shape and subsonic diffuser, separate pressure-recovery curves have been drawn through the experimental points where necessary in order to avoid confusion.

In figures 25 and 26 are presented results of tests of inlets having 25° cone-angle central bodies at a free-stream Mach number of 1.90.

For lower values of θ_l, separation occurs on the central body and buzz starts because of the vortex sheet from the lambda shock. The separation starts for $\theta_l = 40^\circ$. The results for an inlet having a boundary-layer suction slot are also presented in the same figure. Only one suction-slot position was tested. For the range of θ_l tested between $\theta_l = 36^\circ 26'$ and $\theta_l = 39^\circ 8'$, separation was eliminated, and a larger volume-flow regulation obtained. For lower values of θ_l the suction slot was too near the tip of the cone, so that separation occurred behind it on the central body. From these tests it appears that the suction may be effective for inlets having small cone angles; however, the position of the suction slot must be selected by considering the value of θ_l to be used. The measured values of pressure recovery for the minimum stable flow for the same inlet configurations are presented in figure 26.

In figures 27 and 28 are presented data at a free-stream Mach number of 1.9 for an inlet having a 27.5° central-body cone angle. The buzz started for the condition of the vortex sheet at the lip of the cowling. All the configurations tested were choked, but the vortex sheet due to the intersection of the conical shock with the strong shock was outside of the cowling for the condition of maximum entering volume flow. The pressure-recovery values are plotted in figure 28.

The characteristics of inlets having 30° central-body cone angles at a free-stream Mach number of 1.9 are shown in figures 29 and 30. For all configurations tested the inlet was either choked (too large an internal-contraction ratio) or operated with a detached shock in front of the cowling lip (cowlings designed for higher Mach numbers). Consequently, the maximum volume flow was less than the theoretical value. For $\theta_l > 48^\circ$, because of choking effects the vortex sheet was also inside the inlet for the condition of maximum entering volume flow for all configurations with the exception of the inlet having cowling D and a central body 30°-0.80. The same was true for the inlet configuration having cowling D and 30°-1.10 central body for θ_l between $44^\circ 30'$ and 47°. For these conditions, the minimum volume flow was less than the value corresponding to the condition of the vortex at the lip because the low-velocity layer inside the cowling existed even for the condition of maximum-volume flow and had a finite cross section. Therefore, the average Mach number of the stream in the region where separation occurs was lower, so that a larger reduction of flow was possible than for the condition of the vortex sheet at the lip of the cowling.

For the lower values of θ_l, the curved part of the central body extended ahead of the cowling lip; therefore, the flow behind the initial shock was not exactly conical, and the results cannot exactly be applied to conical inlets.

In the same figure are also presented the data on an inlet having a long subsonic diffuser (cowling D, central body 30°-0.8). For this configuration the minimum stable entering volume flow was less than that for the other inlets tested; the vortex sheet could enter the inlet without causing buzz because of the long mixing length, as was previously discussed. The pressure-recovery values for all the 30° cone-angle central bodies are given in figure 30.

Results for inlet configurations having 30° cone-angle central bodies at angles of attack of 8°30' and 9° are shown in figures 31 and 32 and figures 33 and 34, respectively.

In figures 35 to 38 are presented results for 35° and 40° cone-angle central bodies at a Mach number of 1.90. For the 40° cone, the Mach number on the surface of the cone was less than 1, so that the theoretical maximum-flow curves could not be obtained from conical considerations.

The results of tests of inlets tested at a free-stream Mach number of 2.46 are shown in figures 39 to 50.

In figures 39 and 40 are presented data on inlets having 25° cone-angle central bodies at a free-stream Mach number of 2.46.

The experimental results for inlet configurations having a central-body cone angle of 27.5° are shown in figures 41 and 42. The minimum stable volume flow was determined by separation on the central body. For the lower values of θ_l, the curved part of the central body extended ahead of the central body extended ahead of the inlet.

In figures 43 and 44 are presented data for a 30° cone-angle central body at a Mach number of 2.46. For some of the configurations, subcritical conditions occurred for the condition of maximum entering volume flow and are denoted by the flagged symbols. For the lower values of θ_l the minimum stable entering volume flow was determined by separation from the cone surface.

The results for the 35° and 40° central-body cone angles are given in figures 45 to 48. For all the maximum-flow conditions the entering flow was subsonic. All minimum stable entering flow occurred when the outside vortex entered the cowling.

In figures 49 and 50 are shown the results of a modified double-shock central body. The same central body was tested with two cowlings having different entrance diameters, so that the inlets are not geometrically similar externally, and, therefore, represent two different configurations. For these tests, buzz occurred when the outside vortex sheet entered the cowling. Separation occurred on the central body for these two inlet configurations but tended to remain localized.

In figures 51 to 62 are presented data at a free-stream Mach number of 2.70. Flow and pressure-recovery data for inlets having 25° cone-angle central bodies are presented in figures 51 and 52, respectively. For large values of θ_l the external vortex sheet produces buzz, while for the lower values of θ_l separation occurred on the body. However, for this condition, for the central bodies considered the curved part of the bodies was ahead of the cowling entrance. The inlet having cowling A and central body 25°-1.10 at $\theta_l = 35°36'$ was choked and the vortex sheet was inside the cowling for the condition of maximum entering volume flow.

The performance of an inlet (cowling A and central body 25°-1.100S) having a boundary-layer suction slot around the central body is also shown in figure 51. The maximum volume flow for this configuration occurred with subcritical conditions. At $\theta_l = 35°28'$ the vortex sheet was inside the cowling for the condition of maximum entering volume flow.

The results of tests on inlets having 27.5° central-body cone angles are shown in figures 53 and 54. The inlet configurations having cowling A were choked, while for the inlet configurations having cowling C the curved part of the central body was outside the cowling entrance for $\theta_l < 36°$.

In figures 55 and 56 are presented data for inlet configurations having 30° central-body cone angles at a free-stream Mach number of 2.70. The inlet configurations for $\theta_l > 41°$ were choked and the vortex sheet was inside the cowling for the condition of maximum entering volume flow. The value of the maximum entering volume flow for small values of θ_l was less than the theoretical value because the curved part of the central body was outside the cowling entrance. The value of the minimum stable entering volume flow was determined by the external vortex sheet for $\theta_l > 39°$ while the minimum entering for $\theta_l < 39°$ was determined by the vortex sheet from the lambda shock.

The results for inlet configurations having a 35° cone-angle central body are shown in figures 57 and 58. For $\theta_l = 46°50'$ the vortex sheet was inside the cowling for the condition of maximum and minimum entering volume flow. For all the configurations tested a detached shock occurred ahead of the cowling entrance. The curved part of the central body was ahead of the cowling entrance for $\theta_l = 42°50'$.

In figures 59 and 60 are shown the results of tests of a 40° cone-angle central body. A detached shock occurred ahead of the entrance for all the maximum-volume-flow conditions considered. The minimum stable volume flow was determined by the external vortex sheet at the lip. For $\theta_l = 53°24'$ the vortex sheet was inside the cowling for the condition of maximum entering volume flow.

The experimental results for an inlet having a double-shock central body are shown in figures 61 and 62. These tests were performed primarily to check the proposed reasons for buzz for this type of configuration. The buzz started when the external vortex sheet entered the cowling.

An Application of the Results

The results of the tests giving the value of the minimum stable entering volume flow as a function of the cowling-position parameter have been cross-plotted as a function of Mach number in figure 63. For each given cone angle, the value of θ_l selected was such that the conical shock would be at the lip of the cowling at a free-stream Mach number of 2.80. For this value of θ_l the area of the minimum entering-free-stream tube referred to the entrance area has been plotted as a function of flight Mach number. As appears from the curves, the minimum stable entering flow at each Mach number is a function of the central-body cone angle. The minimum value of stable flow at each Mach number was obtained for a cone angle of 27.5° or a 25° central body having boundary-layer suction.

To illustrate the application of such inlets, the curve of required volume flow as a function of flight Mach number for a constant minimum area at the exhaust of the nozzle and constant fuel-air ratio has been shown on the same figure. The pressure recovery used for this curve corresponds to an average value obtained for the inlet having 30°-1.1 central body for the design value of θ_l. The pressure recovery used was 0.61 at $M = 2.70$ and 0.88 at $M = 1.90$.

Figure 63 shows that the required volume flow can be obtained, for example, with a 27.5° or 30° cone without boundary-layer suction or with a 25° cone having boundary-layer suction. Moreover, a ram jet designed for a Mach number of 2.8 can be efficiently operated with increasing fuel-air ratio when the Mach number decreases. At a Mach number of 1.9 the minimum volume flow for the 25° cone-angle central body having boundary-layer suction practically corresponds to the value needed for burning a stoichiometric mixture with a constant minimum exhaust area fixed at the design conditions ($M = 2.8$).

At free-stream Mach numbers somewhat below 1.90 the flow becomes subsonic for the cone angles investigated, so that volume-flow regulation can probably be obtained as the vortex tends to disappear. This possibility was shown in reference 1.

The cone angle of the central body is the most important parameter in determining the minimum value of stable volume flow at any Mach number

for a given design condition. The minimum stable flow decreases as the cone angle decreases, when separation on the central body is avoided.

From an analysis of the data presented it appears possible to obtain steady-flow conditions for a constant-geometry inlet in a Mach number range from $M = 2.8$ to the lowest value tested, $M = 1.90$, for a constant minimum exhaust area and for a constant fuel-air ratio. For cone angles between 25° and 30° the fuel-air ratio can be increased when the Mach number decreases, with a corresponding increase in thrust.

CONCLUDING REMARKS

The aerodynamic instability of inlets having external compression has been investigated. The origin of buzz was found to be related to a velocity discontinuity across a vortex sheet arising from a shock intersection. An analysis of the flow showed that the fluctuations started when the vortex sheet produced separation on the inner surface of the cowling and choked the subsonic diffuser. The mechanism of this separation and choking process has been discussed.

When there was no separation on the central body, the vortex sheet originated at the intersection of the conical shock and the strong shock ahead of the entrance and passed outside the entrance for maximum entering volume flow. As the flow was reduced, the vortex sheet moved inward, and the fluctuations started when it entered the cowling.

When separation occurred on the central body, a lambda shock was formed and another vortex sheet arose from the intersection of the two legs of this shock. This vortex sheet passed inside the entrance, moving outward as the flow was reduced; the fluctuations started when the vortex sheet approached the inner surface of the cowling. For this case the stable range of regulation of entering volume flow was less than for the previous case. When the separation and lambda shocks on the central body were eliminated by boundary-layer suction, buzz was started by the external vortex sheet, as in the previous case.

The minimum value of entering stable volume flow for a given cone angle and Mach number was found to be a function of the cowling-position parameter and decreased when the cowling-position parameter decreased. The stable range of regulation of volume flow was increased by the use of a subsonic diffuser providing increased mixing of the two layers on opposite sides of the vortex sheet.

Both the maximum value and the minimum stable value of entering volume flow decreased appreciably for angles of attack of approximately 9° at a Mach number of 1.9.

For the purpose of obtaining design information, tests were conducted at Mach numbers from 1.90 to 2.70 on a number of nose inlets having various cowling and central-body shapes. Application of the results to inlet design has been discussed. It has been shown that buzz can be avoided throughout the entire range of Mach numbers considered, even for the condition of constant minimum exhaust area.

Langley Aeronautical Laboratory
National Advisory Committee for Aeronautics
Langley Field, Va.

REFERENCES

1. Oswatitsch, Kl.: Der Druckrückgewinn bei Geschossen mit Rückstossantrieb bei hohen Überschallgeschwindigkeiten (Der Wirkungsgrad von Stossdiffusoren). Bericht Nr. 1005, Forsch. und Entwickl. des Heereswaffenamtes (Göttingen), 1944. (Available in English translation as NACA TM 1140.)

2. Ferri, Antonio, and Nucci, Louis M.: Preliminary Investigation of a New Type of Supersonic Inlet. NACA RM L6J31, 1946.

3. Moeckel, W. E., Connors, J. F., and Schroeder, A. H.: Investigation of Shock Diffusers at Mach Number 1.85. I - Projecting Single-Shock Cones. NACA RM E6K27, 1947.

4. Ferri, Antonio, and Nucci, Louis M.: Theoretical and Experimental Analysis of Low Drag Supersonic Inlets Having a Circular Cross Section and a Central Body at Mach Numbers of 3.30, 2.75, and 2.45. NACA RM L8H13, 1948.

TABLE I

INTERNAL COWLING ORDINATES

[See fig. 8; all dimensions in inches]

Station X	Cowling radius					
	A	B	C	D	E	F
0	0.75	0.750	0.750	0.750	0.600	0.718
.1	.75	.757	.763	.773	.623	.748
.171	.75	.762	.772	.788	.639	.770
.2	.75	.764	.775	.792	.646	.774
.3	.75	.770	.787	.799	.662	.792
.347	.75	.773	.792	.800	.667	.800
.4	.75	.778	.795	.800	.675	.800
.5	.75	.785	.800	.800	.683	.800
.6	.75	.791	.800	.800	.687	.800
.7	.75	.797	.800	.800	.690	.800
.8	.75	.800	.800	.800	.693	.800
.9	.75	.800	.800	.800	.696	.800
1.0	.75	.800	.800	.800	.700	.800
4.0	.75	.800	.800	.800	.800	.800
4.2	.75	.800	.800	.800	.800	.800
5.0	.80	.800	.800	.800	.800	.800

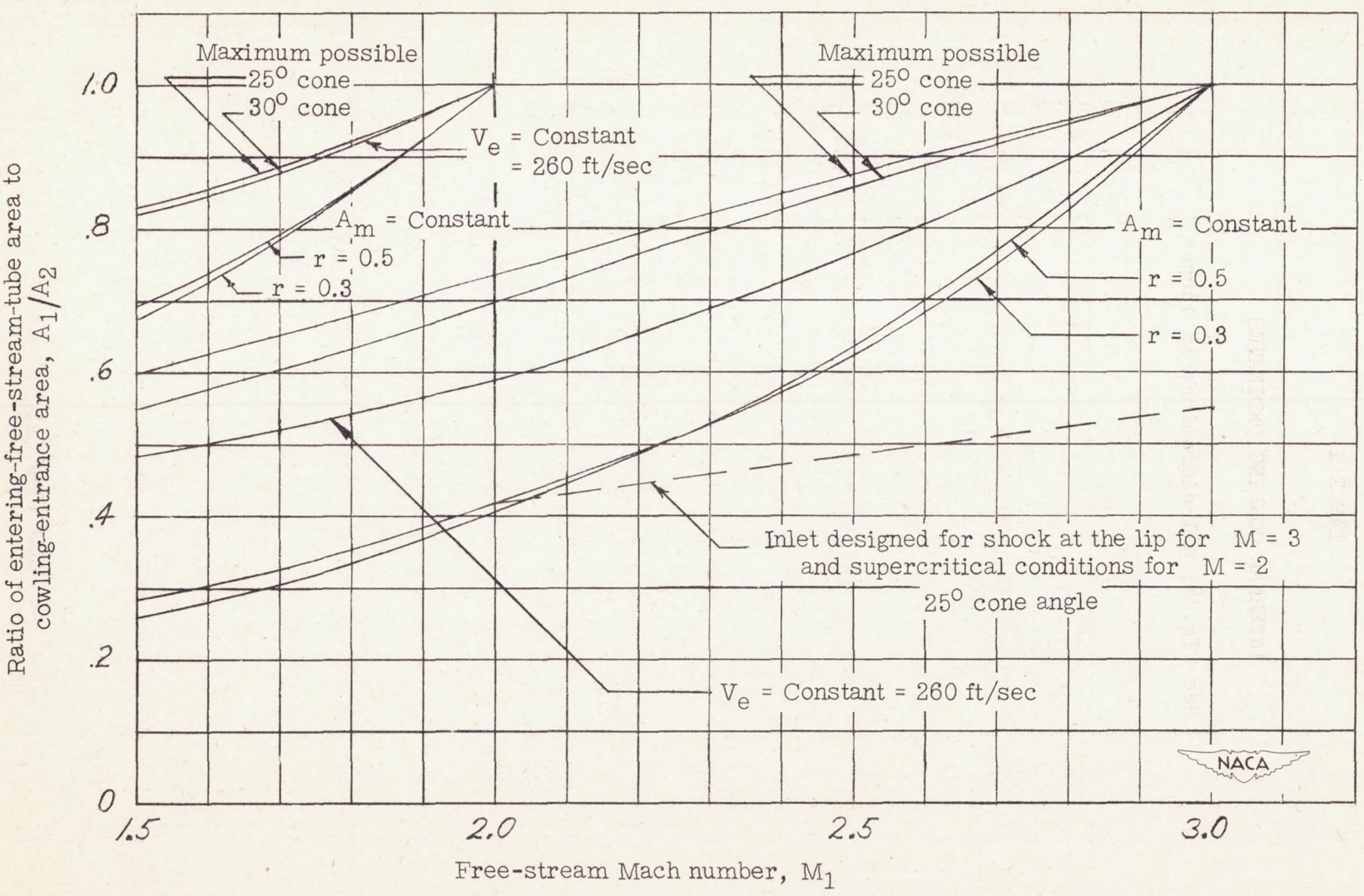

Figure 1.- Variation of the ratio of the entering-free-stream-tube area to cowling-entrance area as a function of Mach number.

(a) Supercritical condition.

(b) Subcritical condition.

Figure 2.- Aerodynamic phenomena of supersonic inlets.

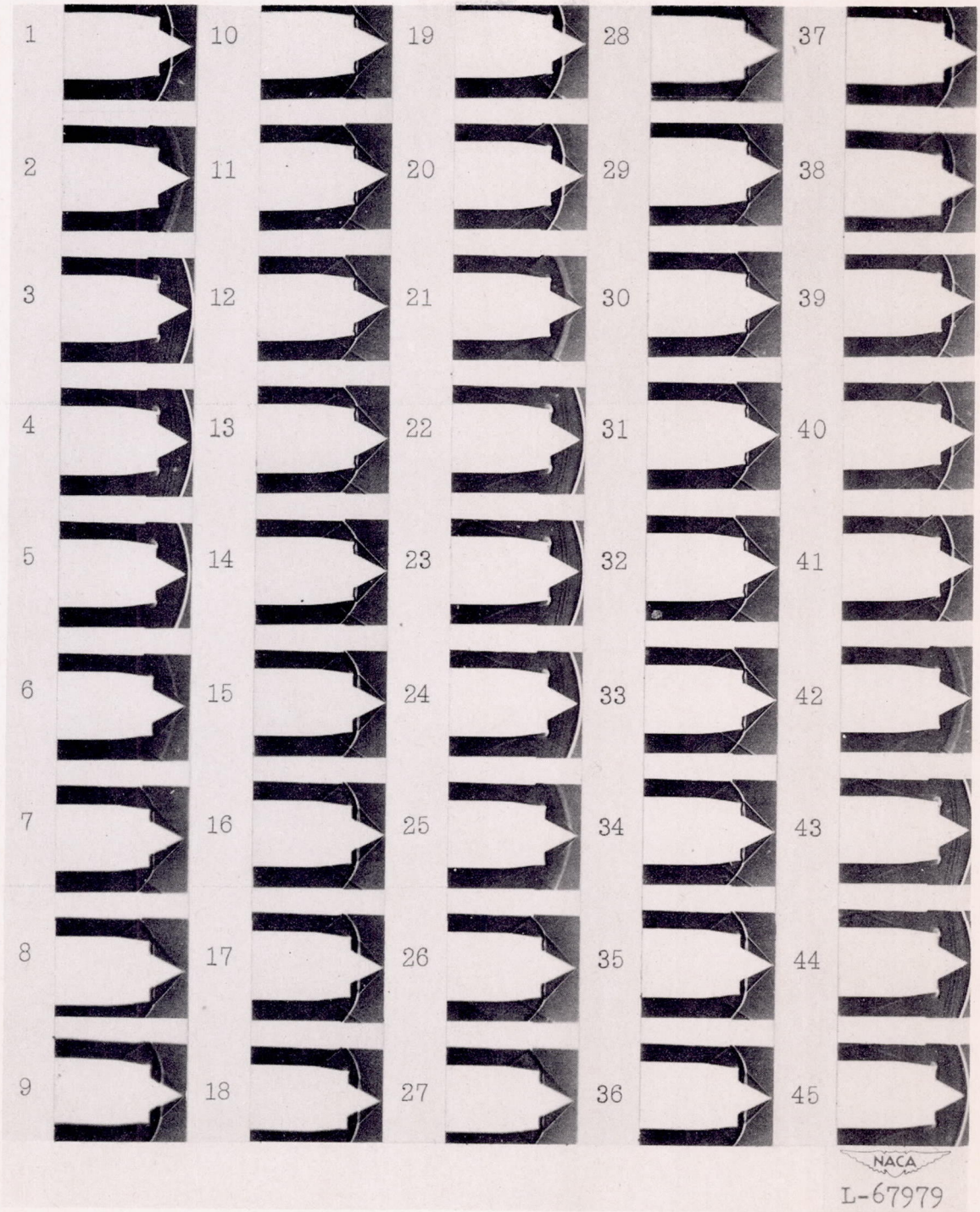

Figure 3.- Typical example of fluctuation phenomena of supersonic inlets having external compression. Inlet having 30°-0.8 central body and cowling E for $\theta_l = 42^{\circ}9'$ at M = 1.90. Motion pictures taken at 64 frames per second.

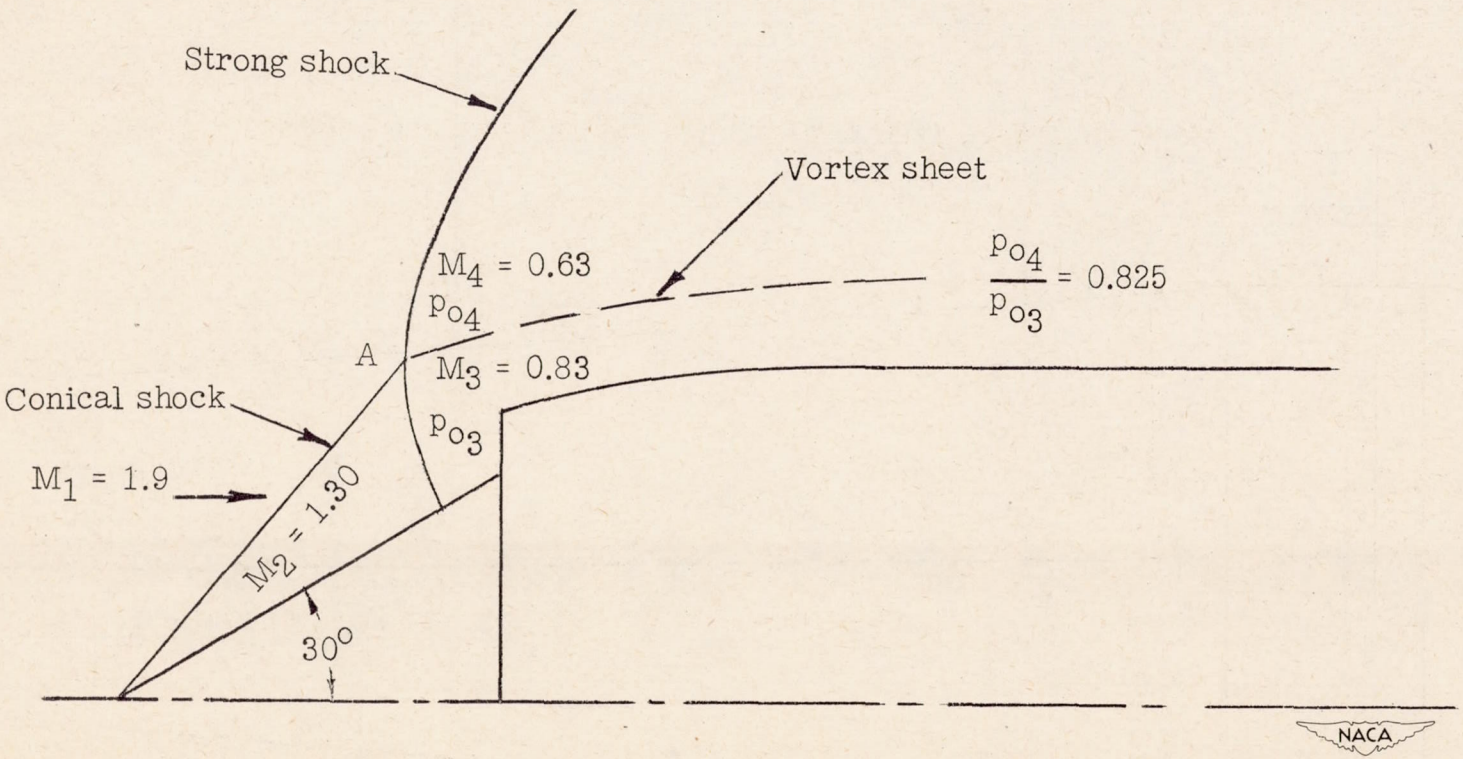

Figure 4.- Aerodynamic phenomena of an inlet having a 30° cone-angle central body for subcritical conditions at M = 1.90.

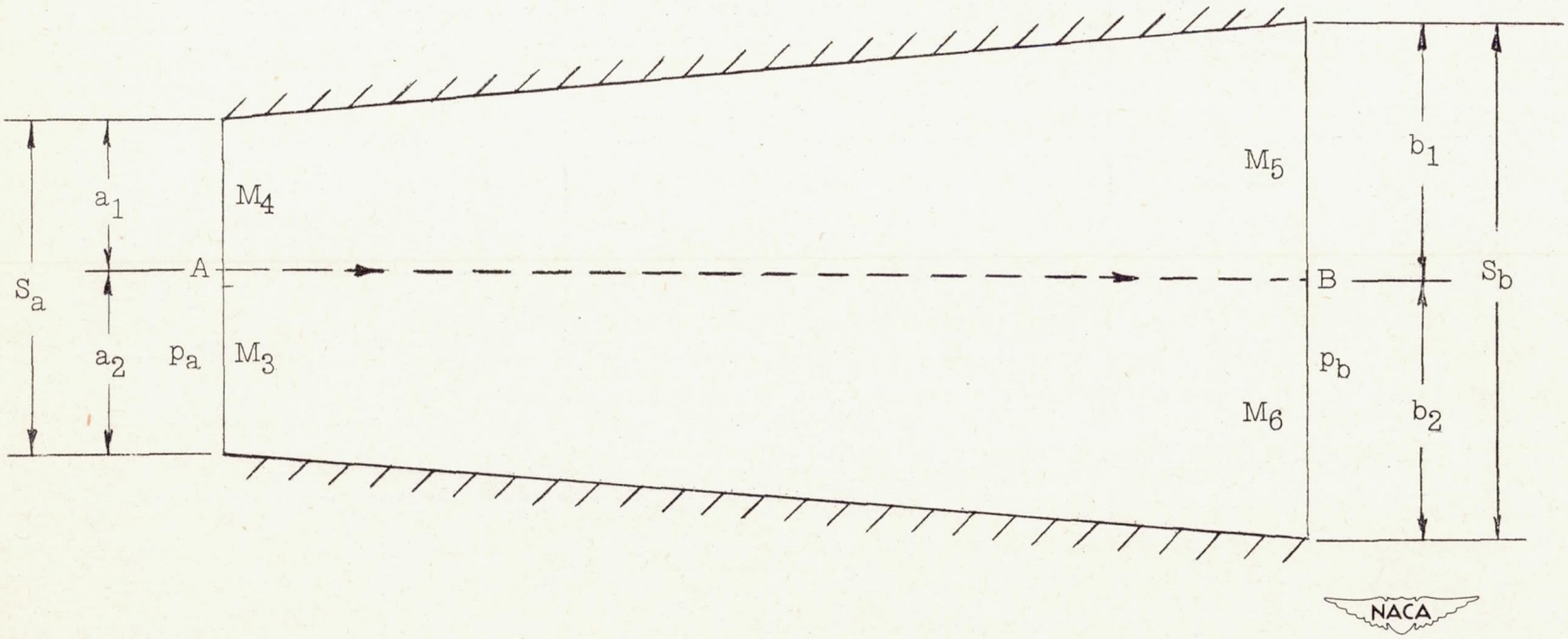

Figure 5.- Subsonic diffusers having two layers of flow having different entropies.

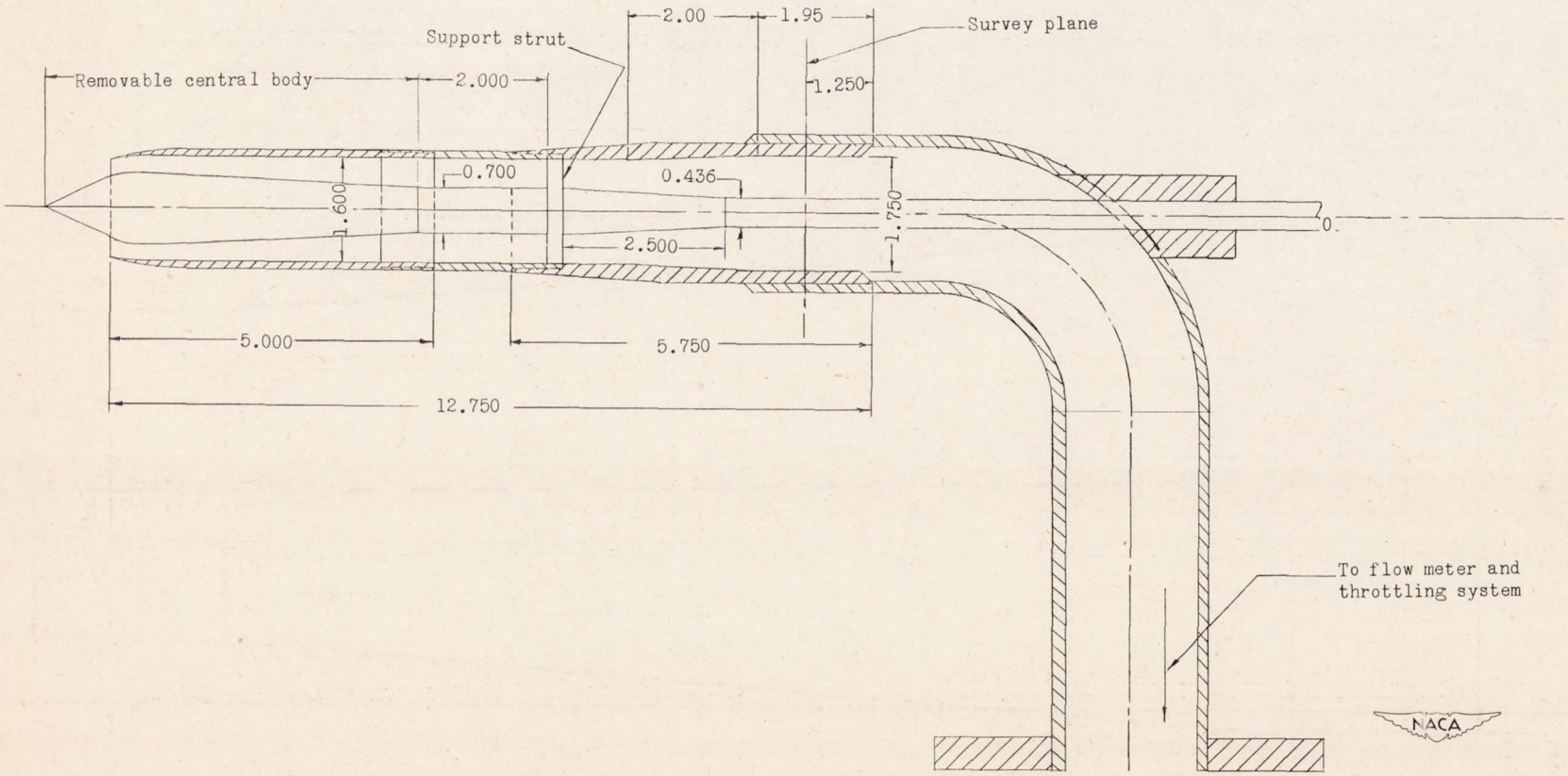

Figure 6.- General configuration of models tested.

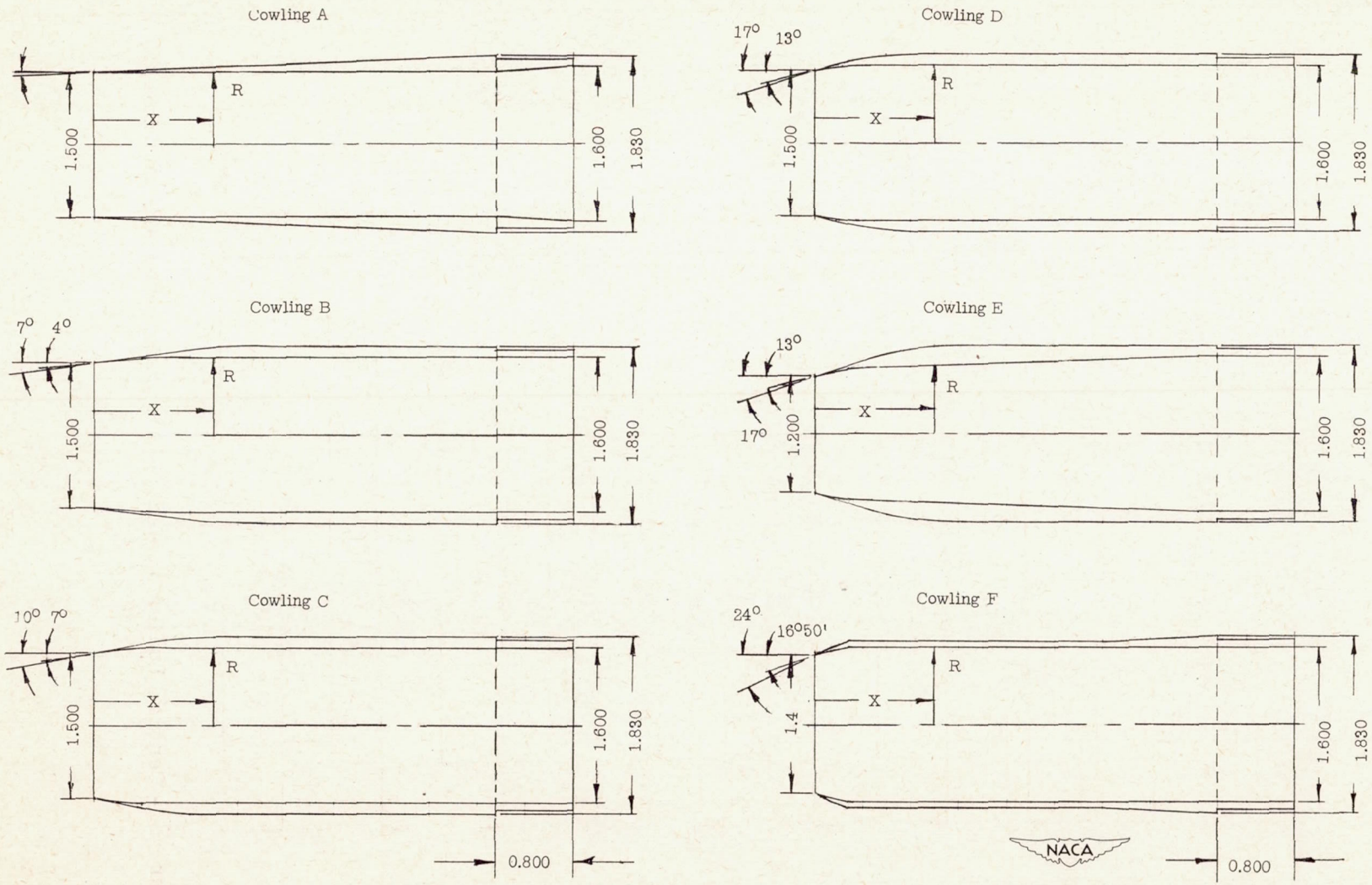

Figure 7.- Cowlings tested. See table I for coordinates.

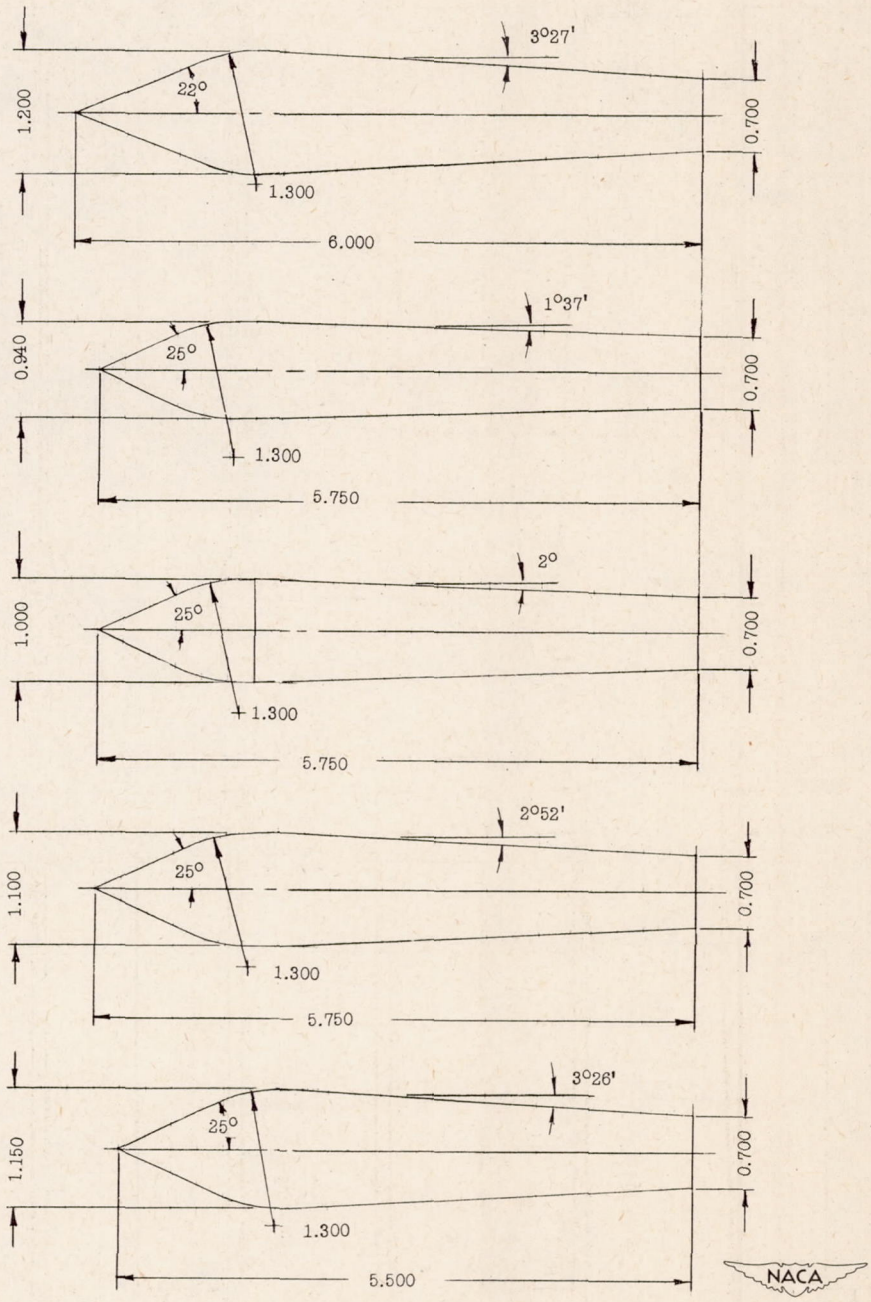

Figure 8.- Central bodies tested. (All dimensions are in inches.)

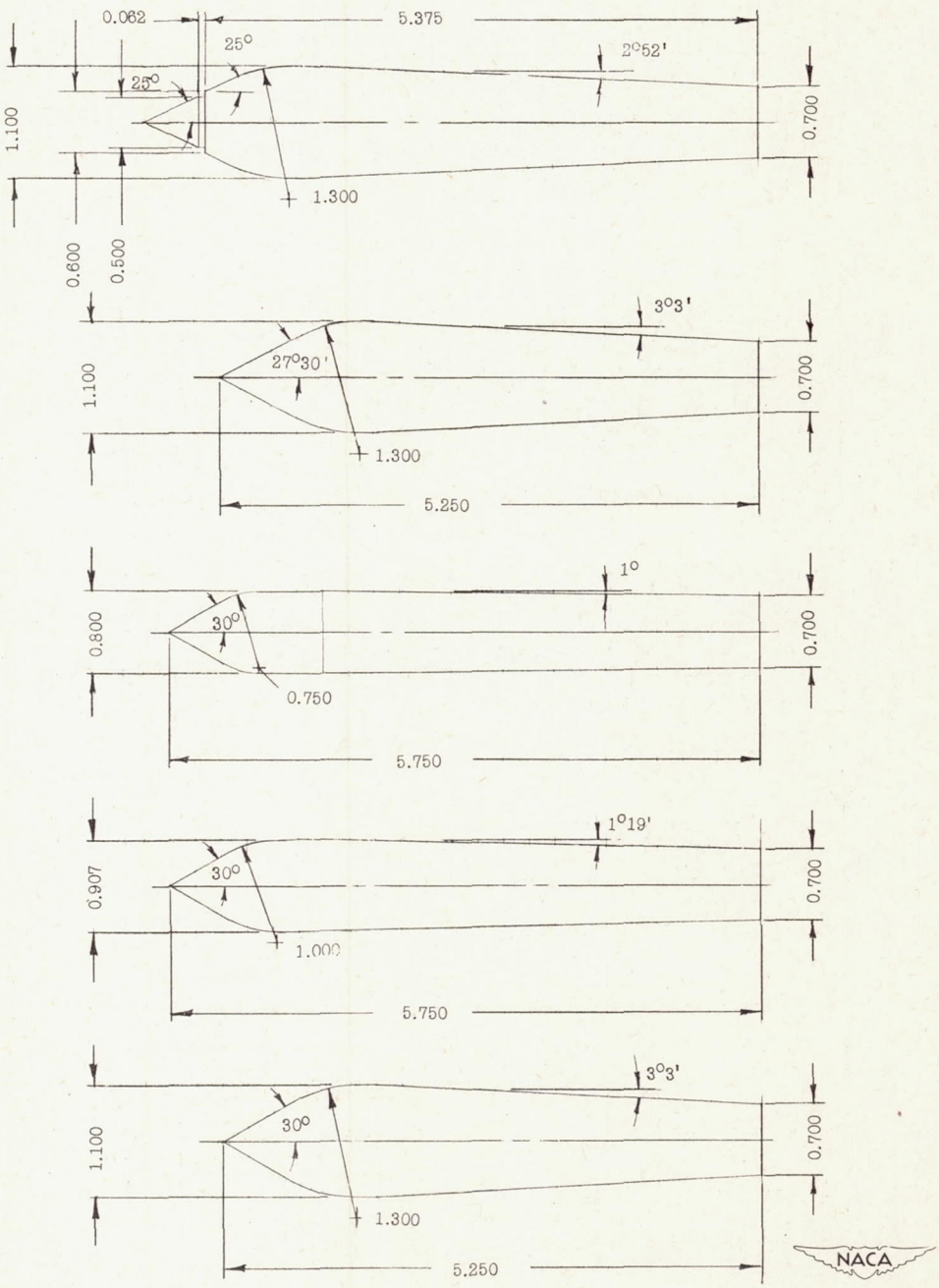

Figure 8.- Continued.

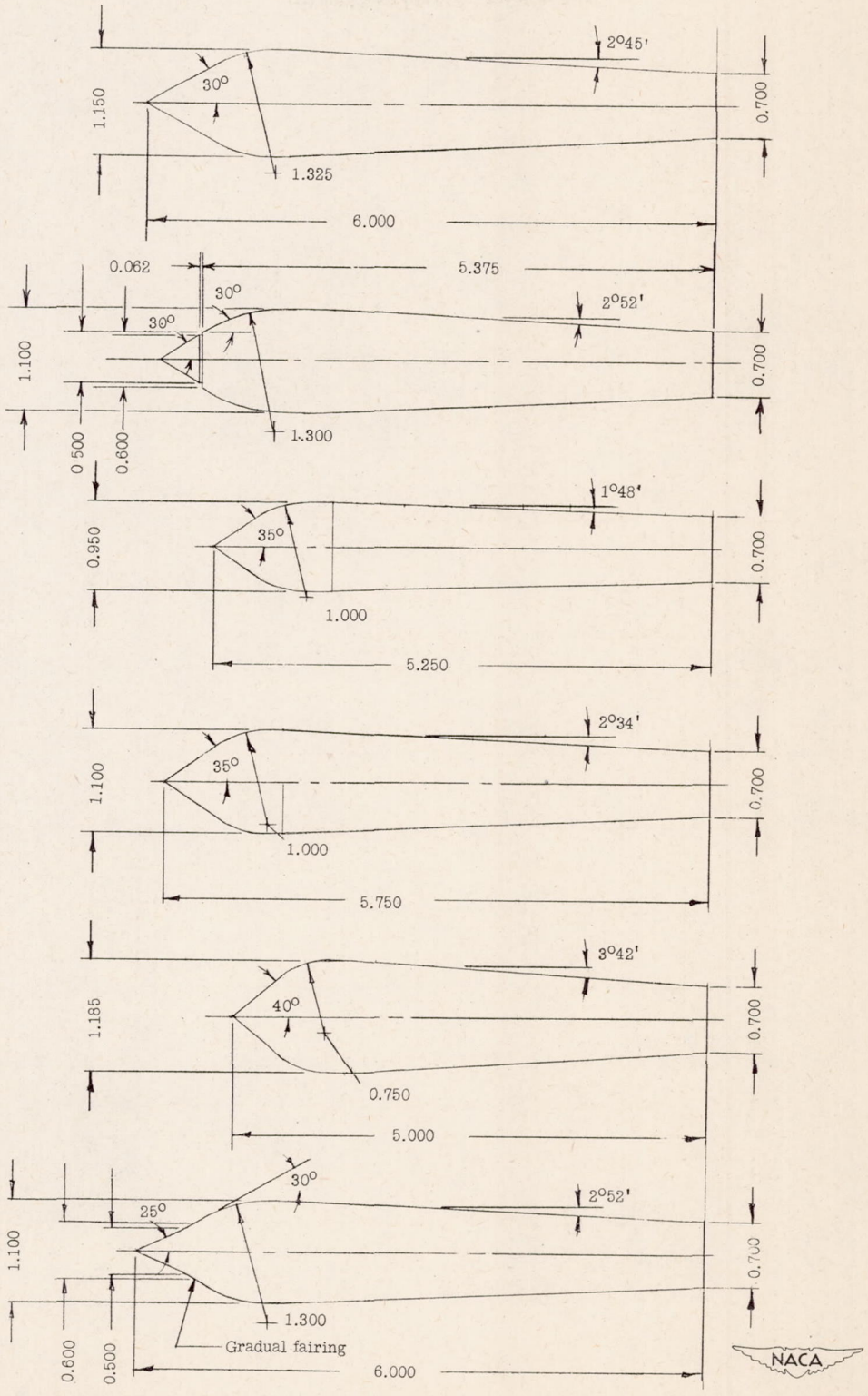

Figure 8.- Concluded.

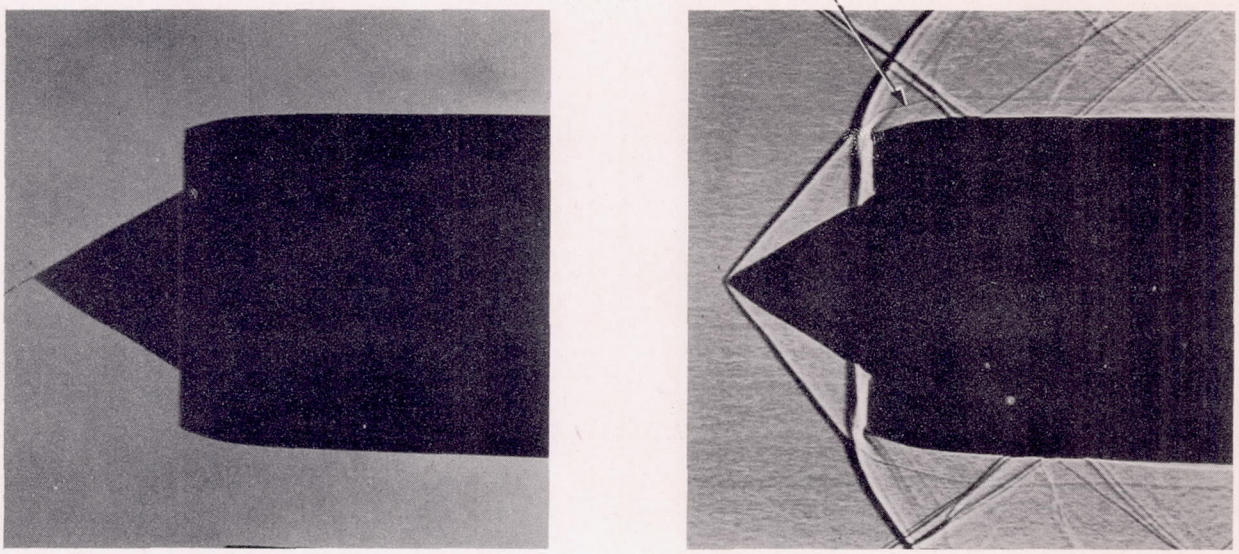

(a) No flow.

(b) $\frac{A_1}{A_2} = 0.76$.

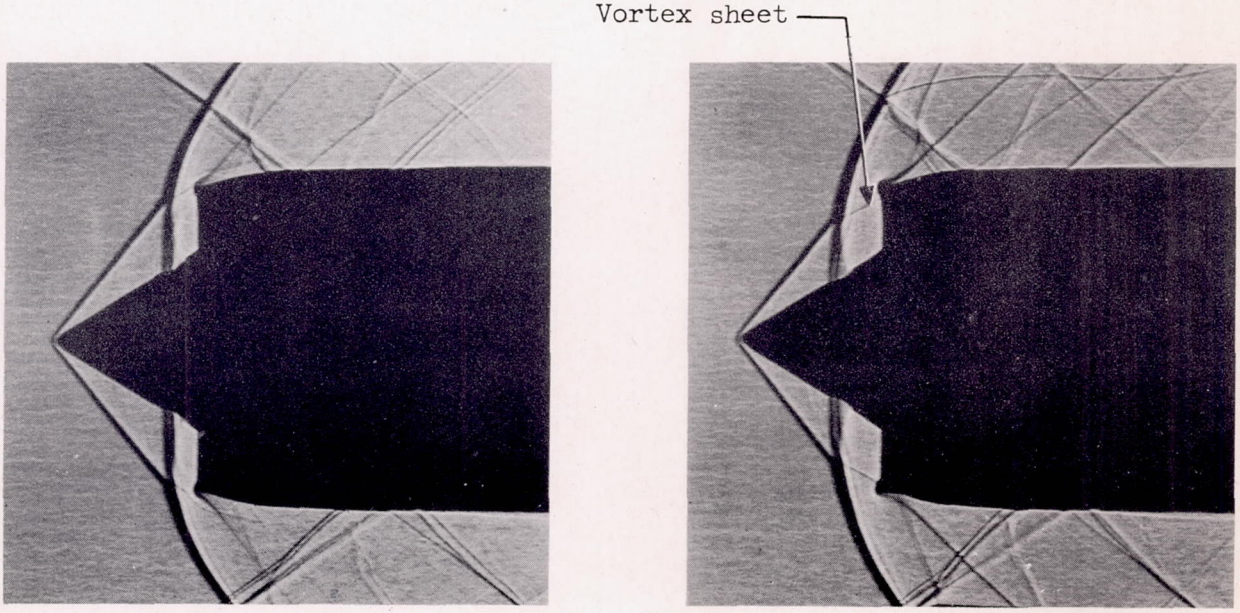

(c) $\frac{A_1}{A_2} = 0.72$.

(d) $\frac{A_1}{A_2} = 0.65$; minimum entering volume flow.

NACA

L-67980

Figure 9.- Shadowgraphs of an inlet having 30°-1.10 central body and cowling D at $\theta_l = 43^\circ 54'$ at M = 1.90 for different values of entering volume flow.

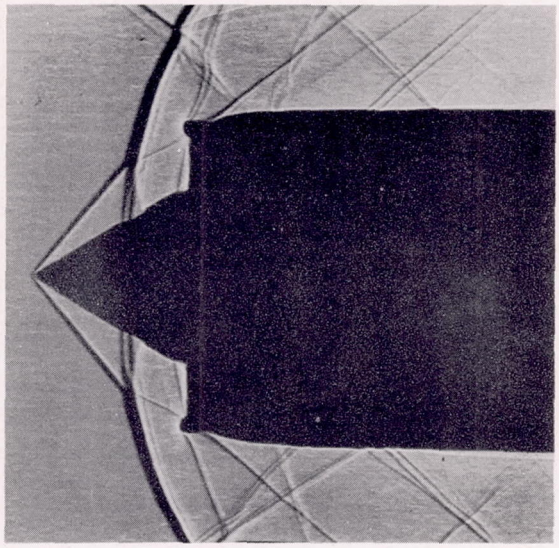

(a) $\theta_l = 41^\circ 48'$; $\frac{A_1}{A_2} = 0.53$.

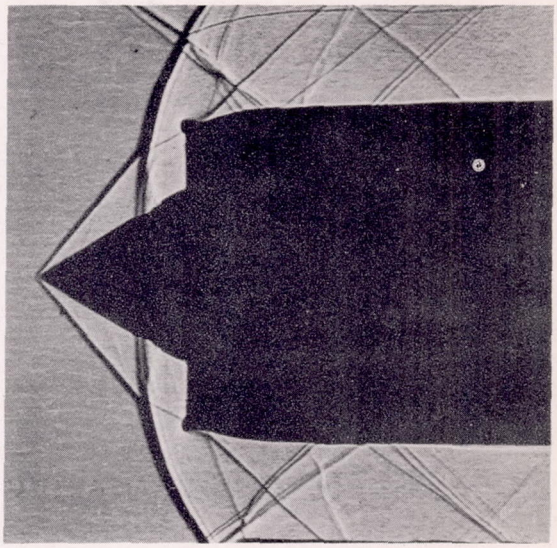

(b) $\theta_l = 42^\circ 50'$; $\frac{A_1}{A_2} = 0.64$.

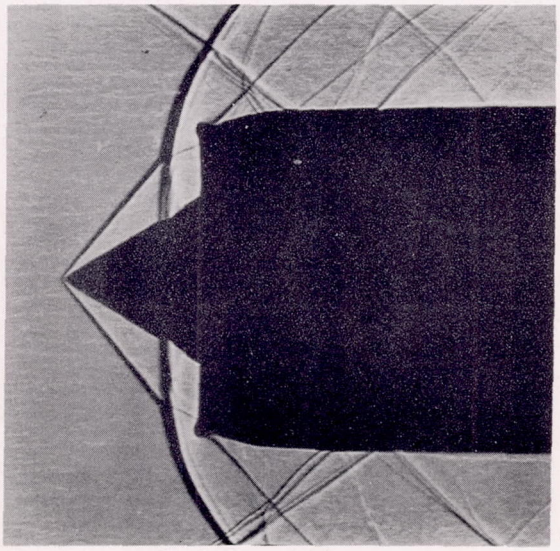

(c) $\theta_l = 45^\circ$; $\frac{A_1}{A_2} = 0.74$.

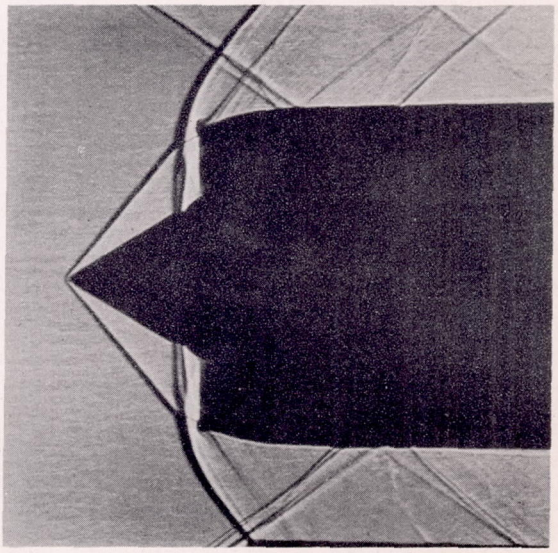

(d) $\theta_l = 46^\circ 11'$; $\frac{A_1}{A_2} = 0.79$.

NACA

L-67981

Figure 10.- Shadowgraphs of inlets having 30°-0.907 central body and cowling D for the condition of minimum stable entering volume flow at each value of θ_l at M = 1.90.

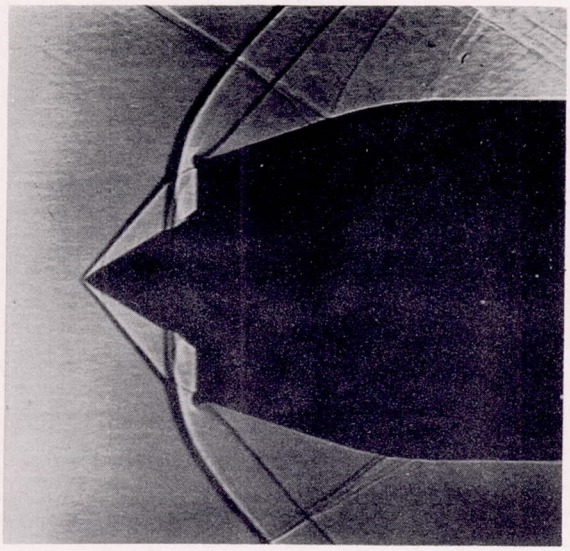

(a) 30°-0.80 central body; cowling E; $\theta_l = 44^{\circ}48'$; $\frac{A_1}{A_2} = 0.71$.

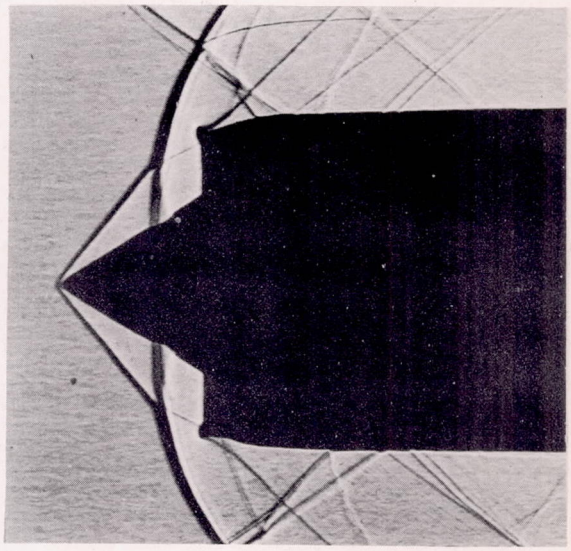

(b) 30°-1.10 central body; cowling D; $\theta_l = 43^{\circ}54'$; $\frac{A_1}{A_2} = 0.65$.

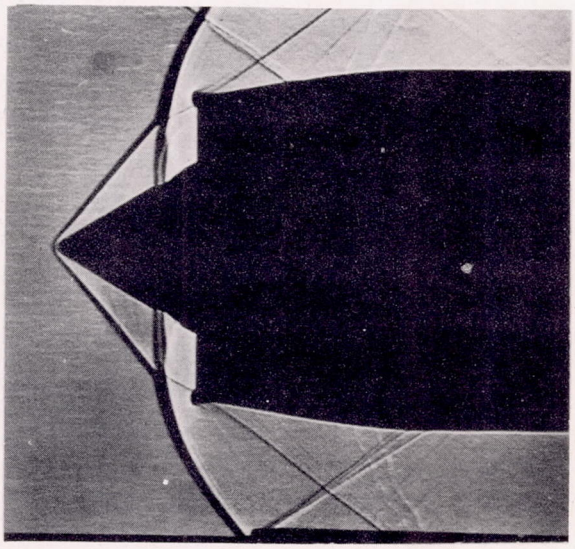

(c) 30°-0.907 central body; cowling C; $\theta_l = 44^{\circ}1'$; $\frac{A_1}{A_2} = 0.68$.

NACA L-67982

Figure 11.- Shadowgraphs of inlets having different central bodies, subsonic diffusers, and cowlings for the condition of minimum entering volume flow at M = 1.90.

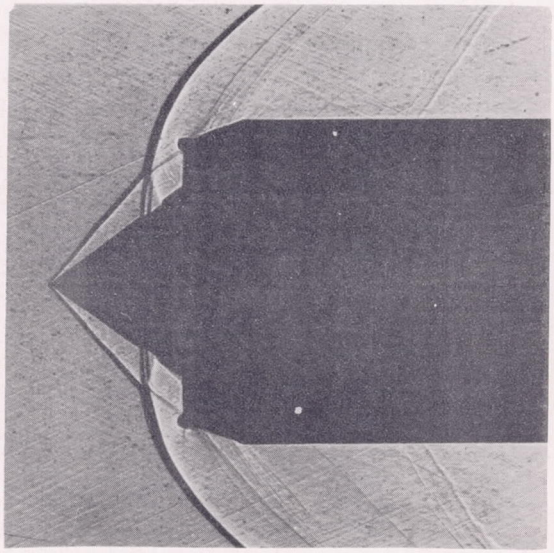

(a) $\theta_l = 44^\circ 52'$; $\frac{A_1}{A_2} = 0.65$.

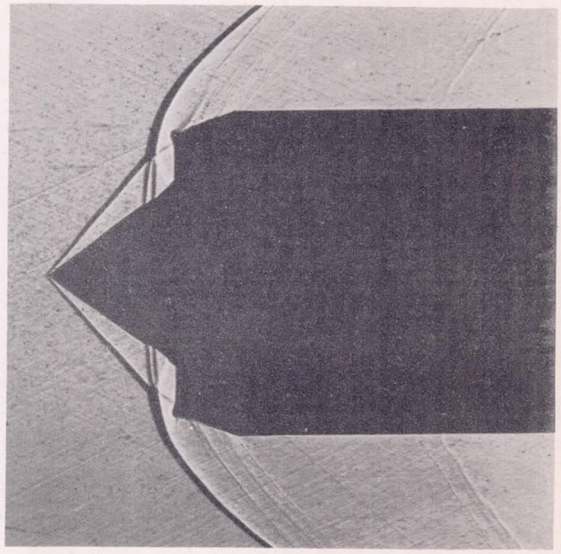

(b) $\theta_l = 46^\circ 2'$; $\frac{A_1}{A_2} = 0.75$.

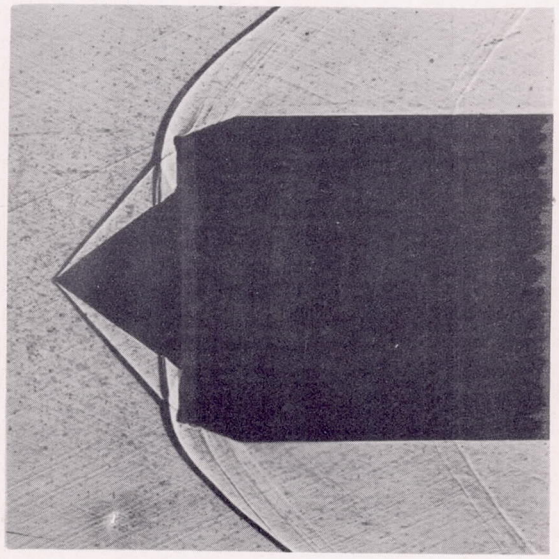

(c) $\theta_l = 46^\circ 50'$; $\frac{A_1}{A_2} = 0.81$.

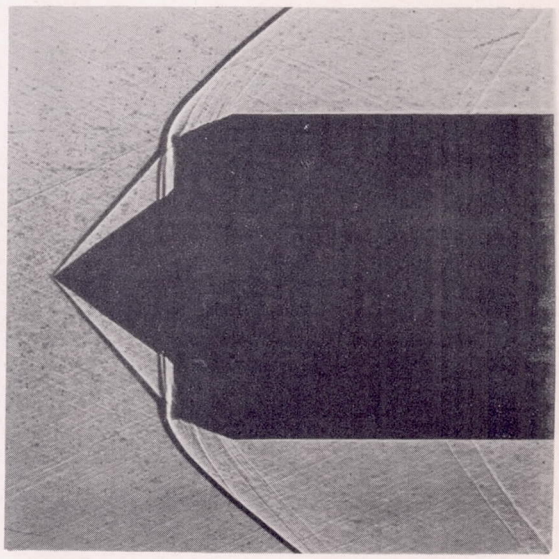

(d) $\theta_l = 48^\circ 5'$; $\frac{A_1}{A_2} = 0.88$.

NACA
L-67983

Figure 12.- Shadowgraphs of inlets having 35°-1.10 central body and cowling F for the condition of minimum stable entering volume flow for various values of θ_l at M = 2.46.

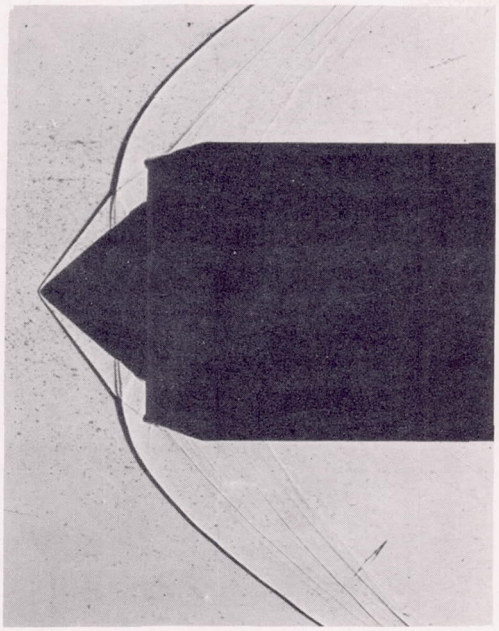

(a) $\theta_l = 48^\circ 33'$; $\frac{A_1}{A_2} = 0.62$.

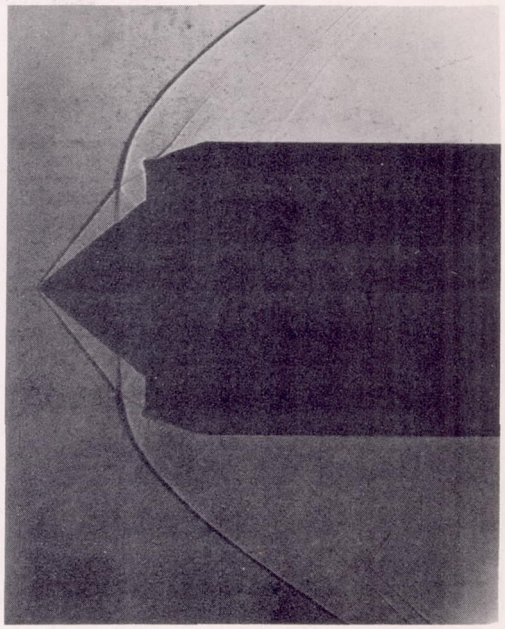

(b) $\theta_l = 48^\circ 58'$; $\frac{A_1}{A_2} = 0.65$.

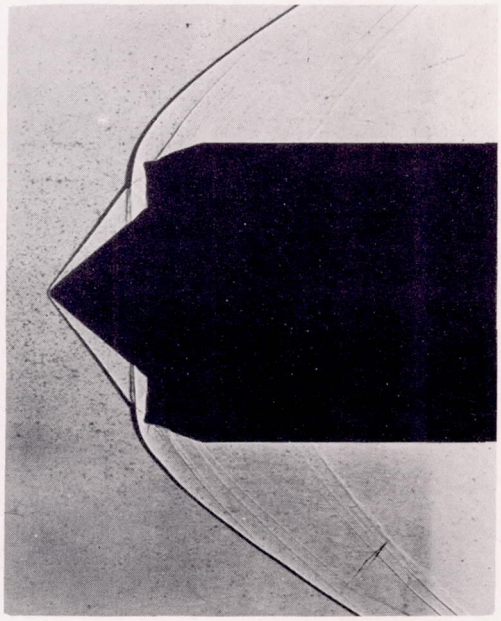

(c) $\theta_l = 51^\circ 16'$; $\frac{A_1}{A_2} = 0.82$.

NACA
L-67984

Figure 13.- Shadowgraphs of inlets having 40°-1.185 central body and cowling F for the condition of minimum stable entering volume flow for various values of θ_l at M = 2.70.

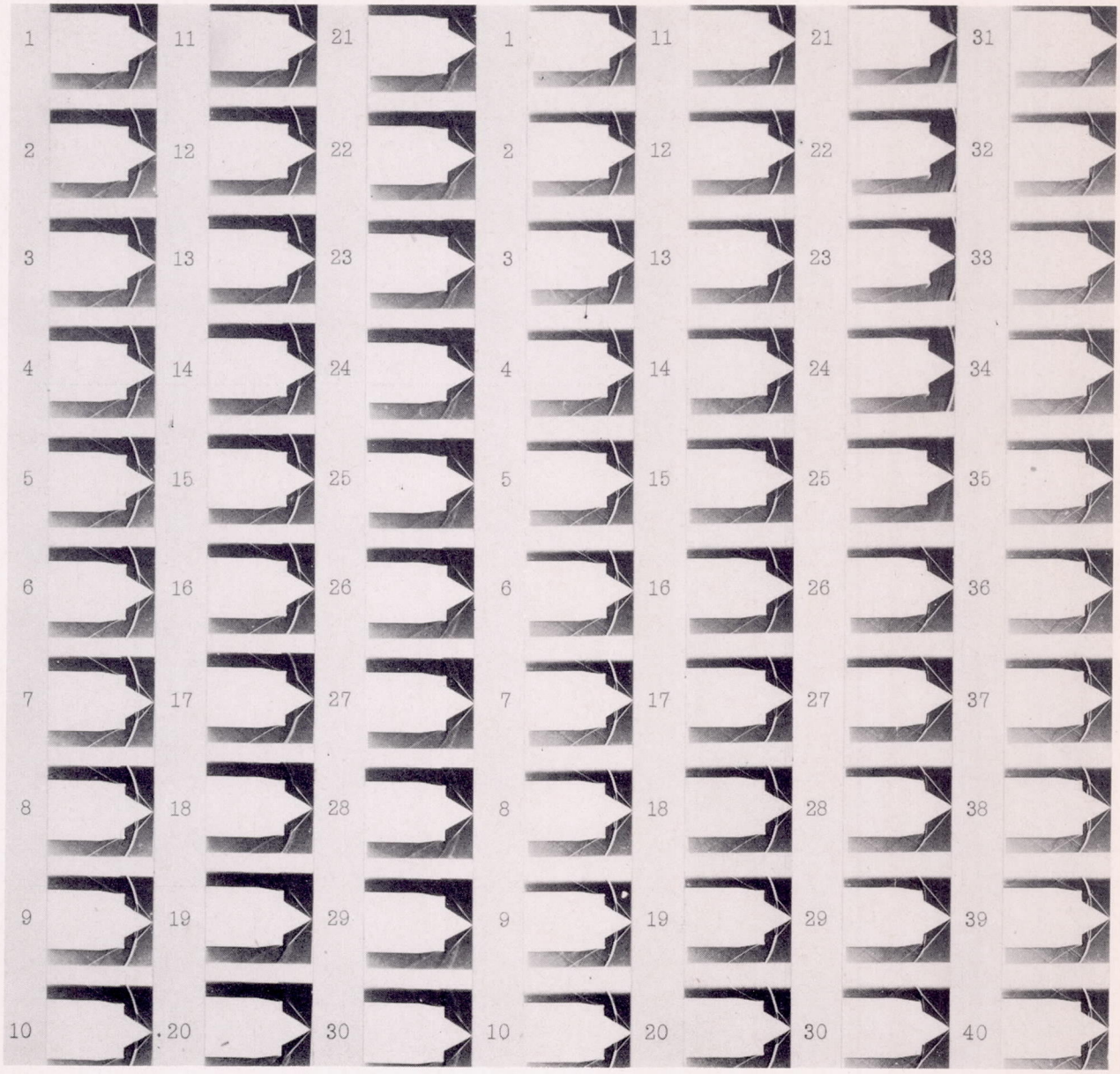

(a) 1-foot, 2-inch-diameter pipe is inserted between model and throttling valve.

(b) 25-foot, 4-inch-diameter pipe is inserted between model and throttling valve.

Figure 14.- Section of motion-picture film showing starting of fluctuations. Inlet having 30°-1.10 central body and cowling B for $\theta_l = 42°$ at $M = 1.90$.

NACA

L-67985

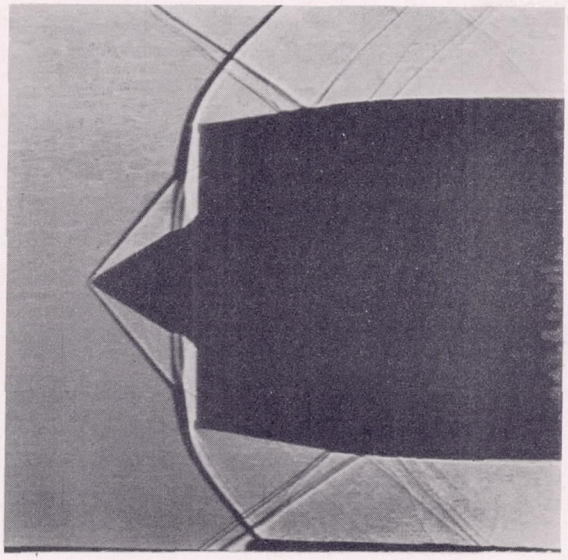

(a) $\frac{A_1}{A_2} = 0.89$; $\frac{p_f}{p_o} = 0.81$.

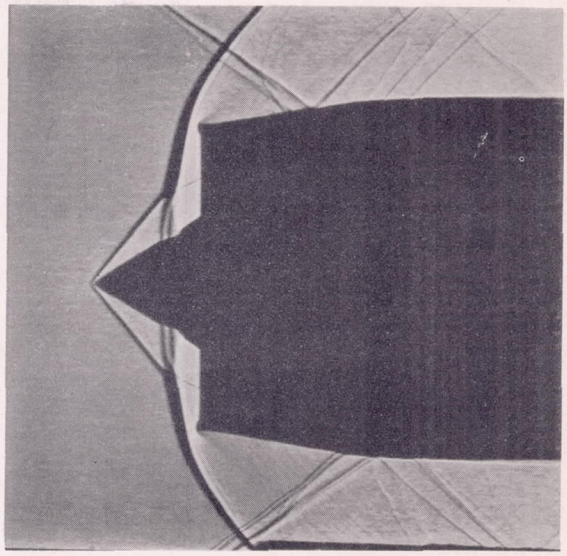

(b) $\frac{A_1}{A_2} = 0.81$; $\frac{p_f}{p_o} = 0.80$.

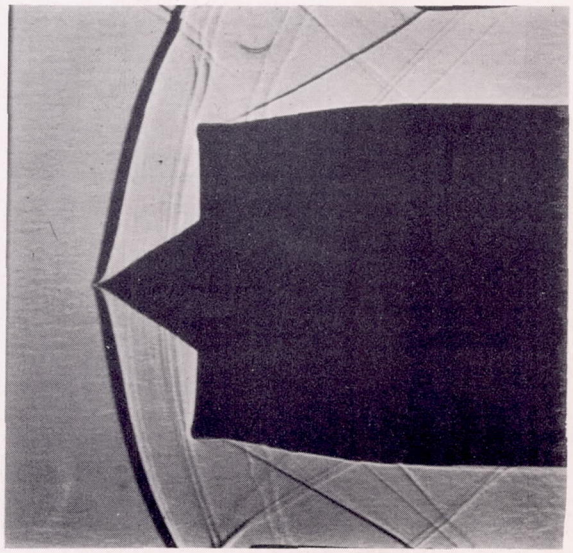

(c) $\frac{A_1}{A_2} = 0.32$; $\frac{p_f}{p_o} = 0.78$.

NACA
L-67986

Figure 15.- Shadowgraphs of an inlet having 30°-0.907 central body and cowling C with $\theta_l = 51^\circ 55'$ for different values of stable entering volume flow at $M = 1.90$.

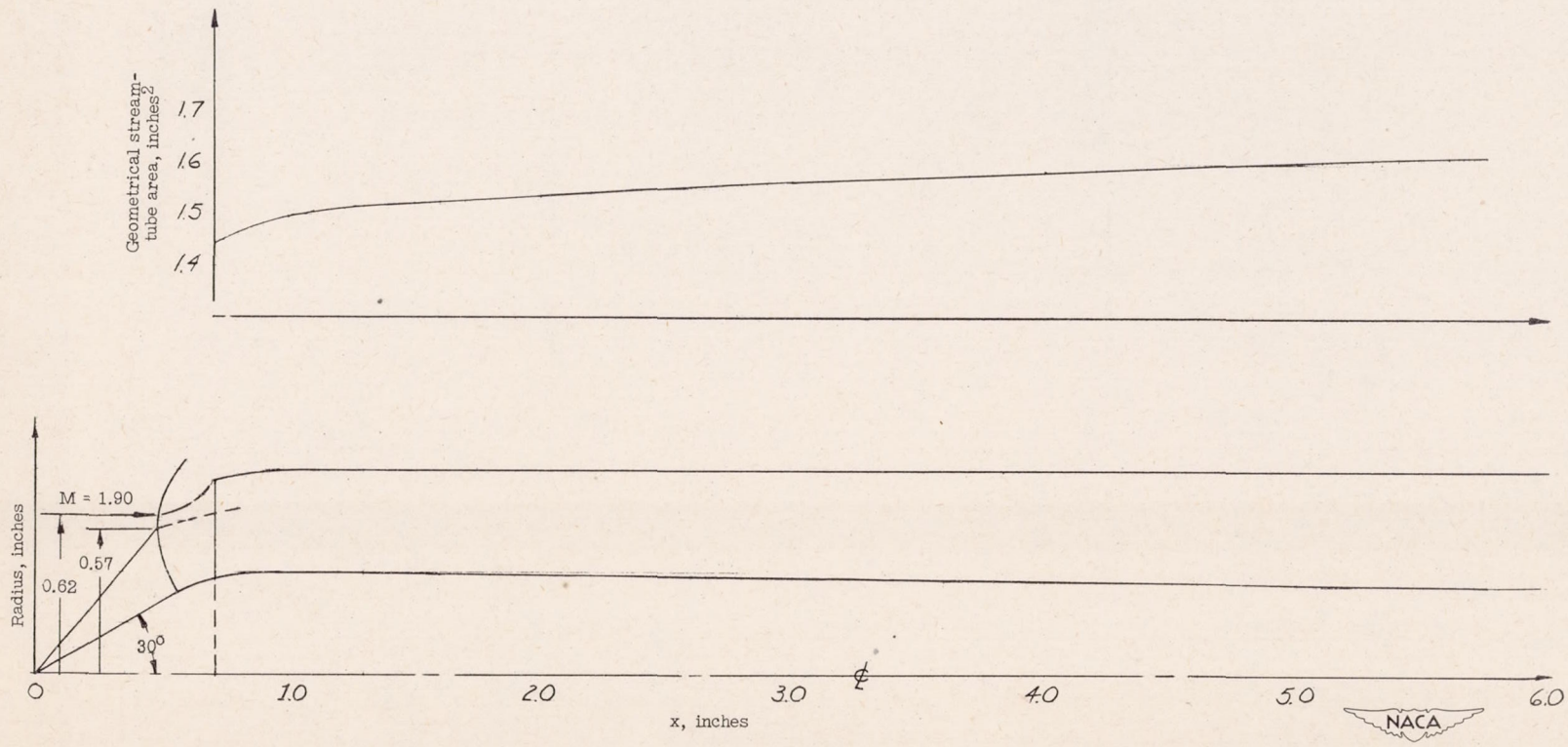

Figure 16.- Inlet having 30°-8 central body and cowling D with $\theta_l = 46°54'$ at M = 1.90.

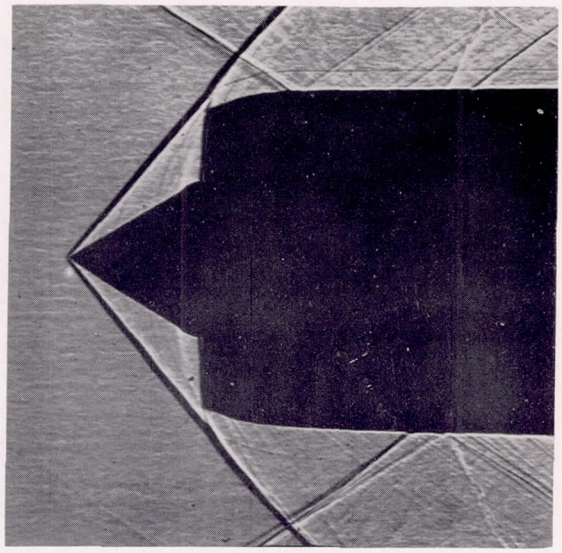

(a) $\frac{A_1}{A_2} = 0.90$.

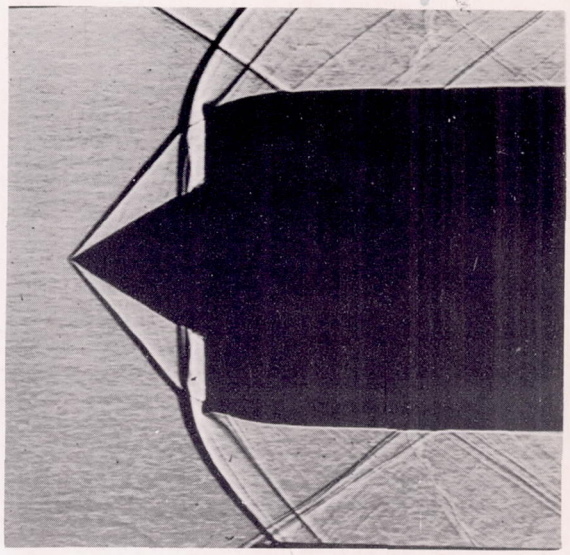

(b) $\frac{A_1}{A_2} = 0.81$.

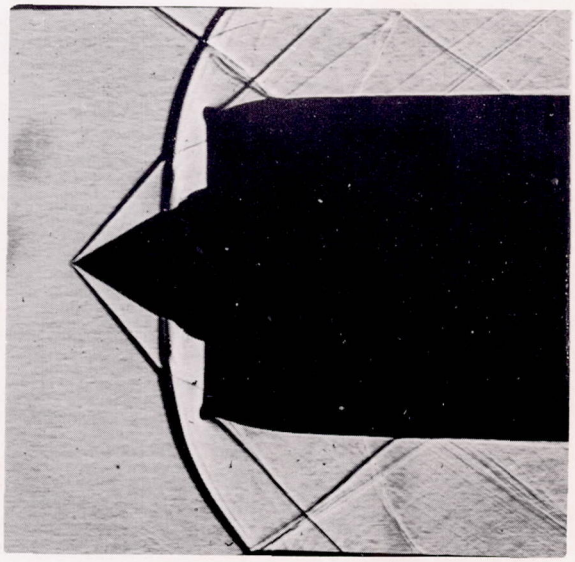

(c) $\frac{A_1}{A_2} = 0.68$; minimum stable entering volume flow.

NACA

L-67987

Figure 17.- Shadowgraphs of an inlet having 30°-0.80 central body and cowling D with $\theta_l = 46^\circ 57'$ for different values of stable entering volume flow at M = 1.90.

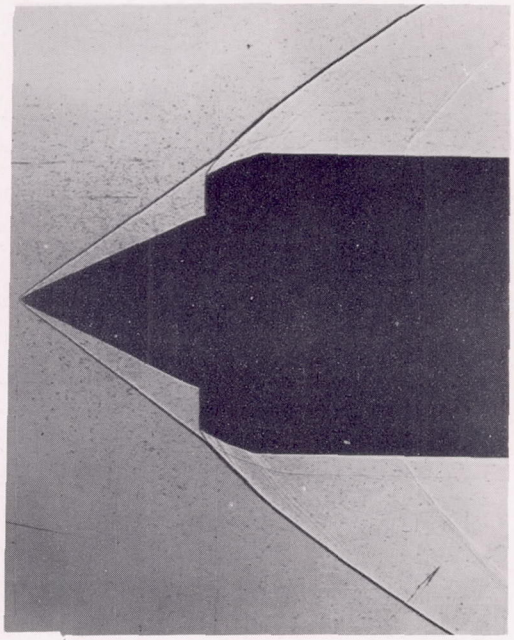

(a) $\frac{A_1}{A_2} = 0.94$; $\frac{p_f}{p_o} = 0.51$.

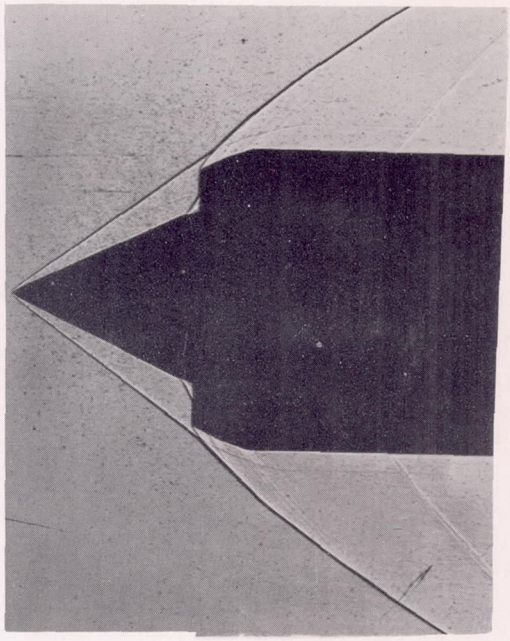

(b) $\frac{A_1}{A_2} = 0.93$; $\frac{p_f}{p_o} = 0.53$

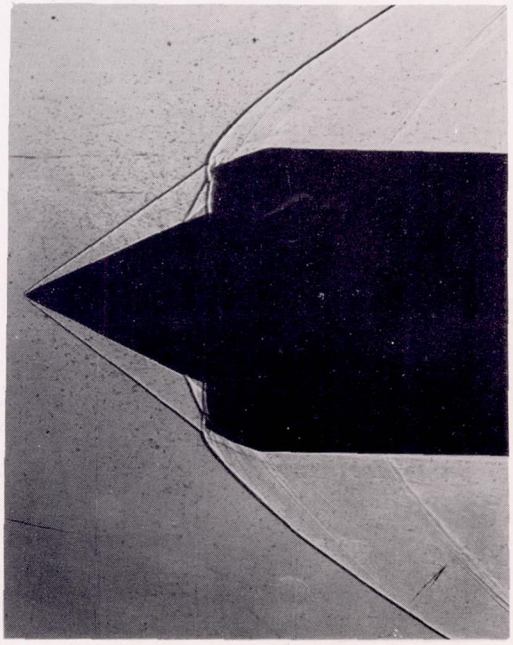

(c) $\frac{A_1}{A_2} = 0.87$; $\frac{p_f}{p_o} = 0.55$; minimum stable entering volume flow.

Figure 18.- Shadowgraphs of an inlet having 25°-1.10 central body and cowling F with $\theta_l = 34^\circ 32'$ for different values of stable entering volume flow at M = 2.70.

NACA

L-67988

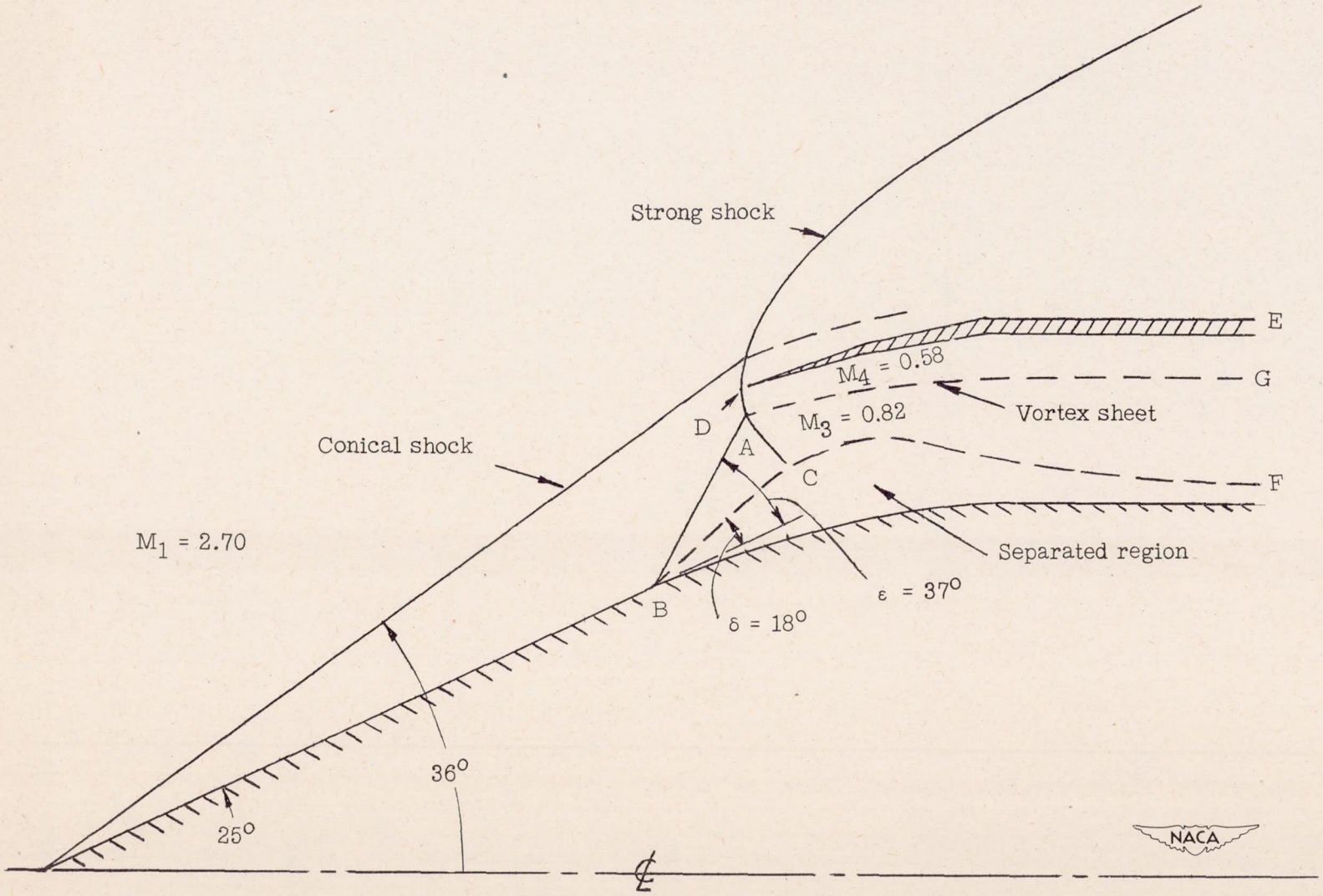

Figure 19.- Aerodynamic phenomena for inlet having 25°-1.10 central body and cowling F with $\theta_l = 34°32'$ at M = 2.70.

CONFIDENTIAL

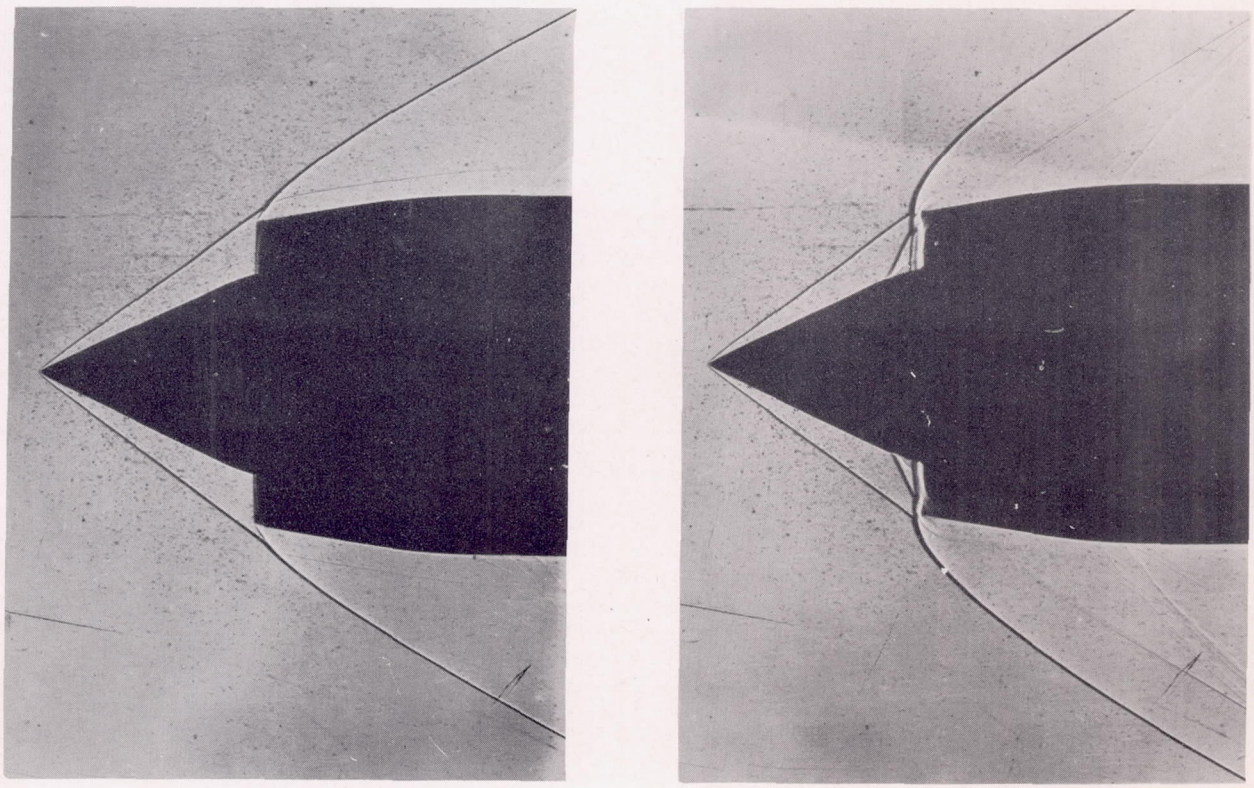

(a) $\frac{A_1}{A_2} = 0.90$.

(b) $\frac{A_1}{A_2} = 0.77$.

Figure 20.- Shadowgraphs of an inlet having 25°-1.10 central body and cowling C with $\theta_l = 33^\circ 14'$ for maximum and minimum entering volume flow at $M = 2.70$.

NACA

L-67989

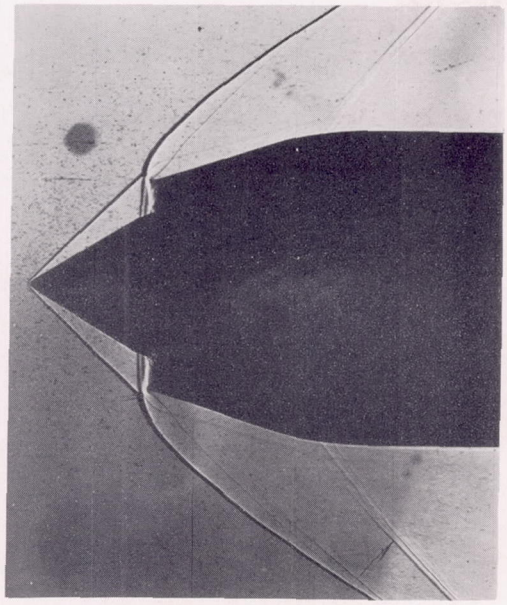

(a) 30°-1.10 central body; $\frac{A_1}{A_2} = 0.66$; minimum entering volume flow without suction.

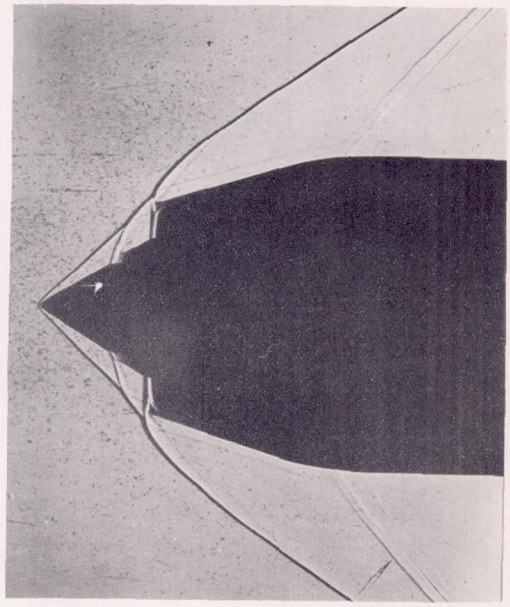

(b) 30°-30°-1.10 suction central body; $\frac{A_1}{A_2} = 0.76$.

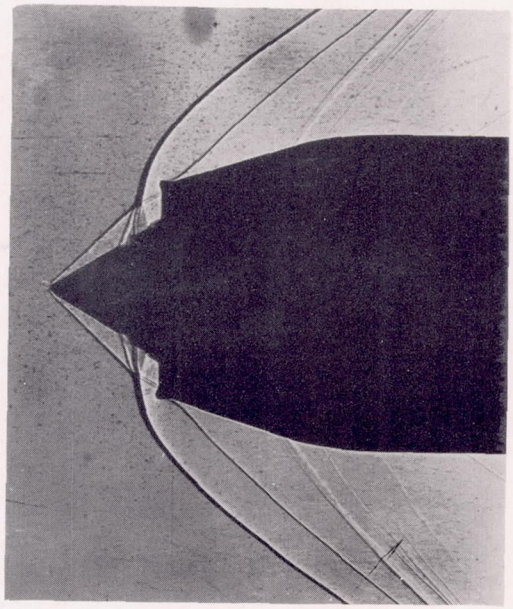

(c) 30°-30°-1.10 suction central body; minimum stable entering volume flow; $\frac{A_1}{A_2} = 0.60$.

NACA L-67990

Figure 21.- Shadowgraphs of inlets having 30° central bodies with and without suction and cowling E with $\theta_l = 38^{\circ}40'$ at $M = 2.46$.

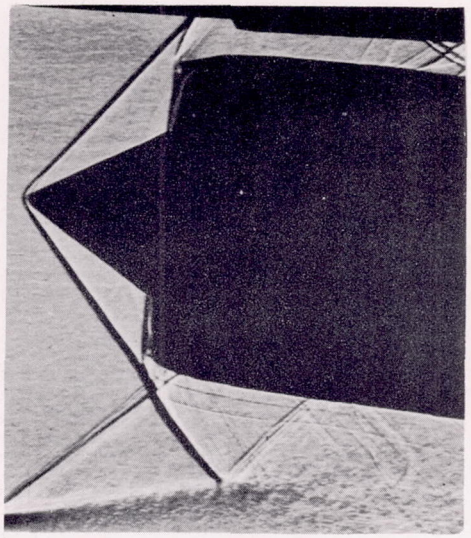

(a) $\alpha = 9^\circ$; $\frac{A_1}{A_2} = 0.85$; maximum entering volume flow.

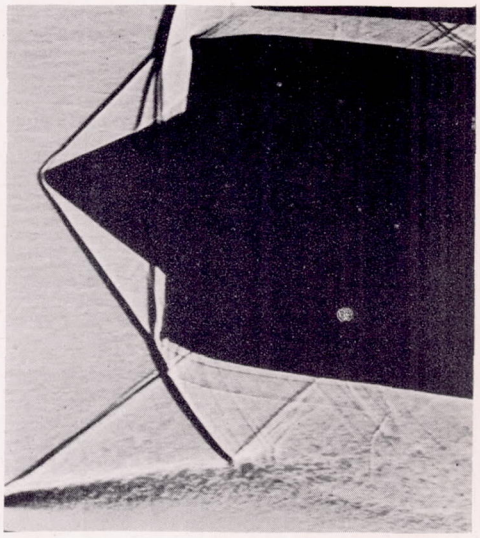

(b) $\alpha = 9^\circ$; $\frac{A_1}{A_2} = 0.77$.

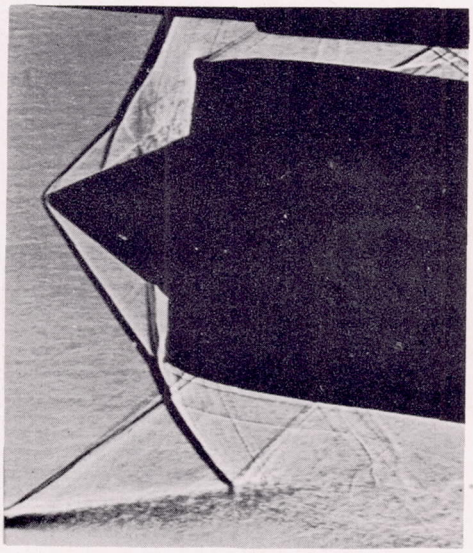

(c) $\alpha = 9^\circ$; $\frac{A_1}{A_2} = 0.71$; minimum entering volume flow.

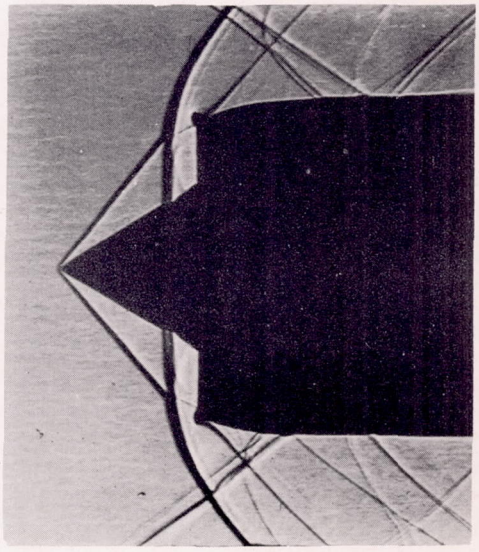

(d) $\alpha = 0^\circ$; $\frac{A_1}{A_2} = 0.78$; minimum entering volume flow.

NACA
L-67991

Figure 22.- Shadowgraphs of an inlet having 30°-0.907 central body and cowling D with $\theta_l = 45^\circ 46'$ with different values of entering volume flow at $\alpha = 9^\circ$ and 0° at M = 1.90.

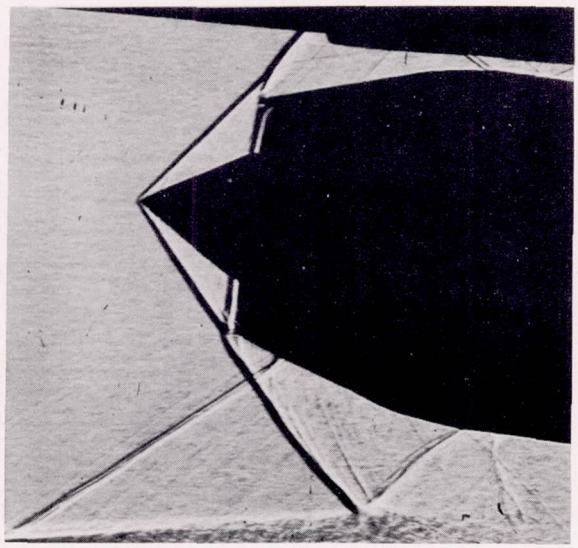

(a) $\alpha = 8^{\circ}30'$; $\frac{A_1}{A_2} = 0.85$;
maximum entering volume flow.

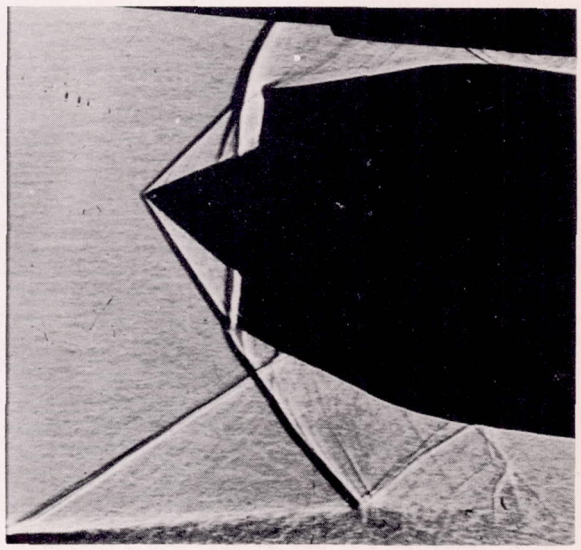

(b) $\alpha = 8^{\circ}30'$; $\frac{A_1}{A_2} = 0.74$;
minimum entering volume flow.

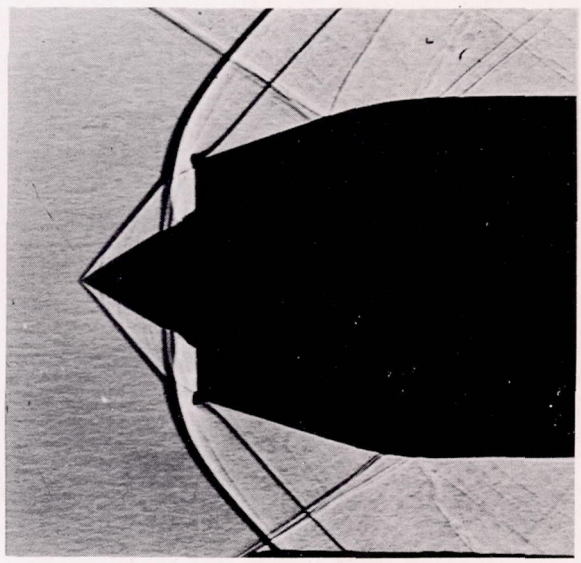

(c) $\alpha = 0^{\circ}$; $\frac{A_1}{A_2} = 0.81$;
minimum entering volume flow.

Figure 23.- Shadowgraphs of an inlet having 30°-0.80 central body and cowling E with $\theta_l = 46^{\circ}14'$ with different values of entering volume flow at $\alpha = 8^{\circ}30'$ and 0° at M = 1.90.

NACA
L-67992

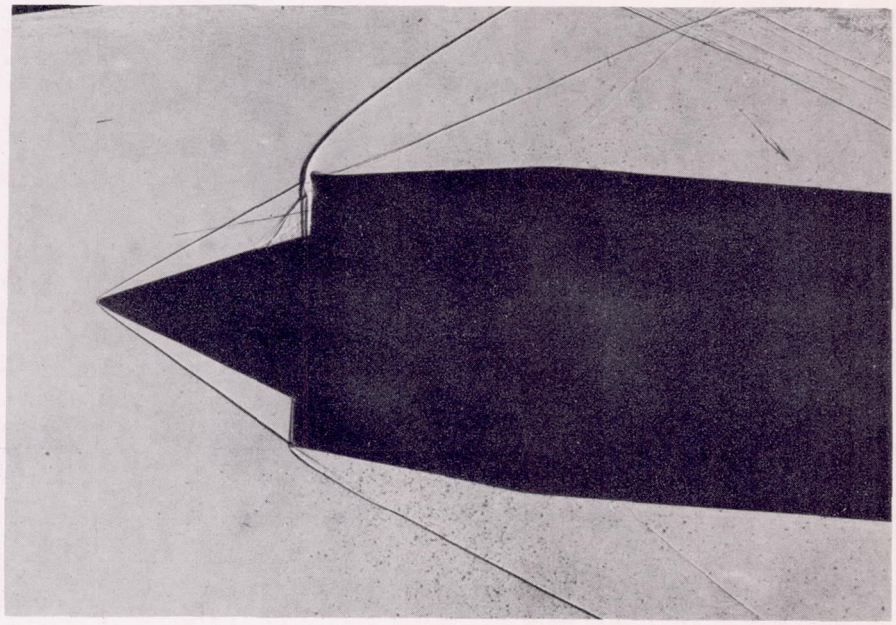

(a) $\alpha = 4^{\circ}$; $\theta_l = 33^{\circ}50'$; $\frac{A_1}{A_2} = 0.95$.

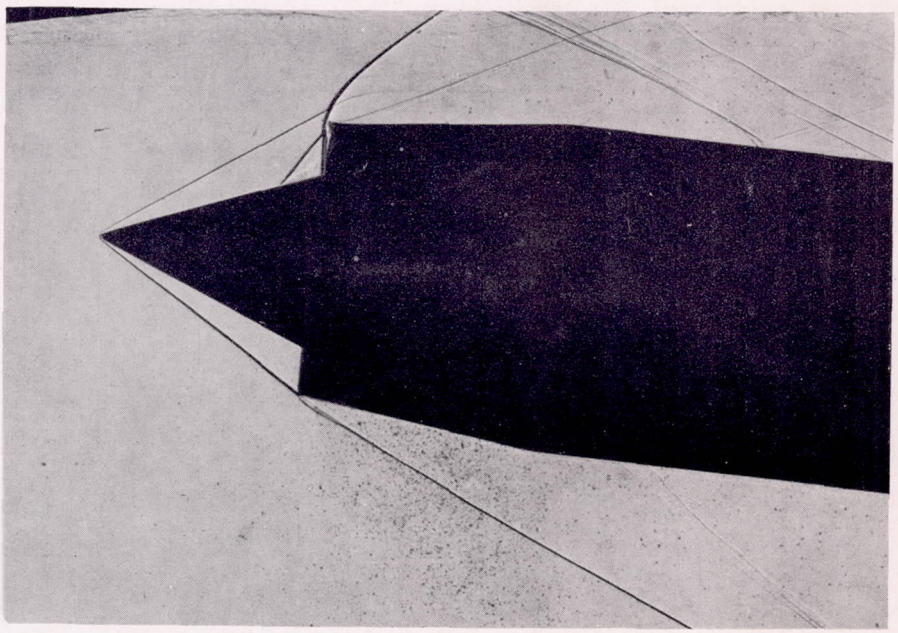

(b) $\alpha = 6^{\circ}$; $\theta_l = 32^{\circ}25'$; $\frac{A_1}{A_2} = 0.95$.

Figure 24.- Shadowgraphs of an inlet having a 22°-1.20 central body and cowling B for the conditions of minimum stable volume flow at $\alpha = 4^{\circ}$ and 6° at M = 2.70.

NACA
L-67993

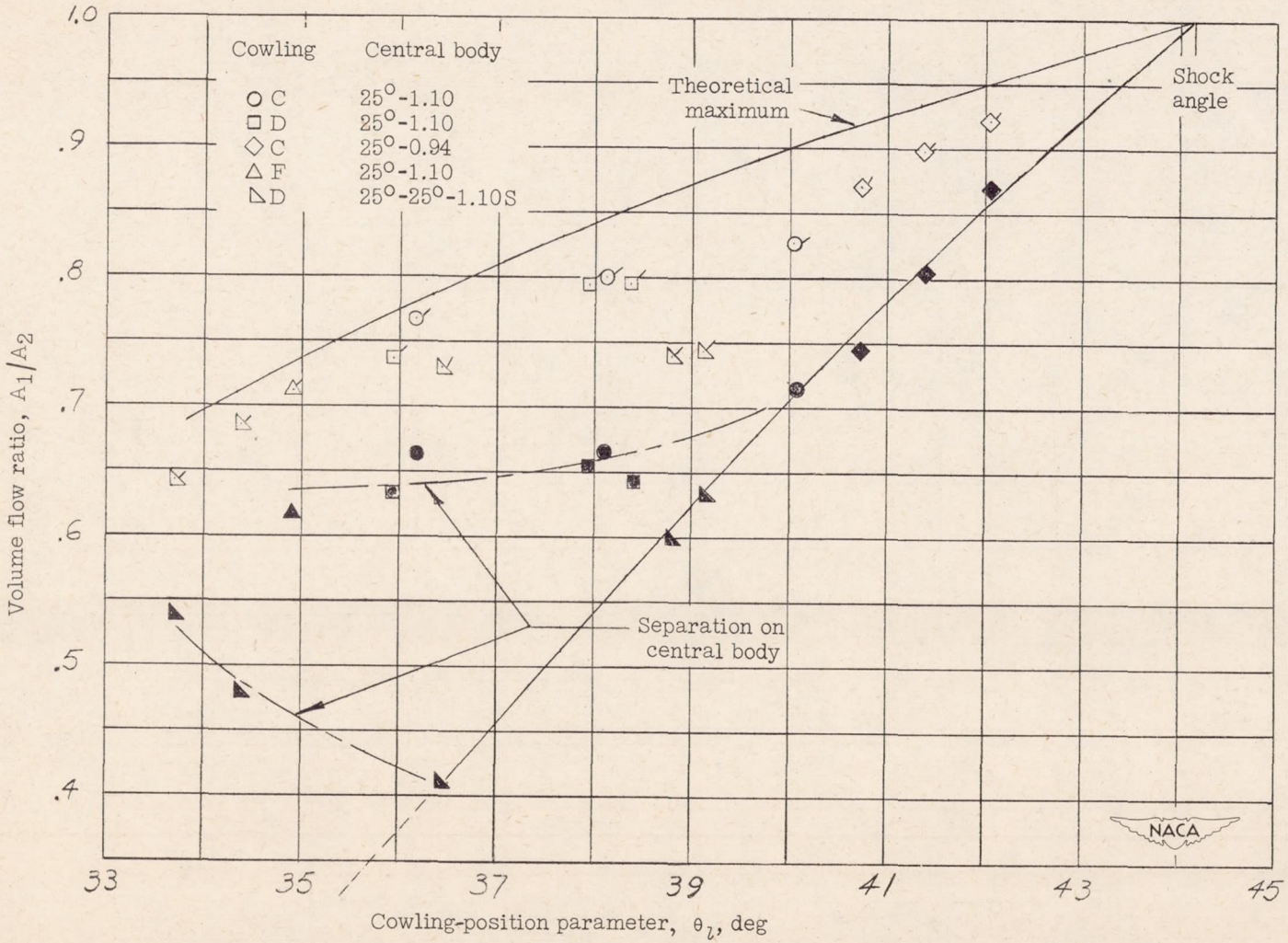

Figure 25.- Volume-flow regulation of inlets having 25° cone-angle central bodies as a function of the cowling-position parameter at M = 1.90.

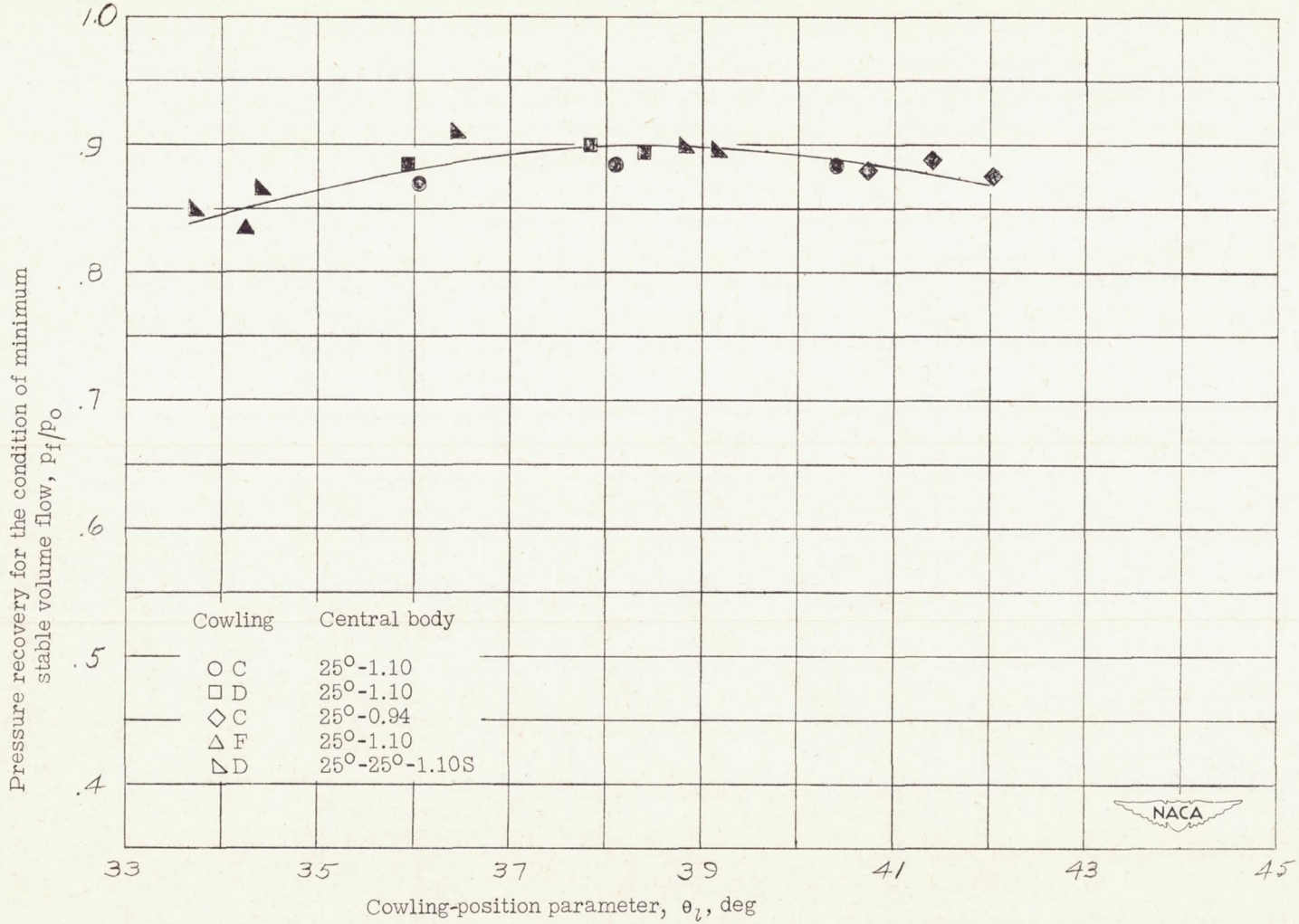

Figure 26.- Pressure recovery of inlets having 25° cone-angle central bodies as a function of the cowling-position parameter at M = 1.90.

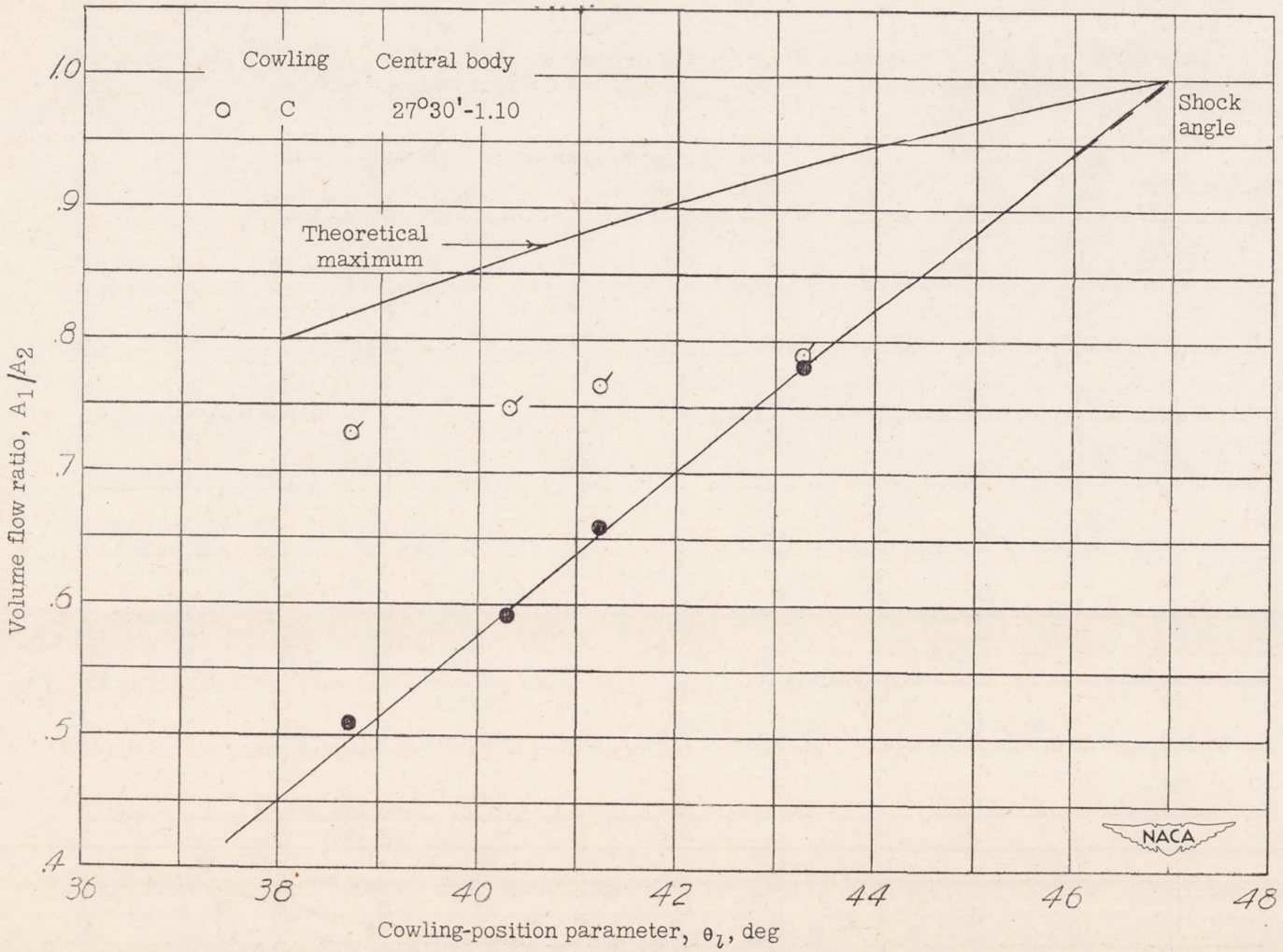

Figure 27.- Volume-flow regulation of inlets having 27°30' cone-angle central bodies as a function of the cowling-position parameter at M = 1.90.

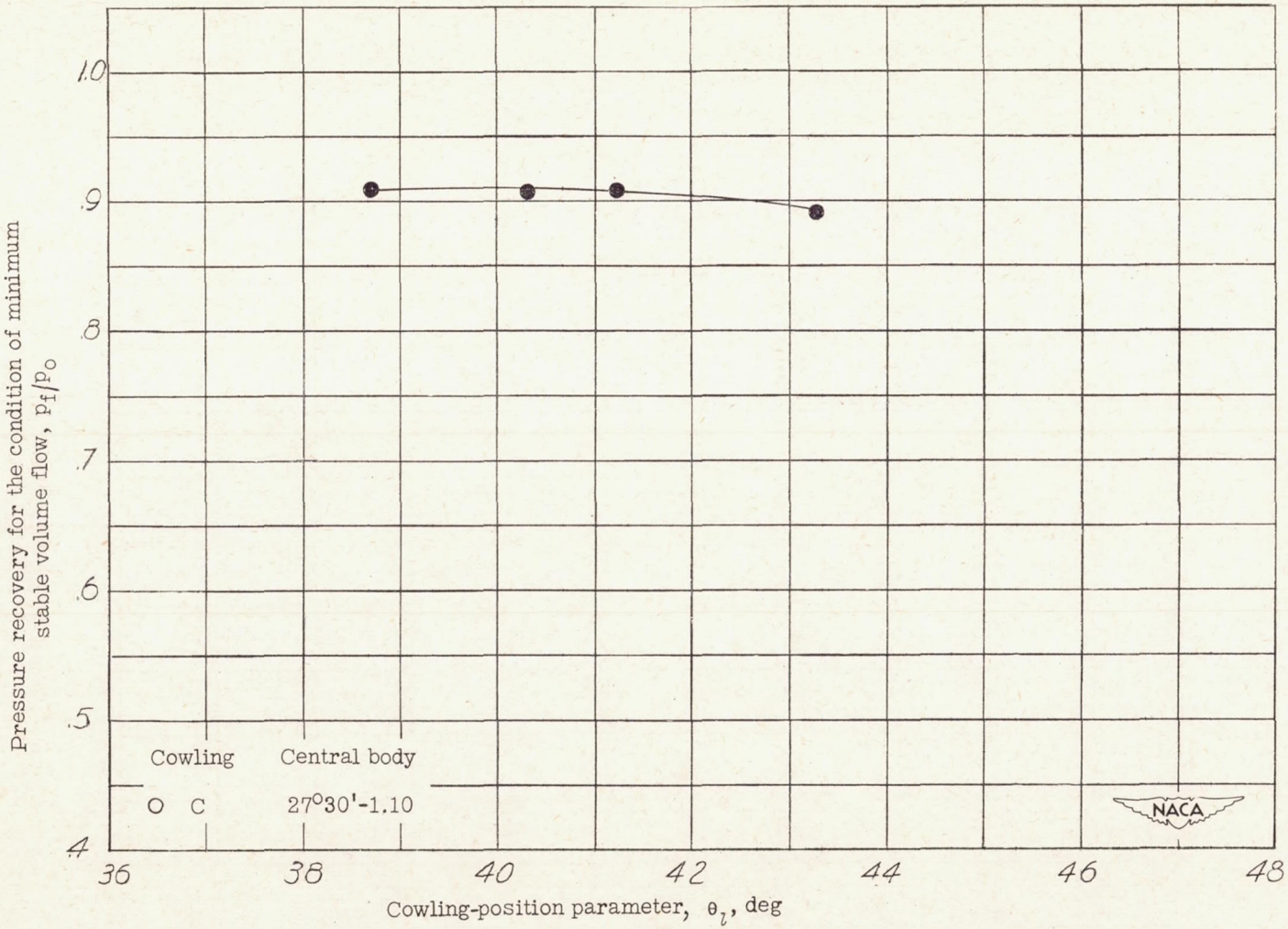

Figure 28.- Pressure recovery of inlets having 27°30' cone-angle central bodies as a function of the cowling-position parameter at M = 1.90.

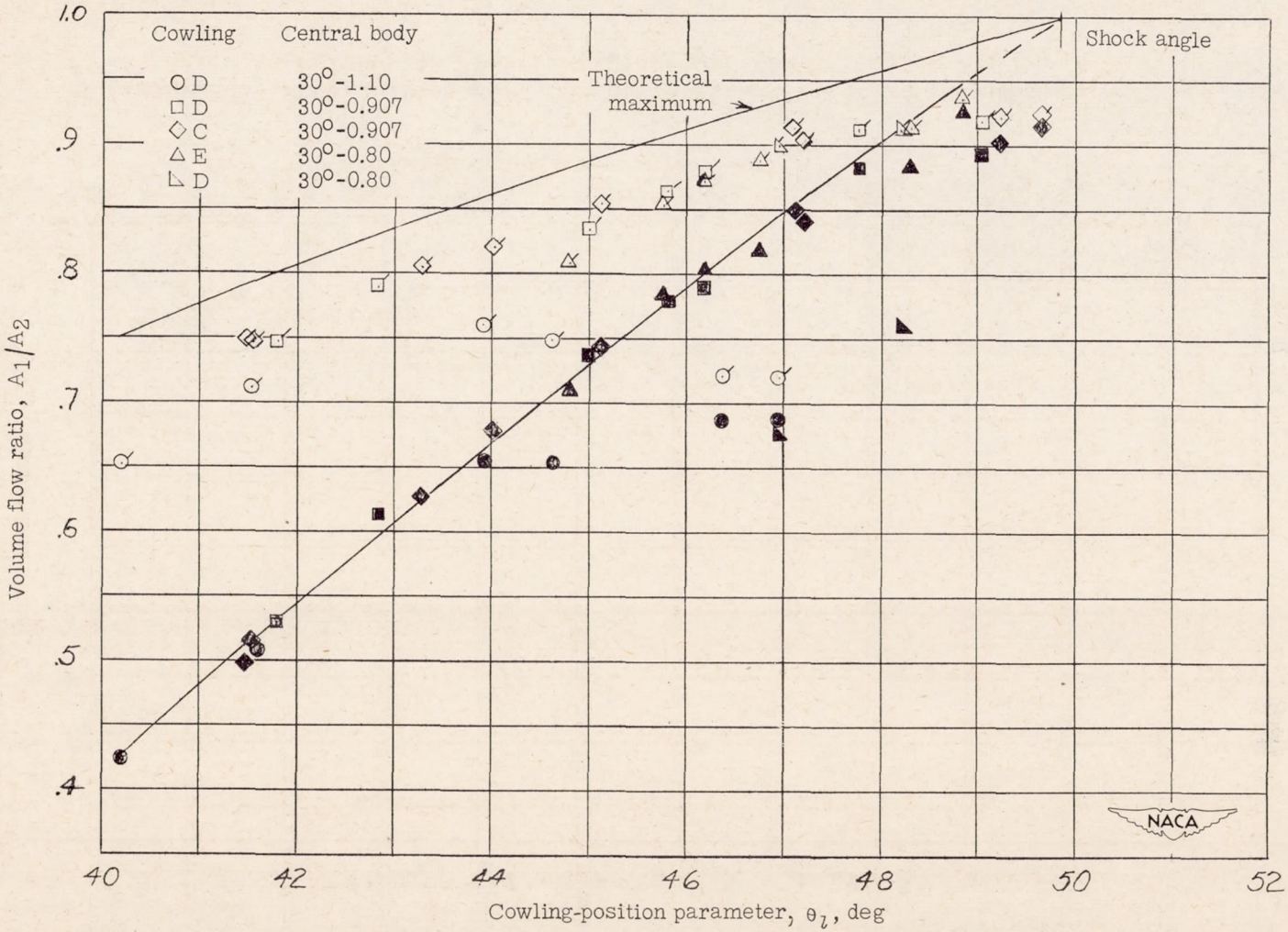

Figure 29.- Volume-flow regulation of inlets having 30° cone-angle central bodies as a function of the cowling-position parameter at M = 1.90.

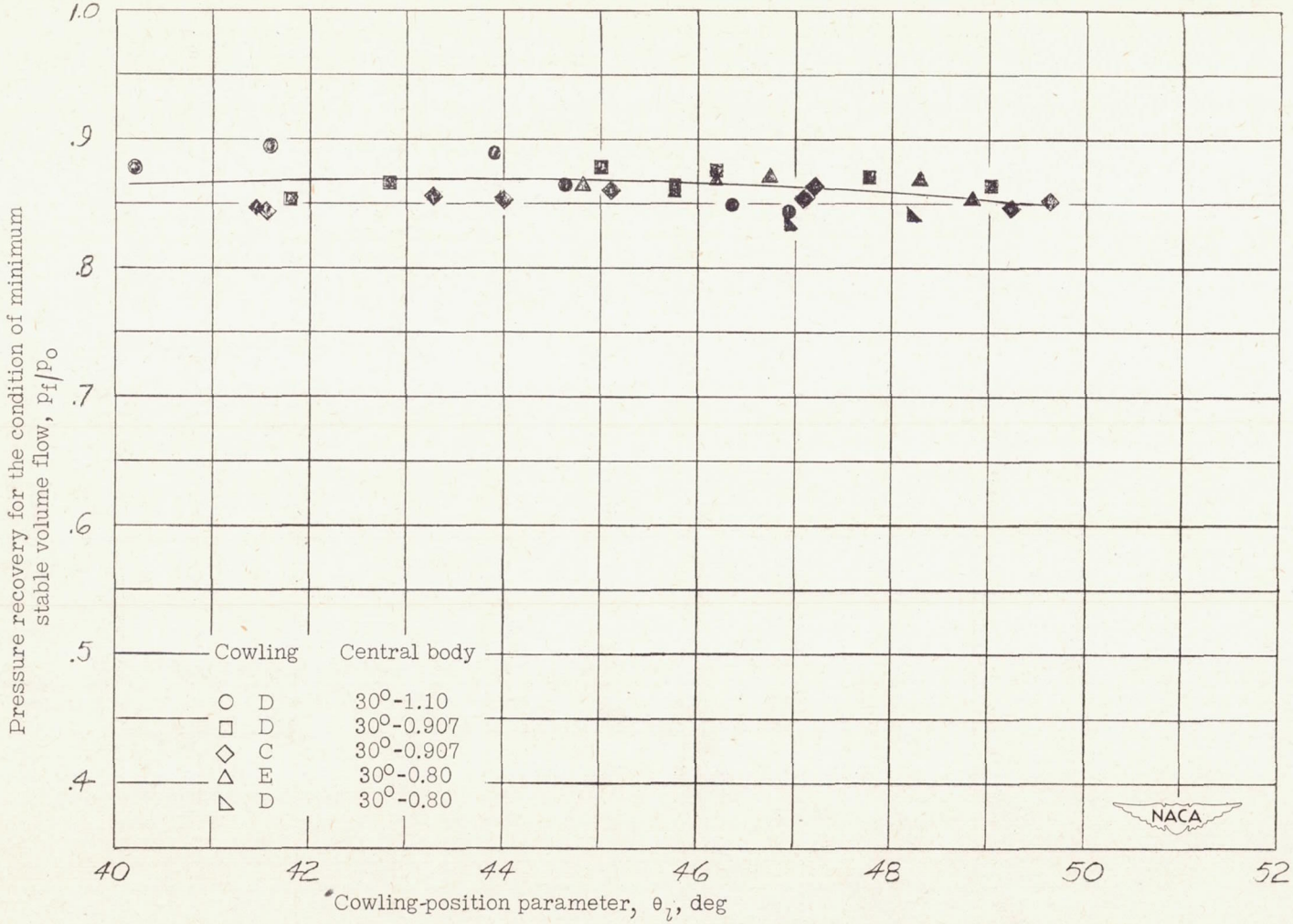

Figure 30.- Pressure recovery of inlets having 30° cone-angle central bodies as a function of the cowling-position parameter at M = 1.90.

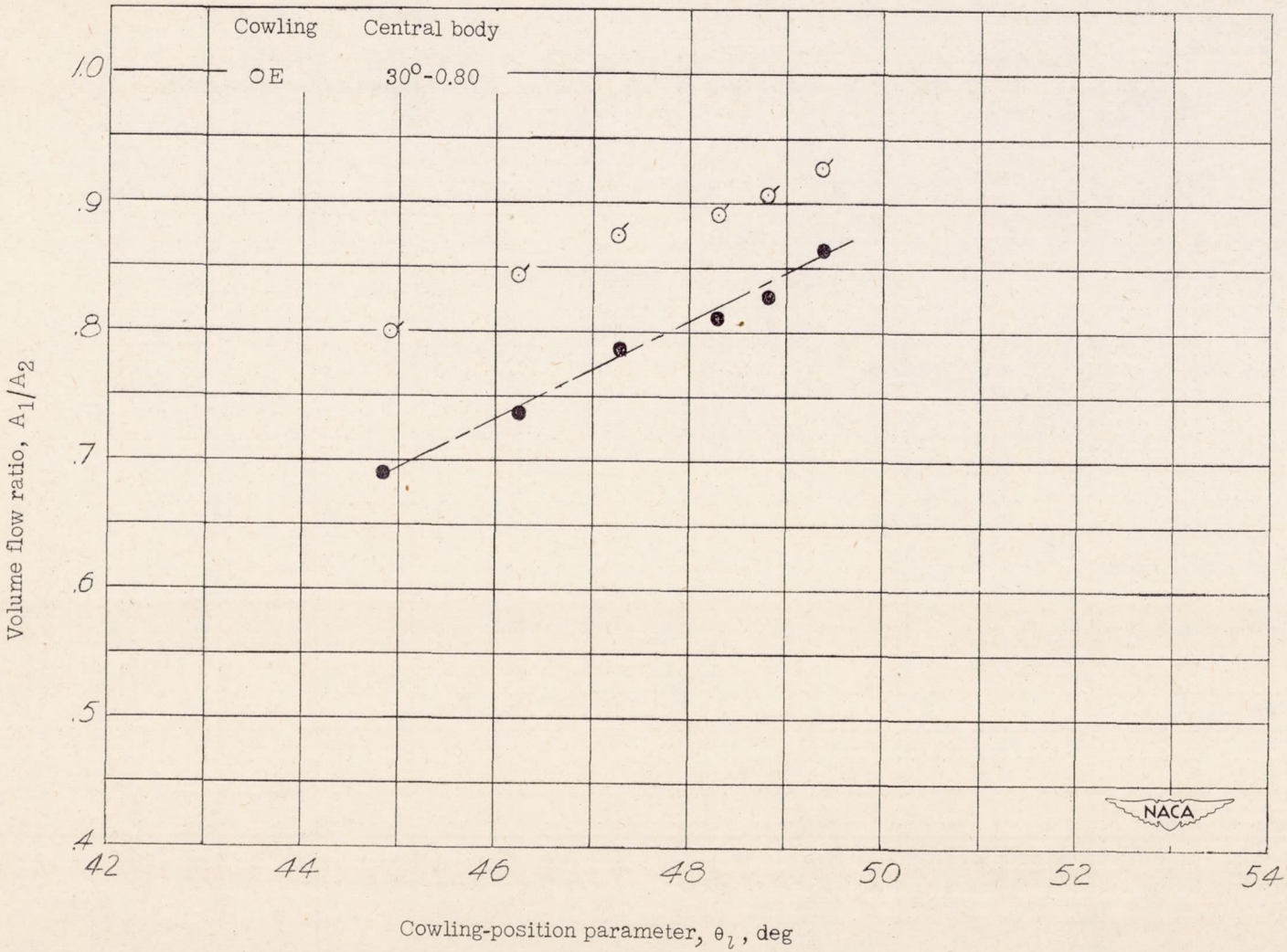

Figure 31.- Volume-flow regulation of inlets having 30° cone-angle central bodies as a function of the cowling-position parameter for $\alpha = 8°30'$ at $M = 1.90$.

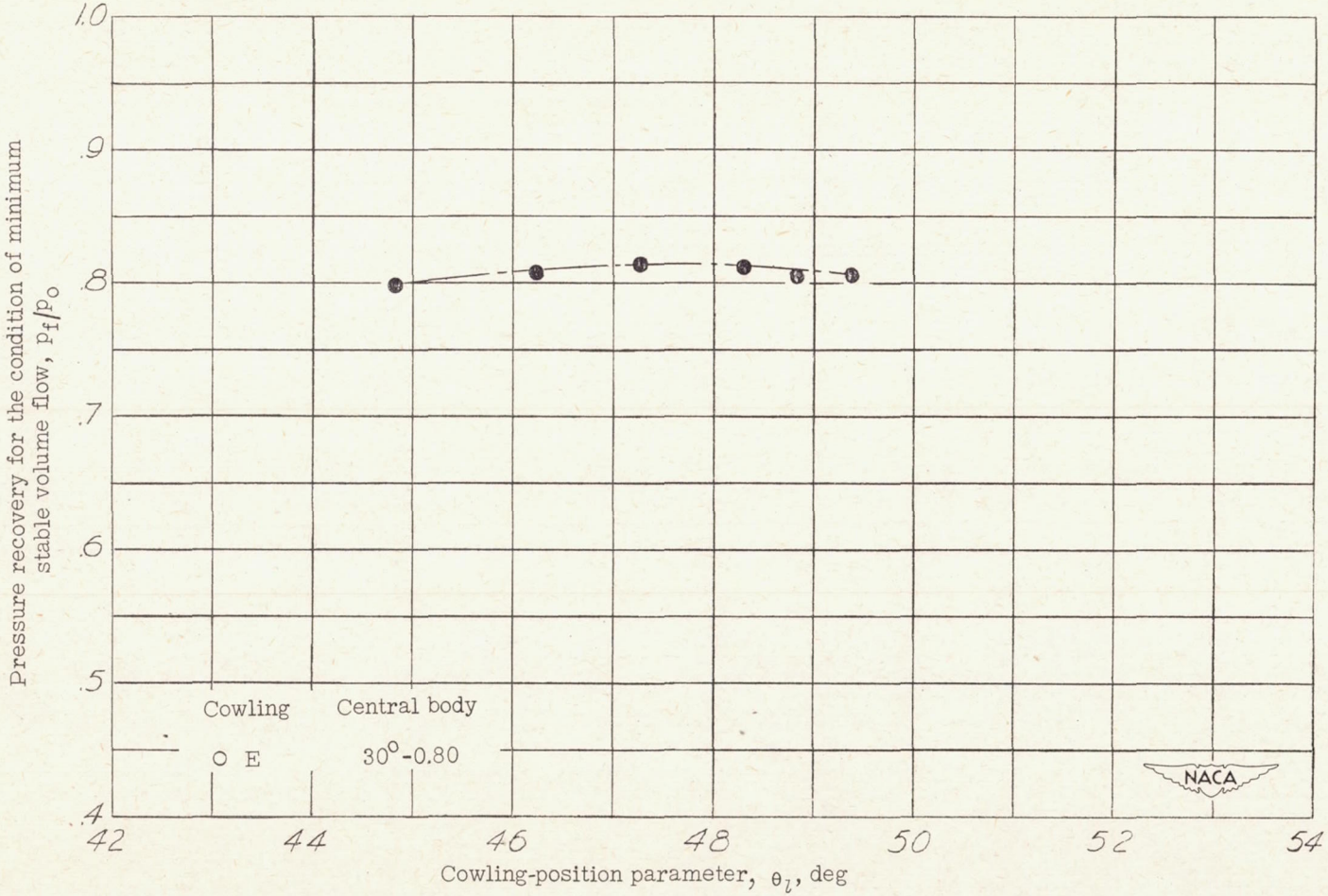

Figure 32.- Pressure recovery of inlets having 30° cone-angle central bodies as a function of the cowling-position parameter for $\alpha = 8°30'$ at $M = 1.90$.

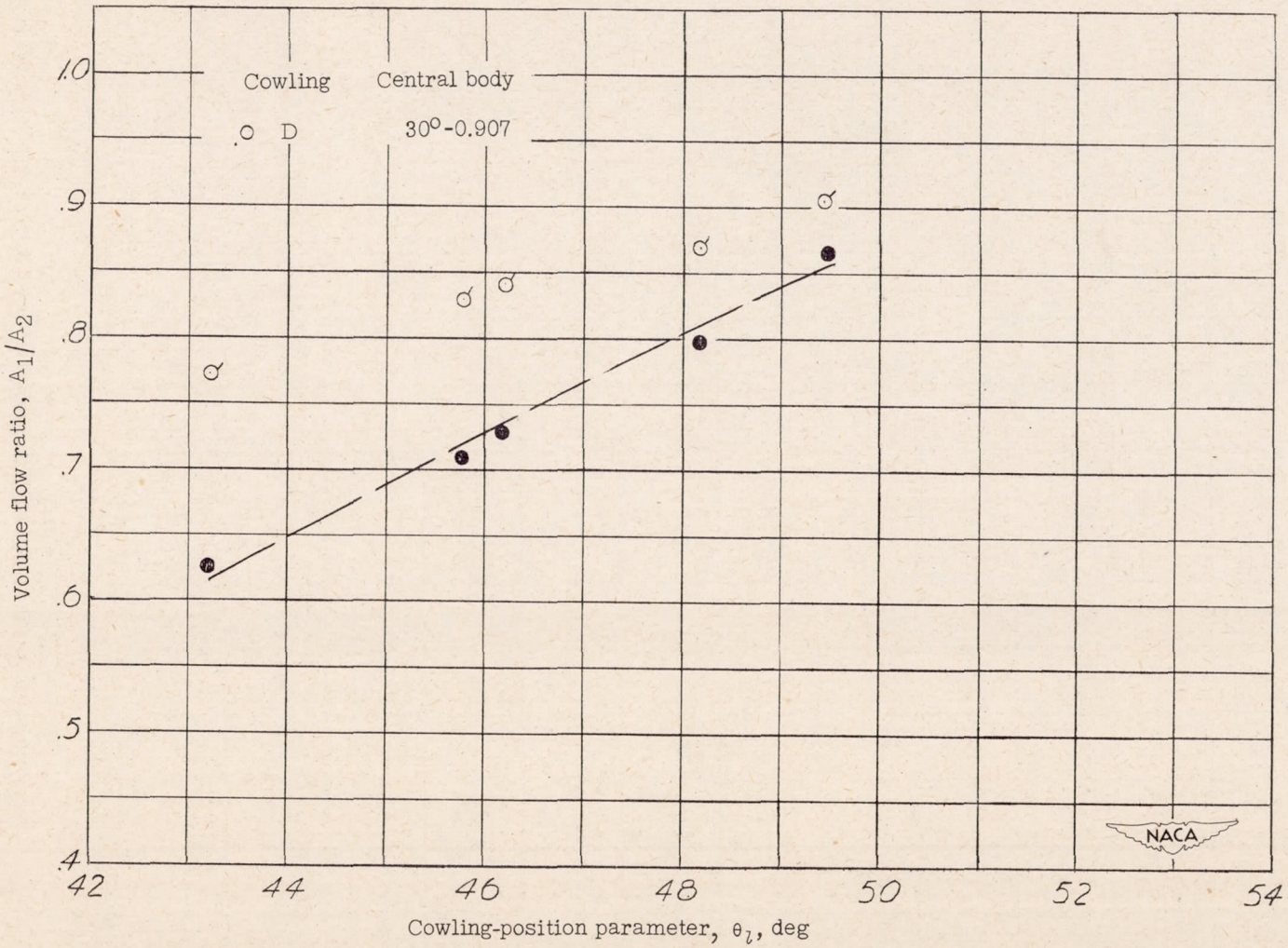

Figure 33.- Volume-flow regulation of inlets having 30° cone-angle central bodies as a function of the cowling-position parameter for $\alpha = 9^\circ$ at M = 1.90.

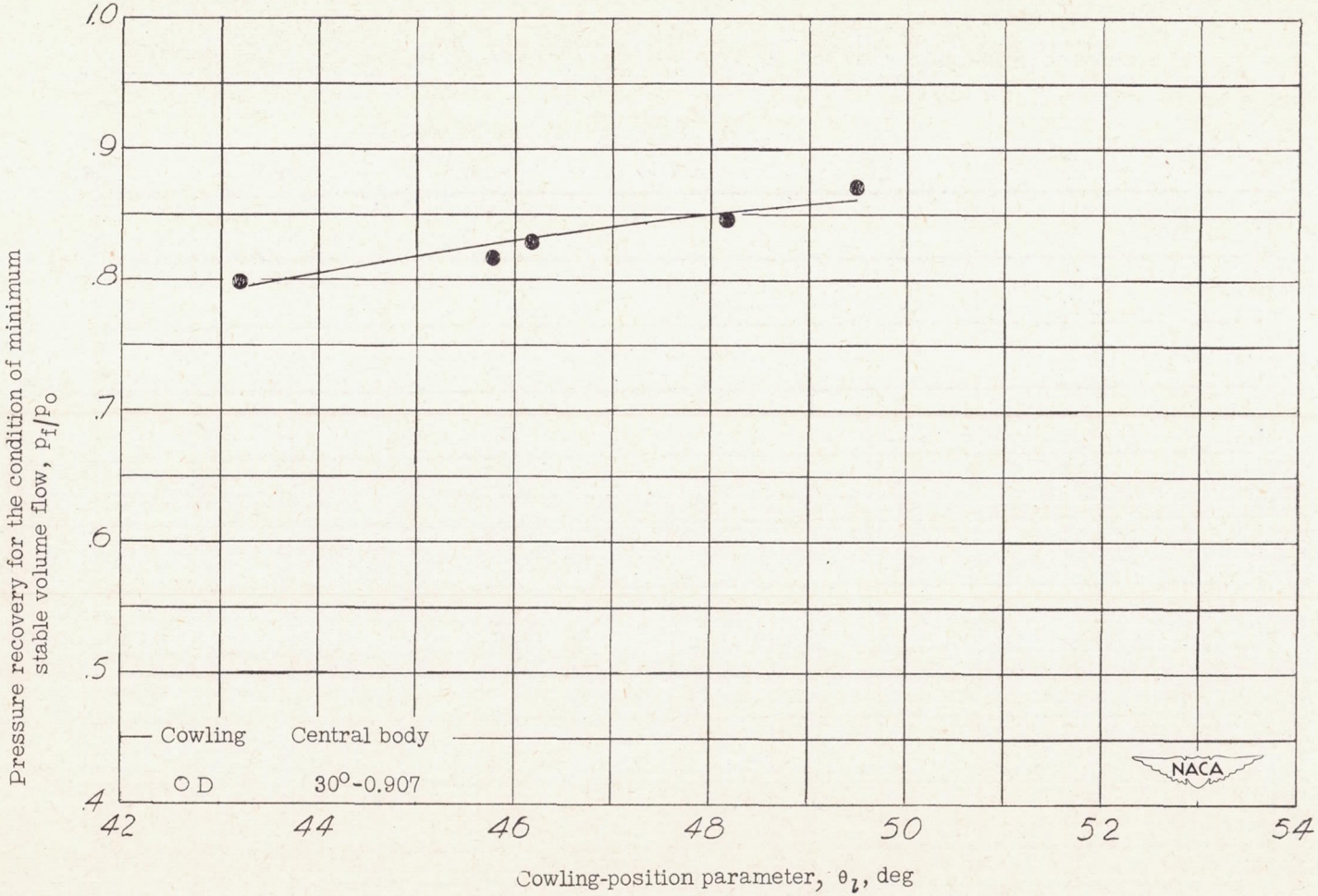

Figure 34.- Pressure recovery of inlets having 30° cone-angle central bodies as a function of the cowling-position parameter for $\alpha = 9°$ at $M = 1.90$.

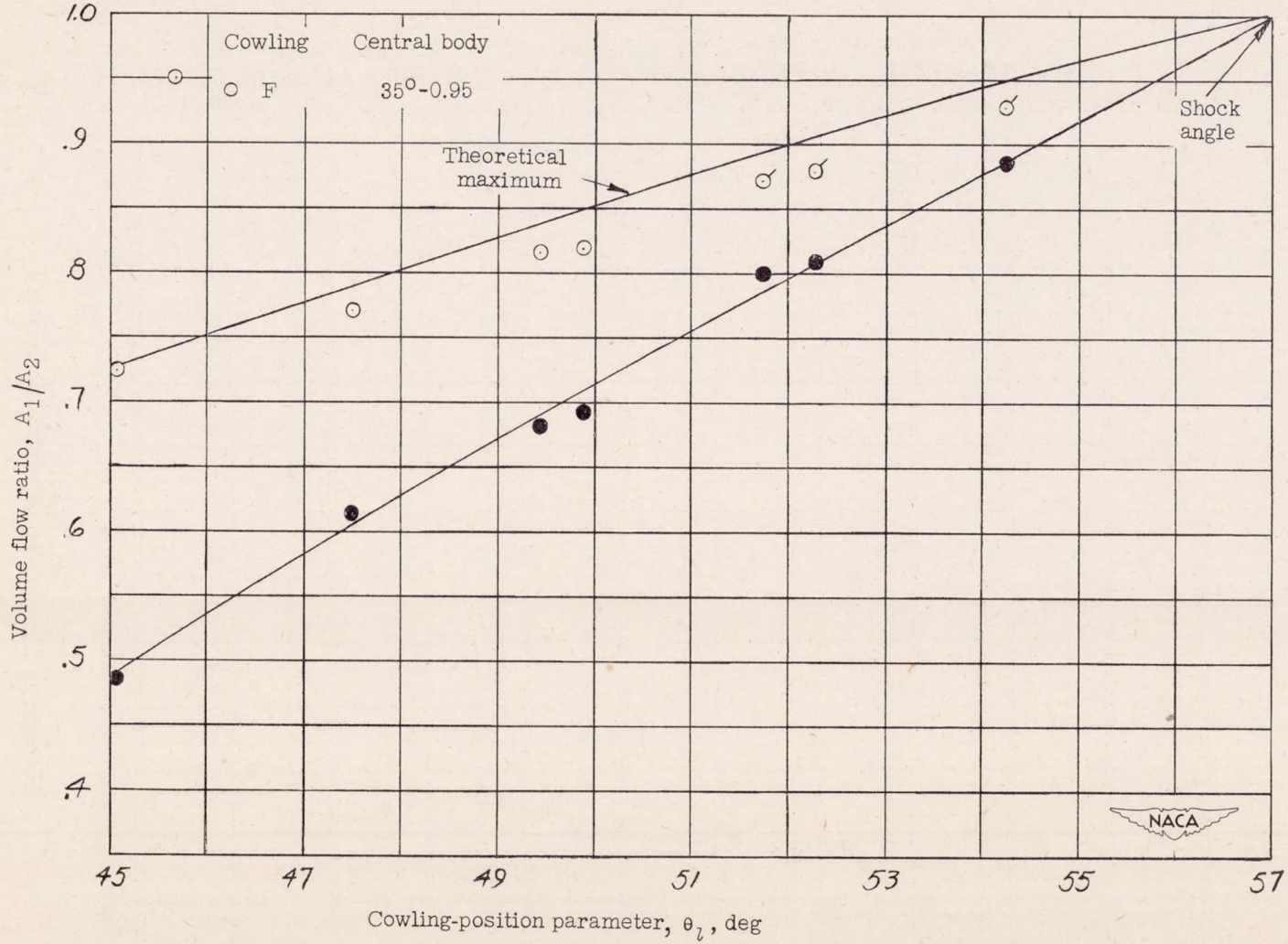

Figure 35.- Volume-flow regulation of inlets having 35° cone-angle central bodies as a function of the cowling-position parameter at M = 1.90.

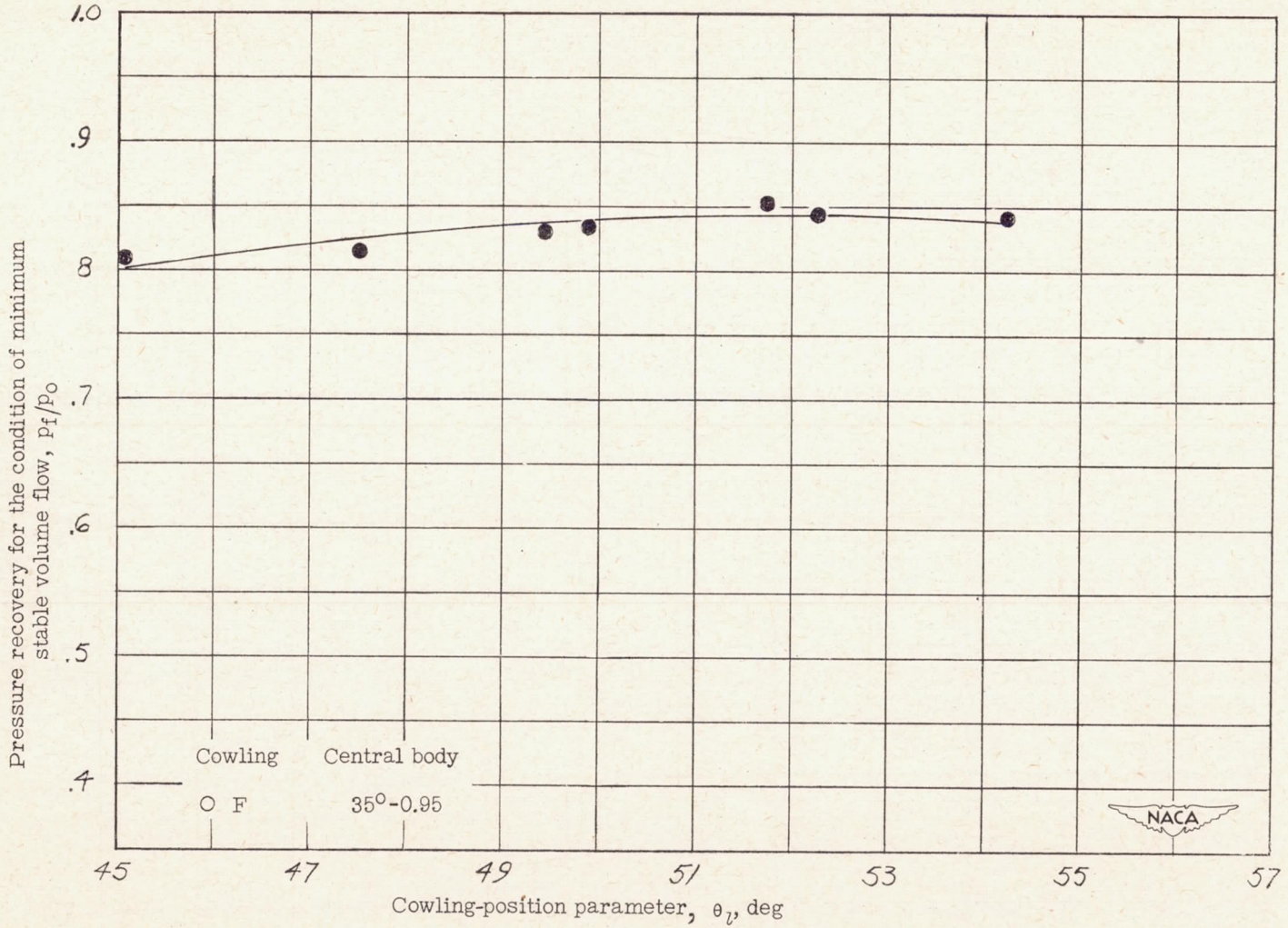

Figure 36.- Pressure recovery of inlets having 35° cone-angle central bodies as a function of the cowling-position parameter at M = 1.90.

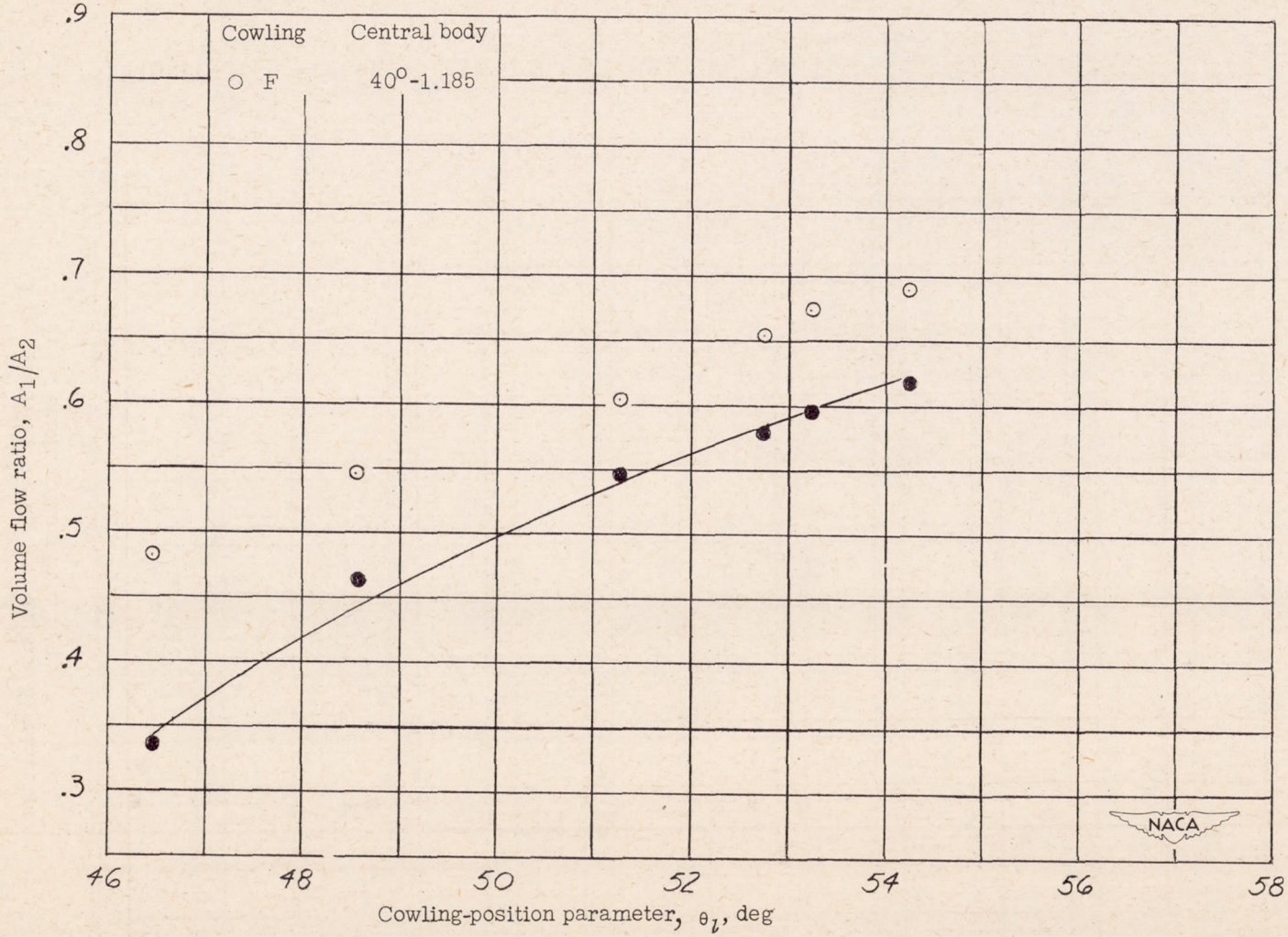

Figure 37.- Volume-flow regulation of inlets having 40° cone-angle central bodies as a function of the cowling-position parameter at M = 1.90.

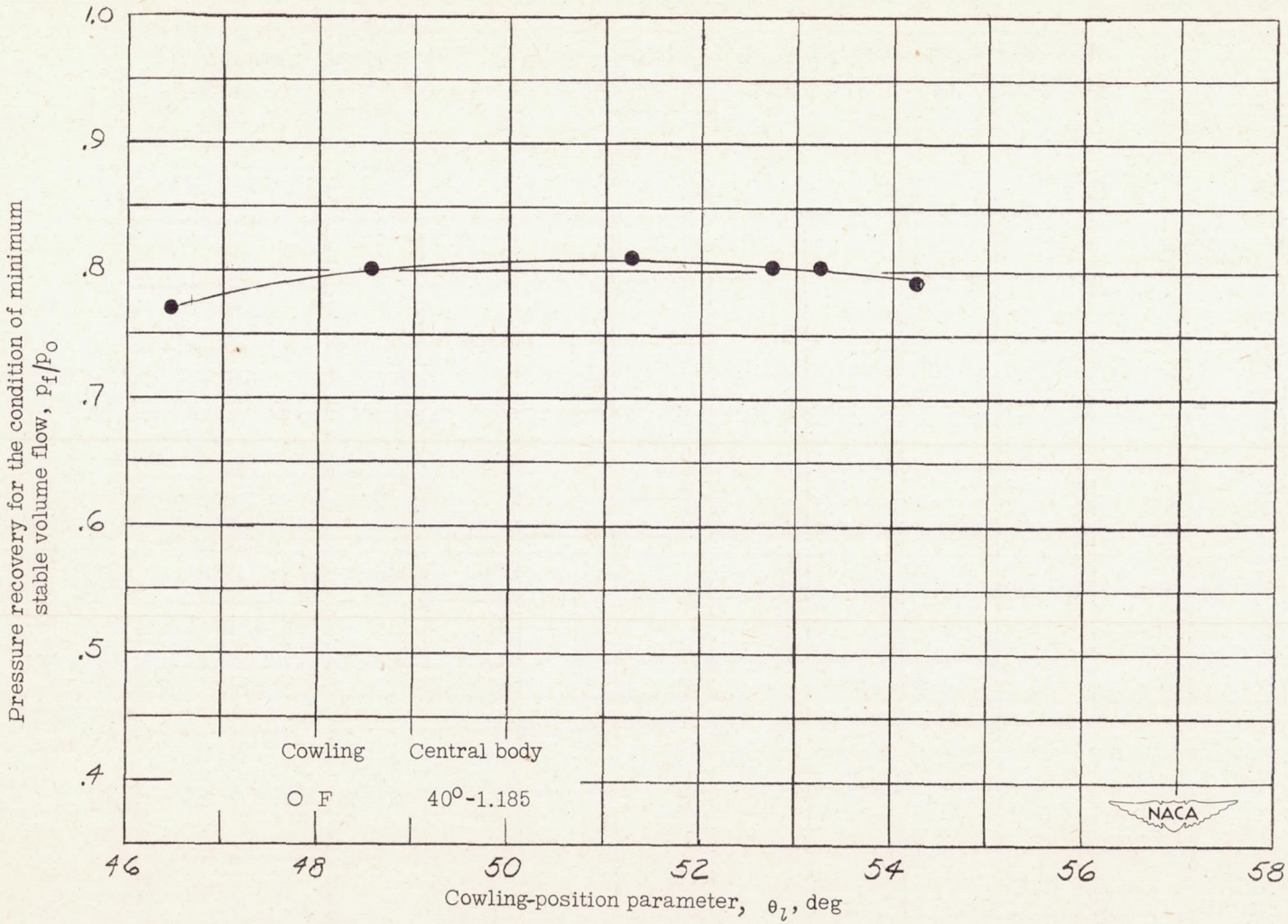

Figure 38.- Pressure recovery of inlets having 40° cone-angle central bodies as a function of the cowling-position parameter at M = 1.90.

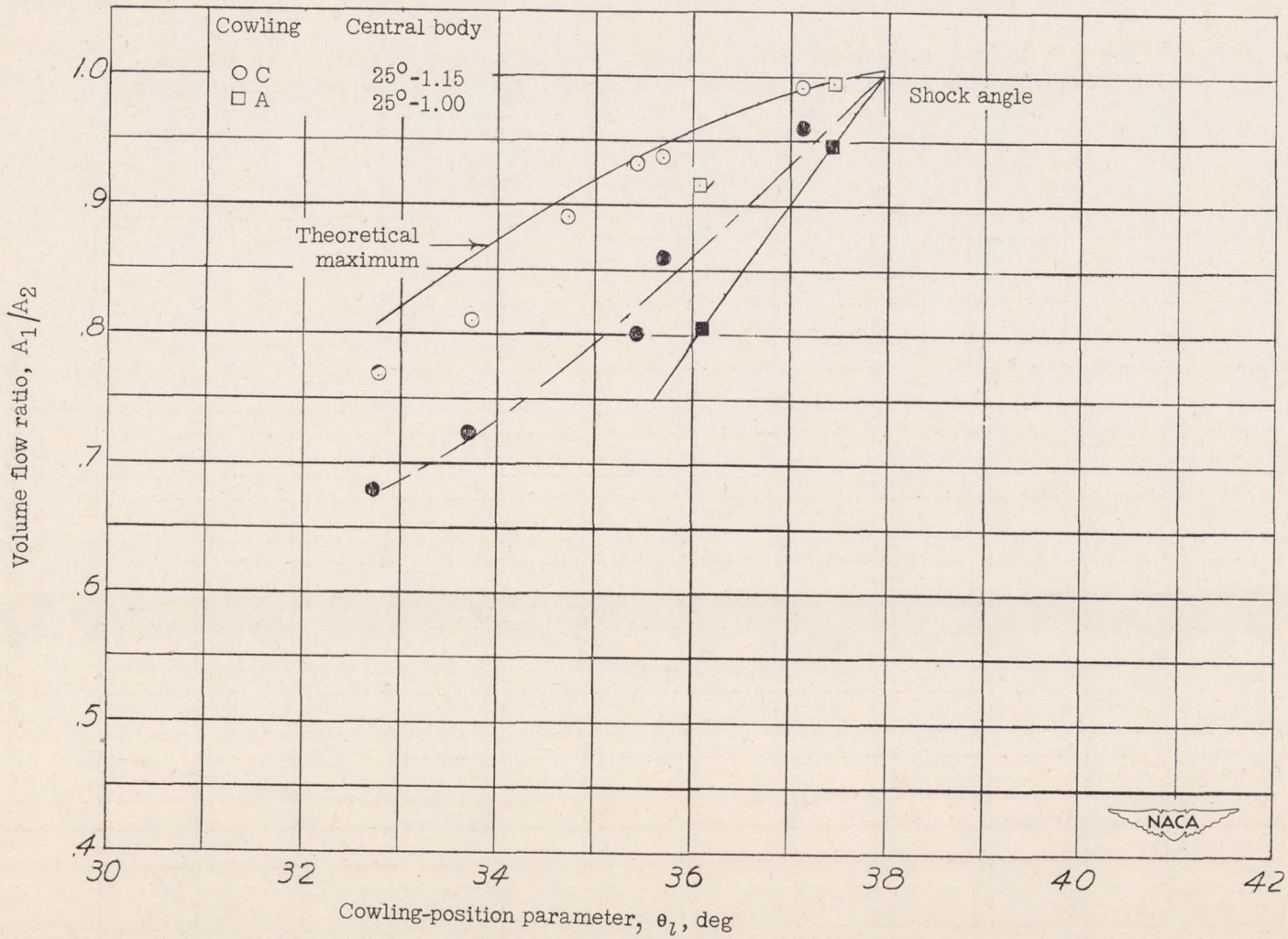

Figure 39.- Volume-flow regulation of inlets having 25° cone-angle central bodies as a function of the cowling-position parameter at M = 2.46.

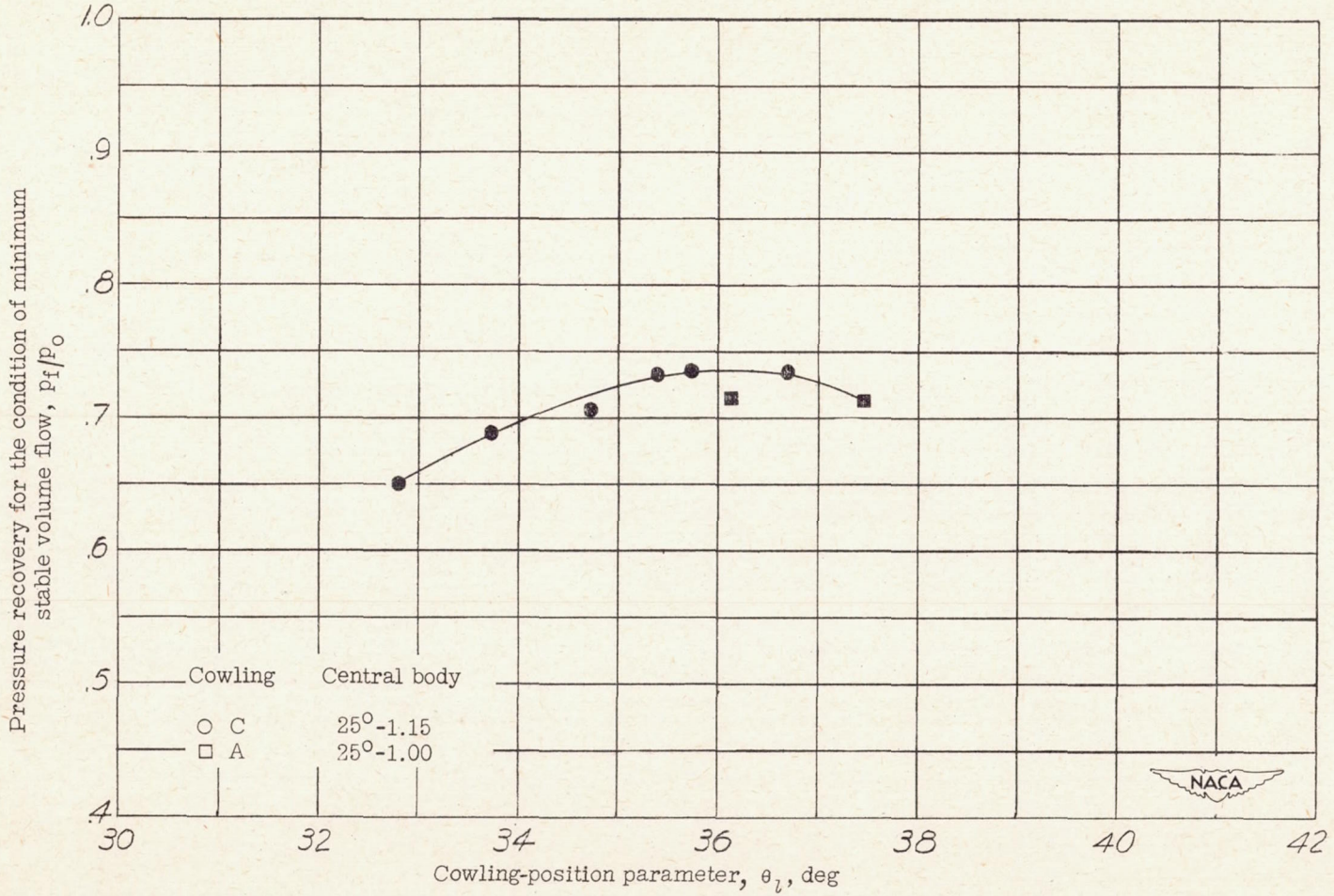

Figure 40.- Pressure recovery of the inlets having 25° cone-angle central bodies as a function of the cowling-position parameter at M = 2.46.

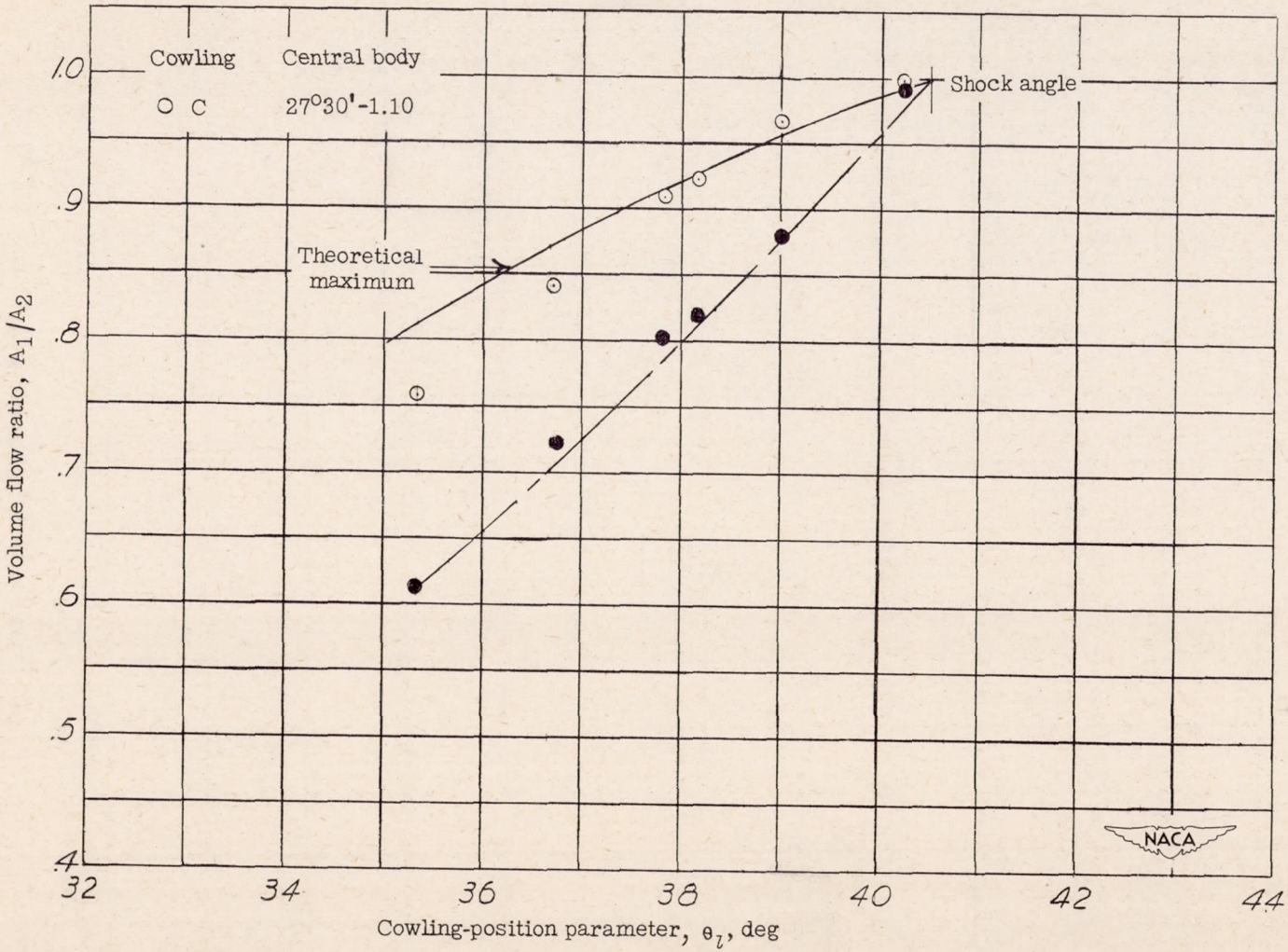

Figure 41.- Volume-flow regulation of inlets having 27°30' cone-angle central bodies as a function of the cowling-position parameter at M = 2.46.

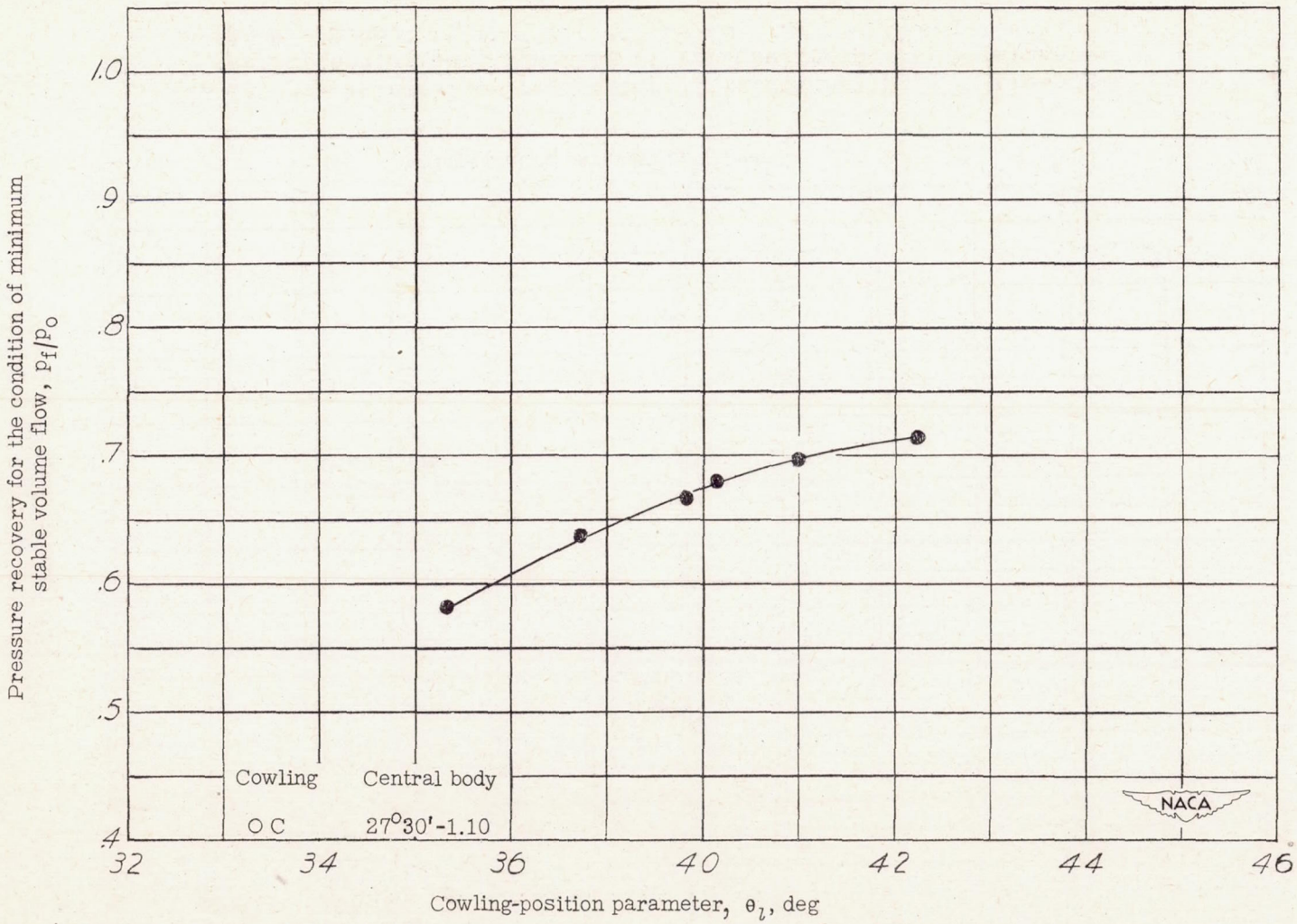

Figure 42.- Pressure recovery of the inlets having 27°30' cone-angle central bodies as a function of the cowling-position parameter at M = 2.46.

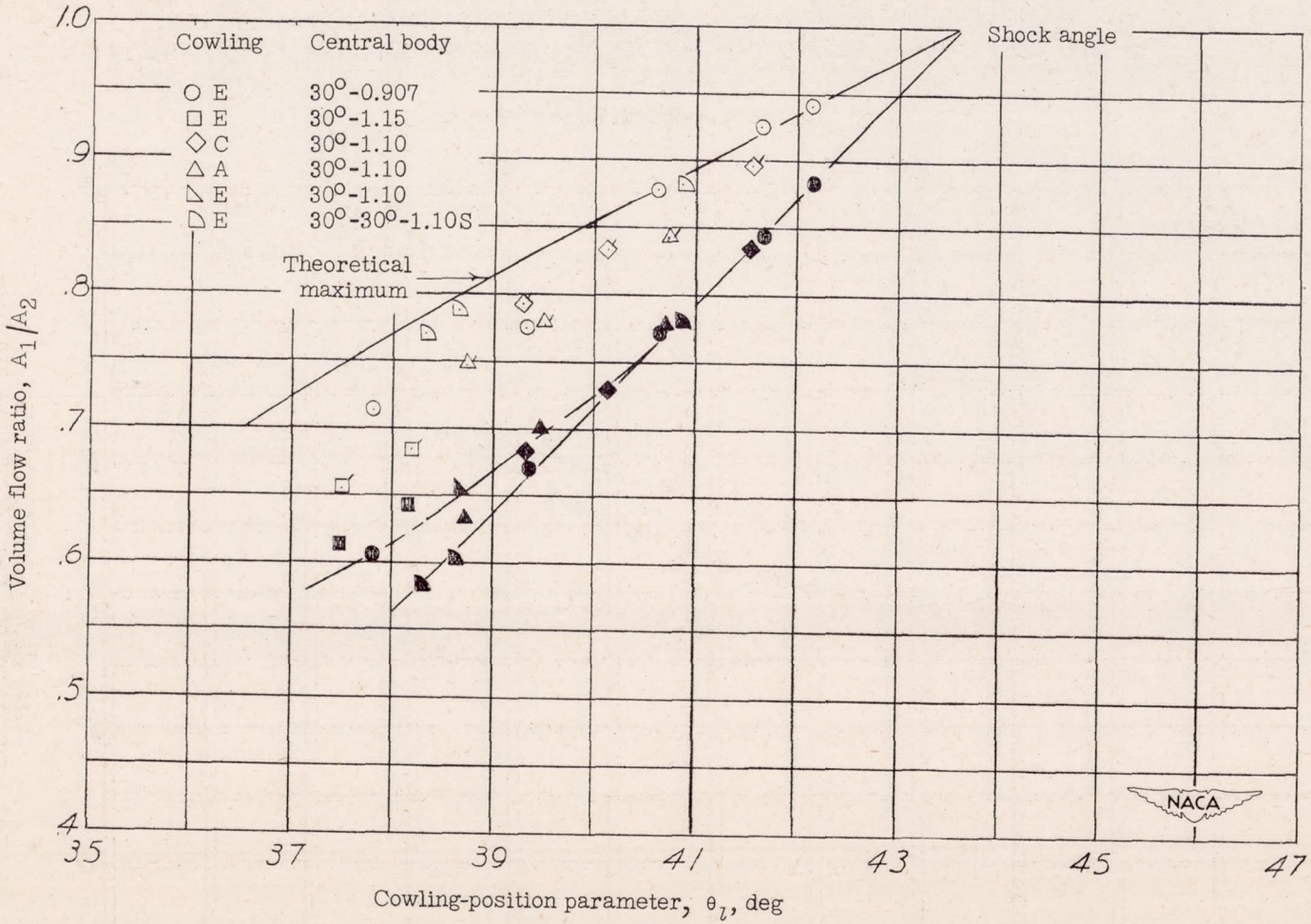

Figure 43.- Volume-flow regulation of inlets having 30° cone-angle central bodies as a function of the cowling-position parameter at M = 2.46.

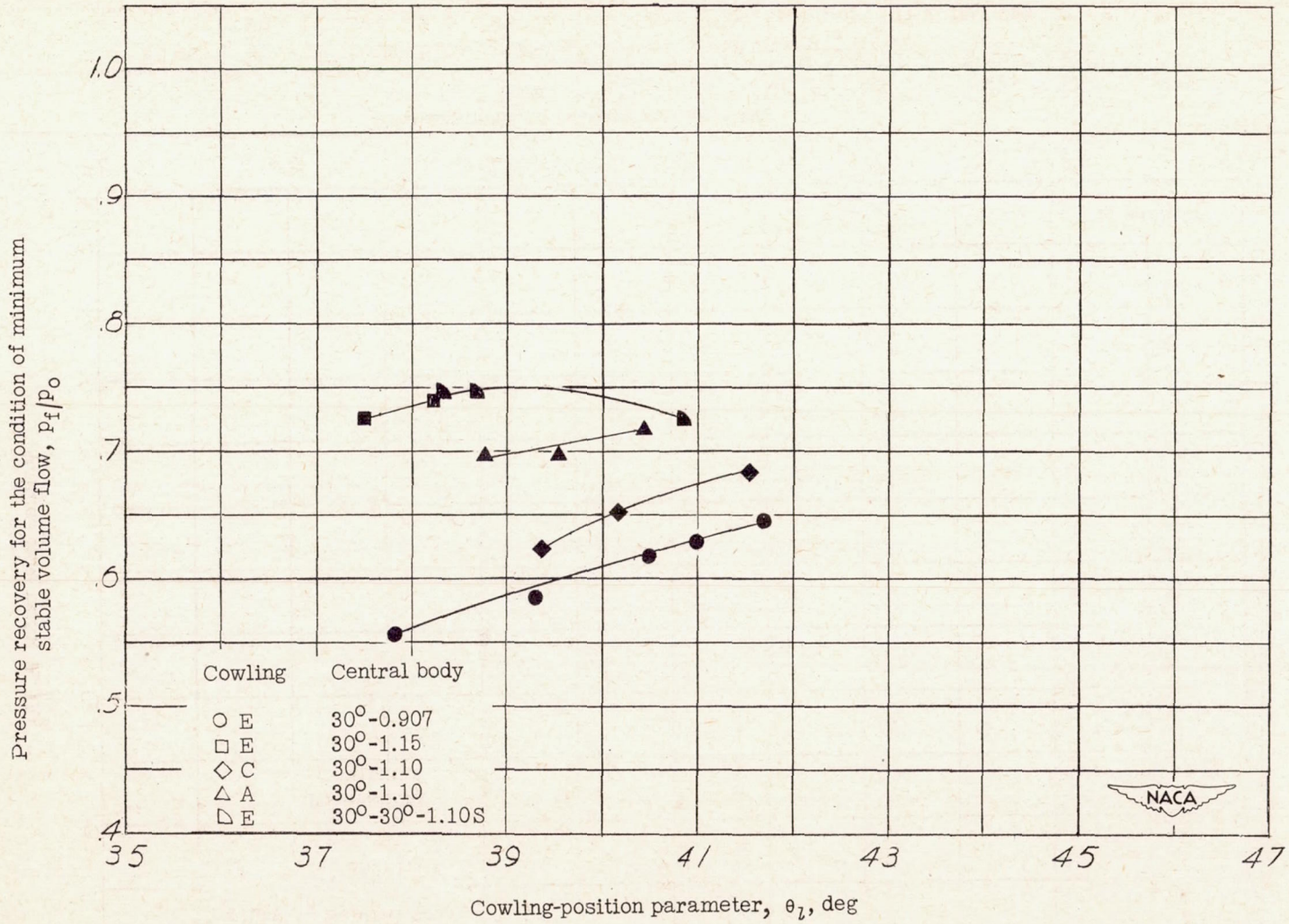

Figure 44.- Pressure recovery of inlets having 30° cone-angle central bodies as a function of the cowling-position parameter at M = 2.46.

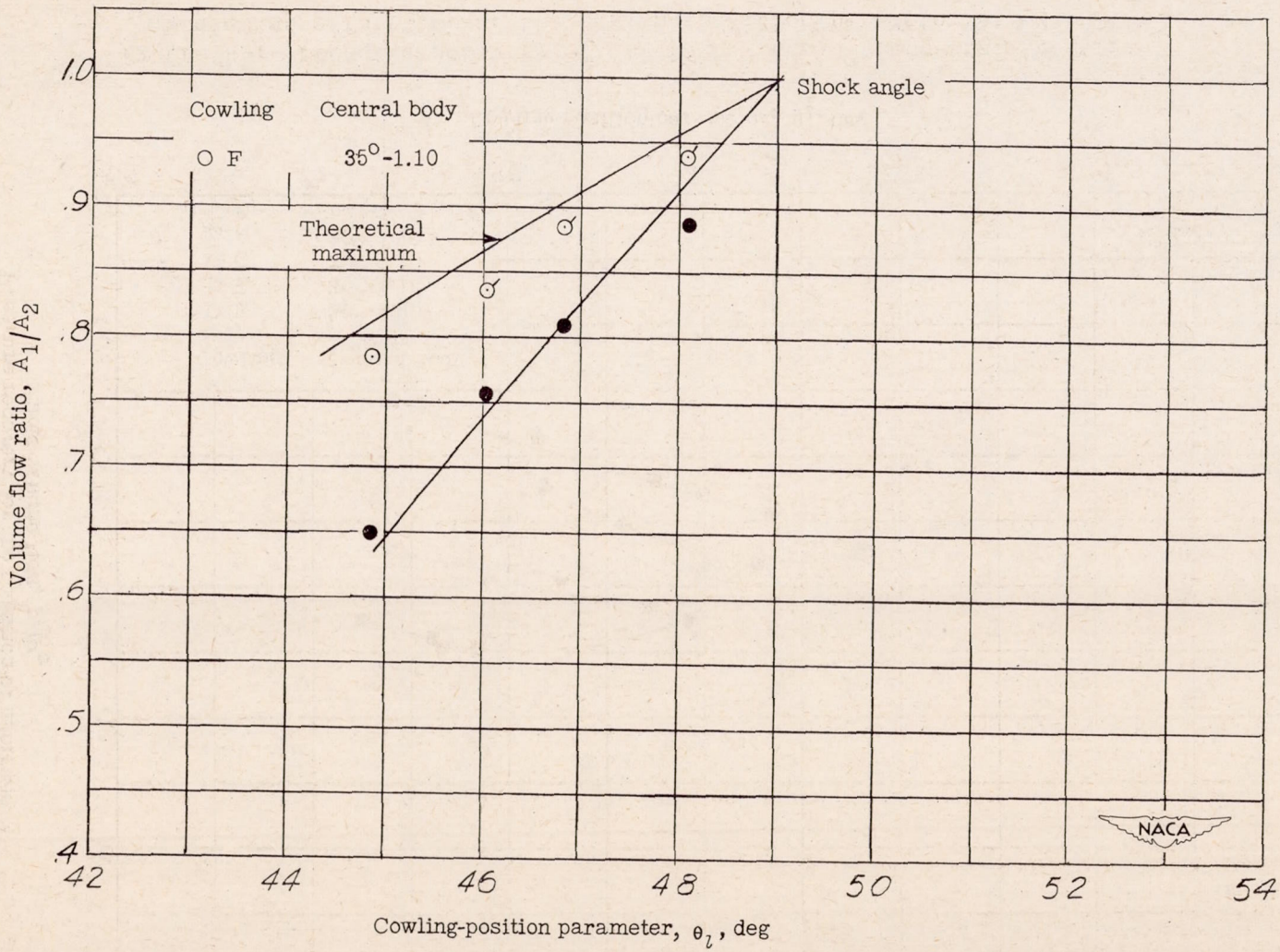

Figure 45.- Volume-flow regulation of inlets having 35° cone-angle central bodies as a function of the cowling-position parameter at M = 2.46.

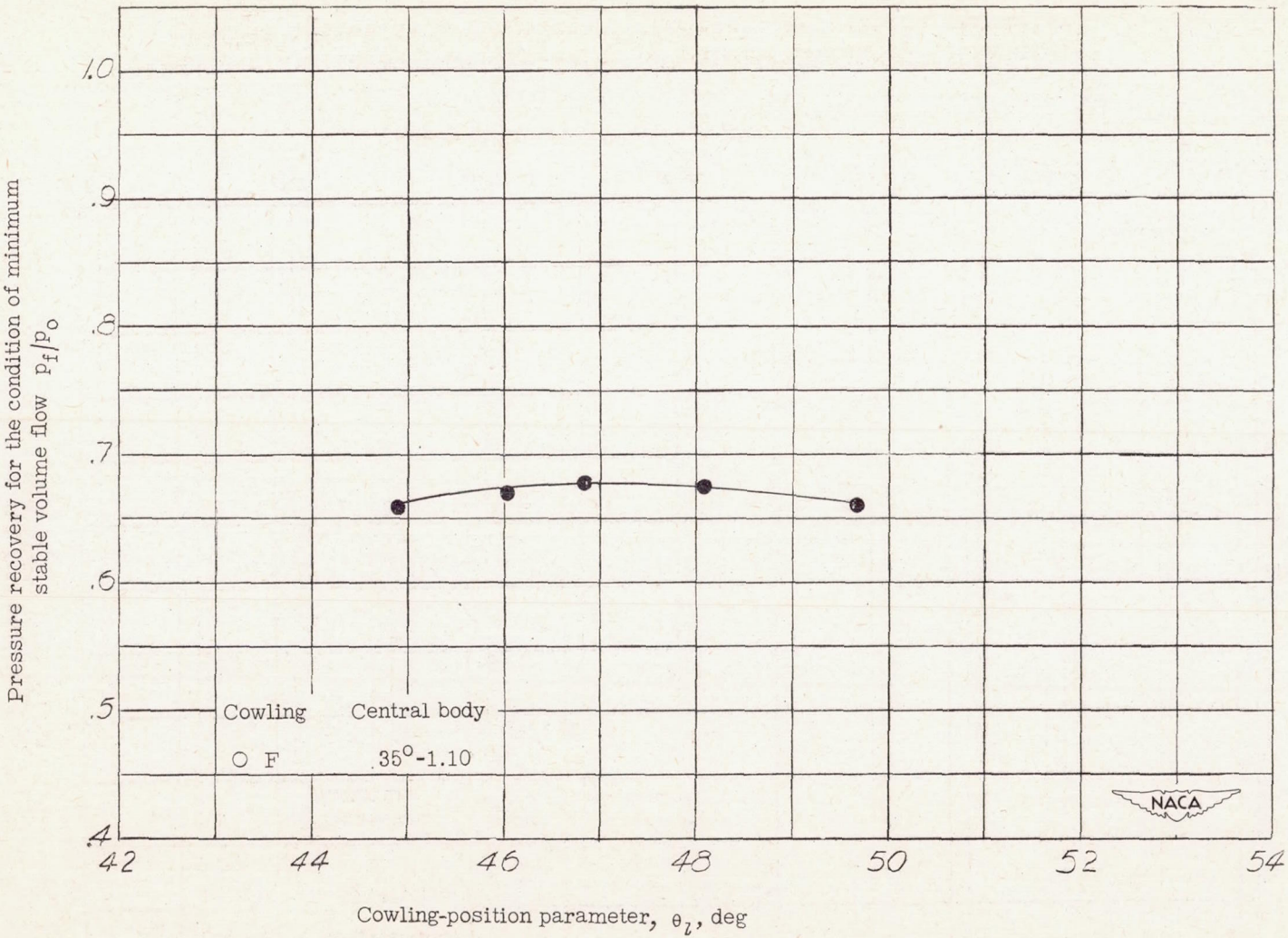

Figure 46.- Pressure recovery of inlets having 35° cone-angle central bodies as a function of the cowling-position parameter at M = 2.46.

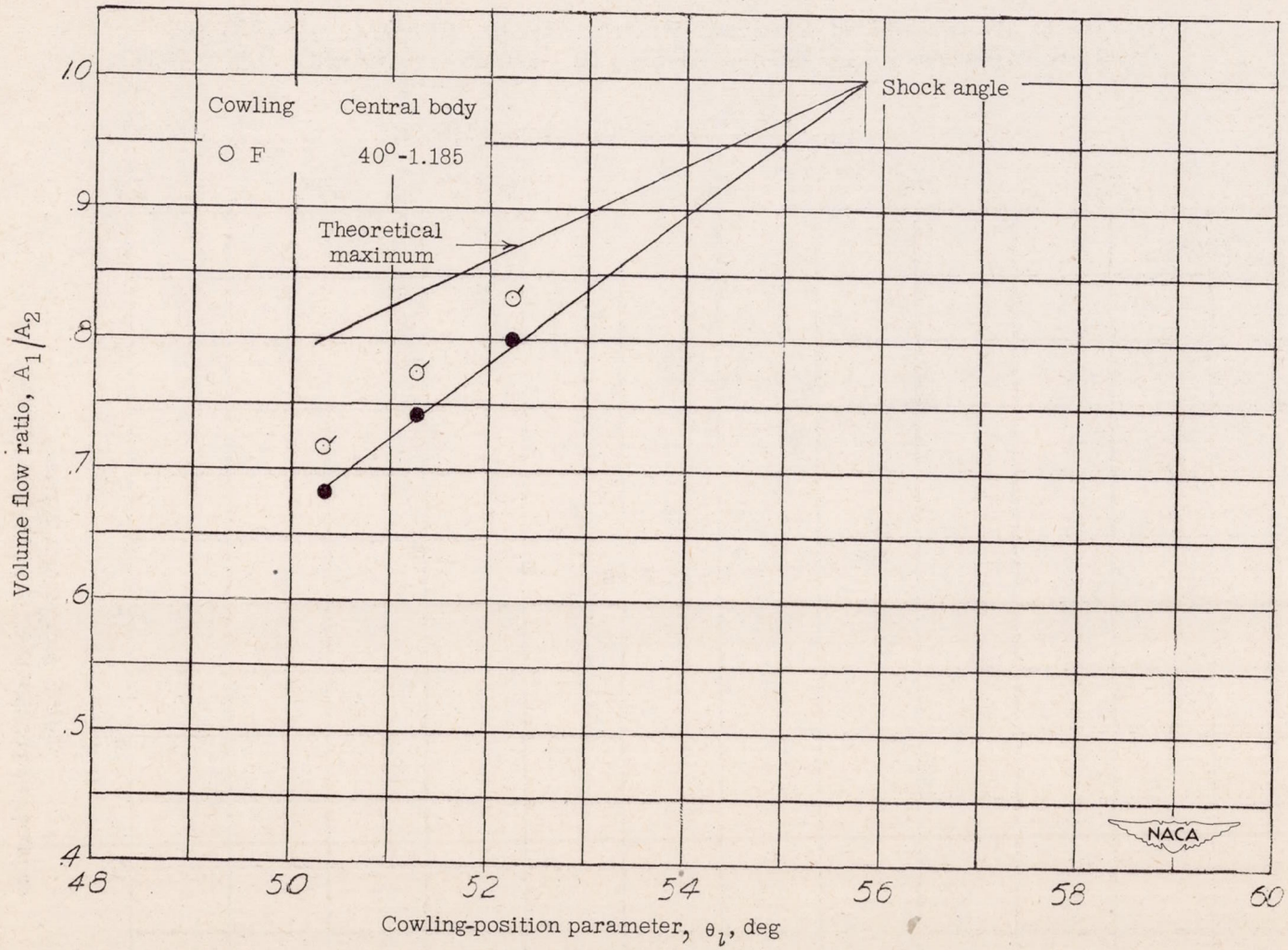

Figure 47.- Volume-flow regulation of inlets having 40° cone-angle central bodies as a function of the cowling-position parameter at M = 2.46.

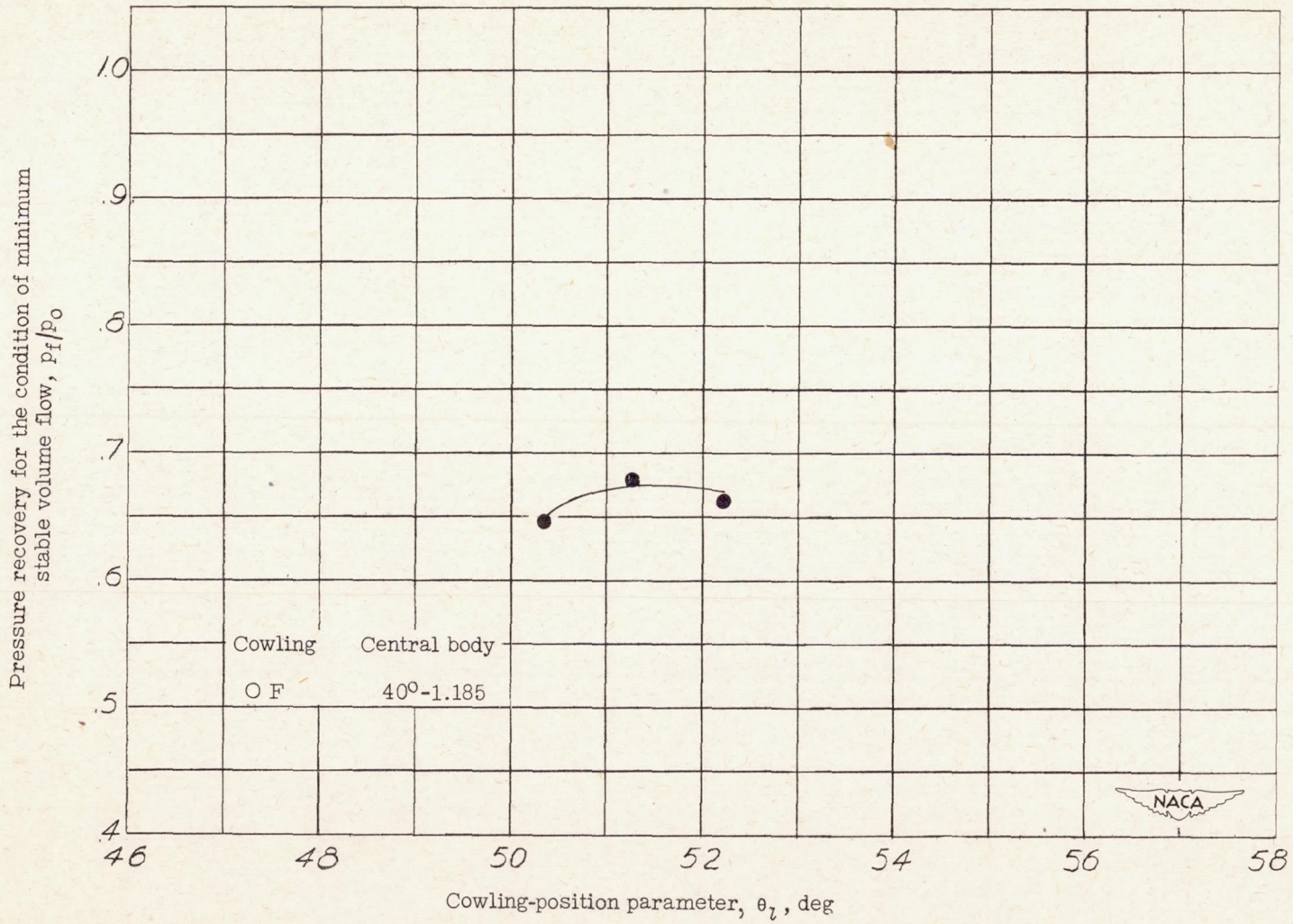

Figure 48.- Pressure recovery of inlets having 40° cone-angle central bodies as a function of the cowling-position parameter at M = 2.46.

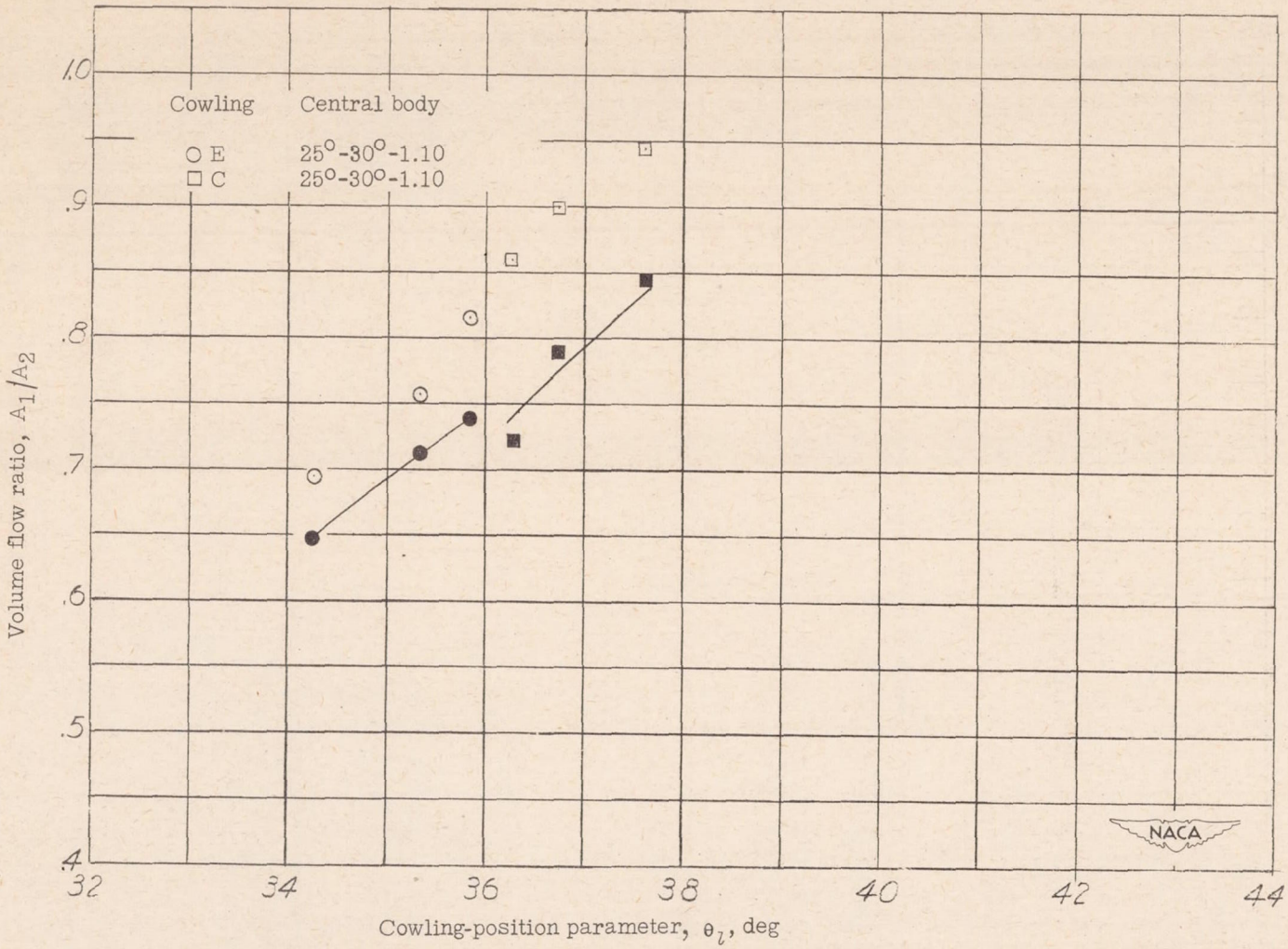

Figure 49.- Volume-flow regulation of inlets having 25°-30°-1.10 central body as a function of the cowling-position parameter at M = 2.46.

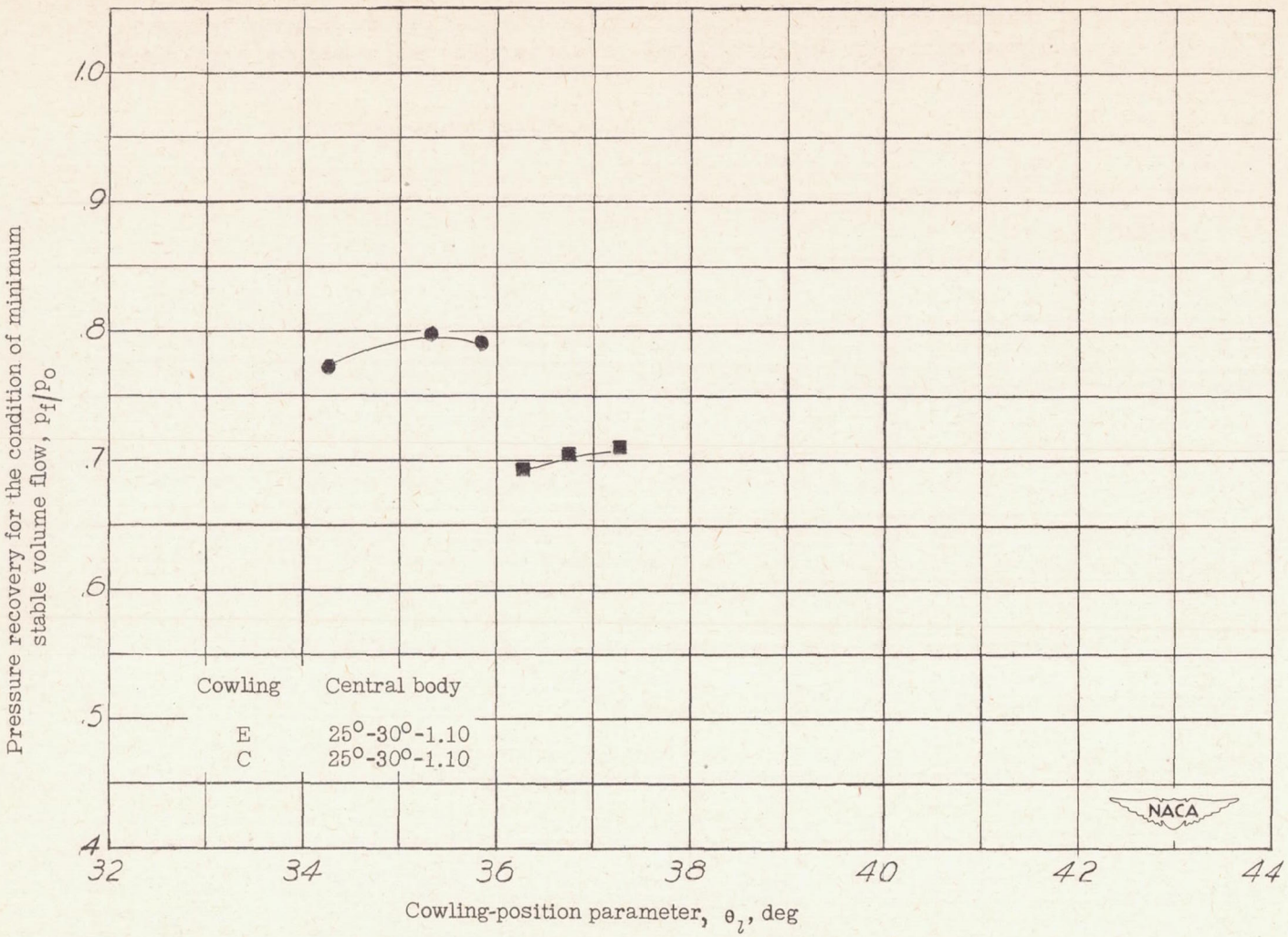

Figure 50.- Pressure recovery of inlets having 25°-30°-1.10 central body as a function of the cowling-position parameter at M = 2.46.

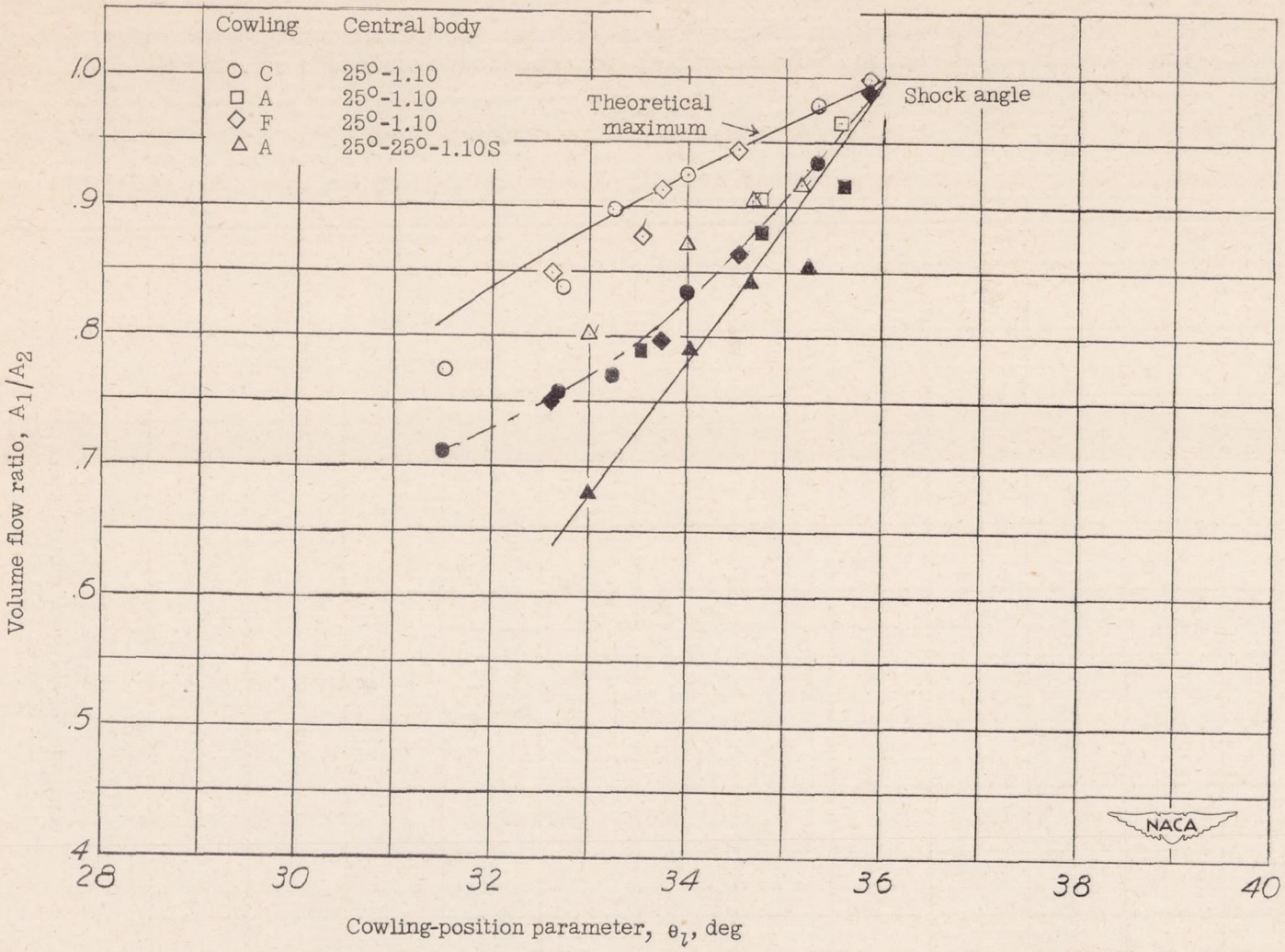

Figure 51.- Volume-flow regulation of inlets having 25° cone-angle central bodies as a function of the cowling-position parameter at M = 2.70.

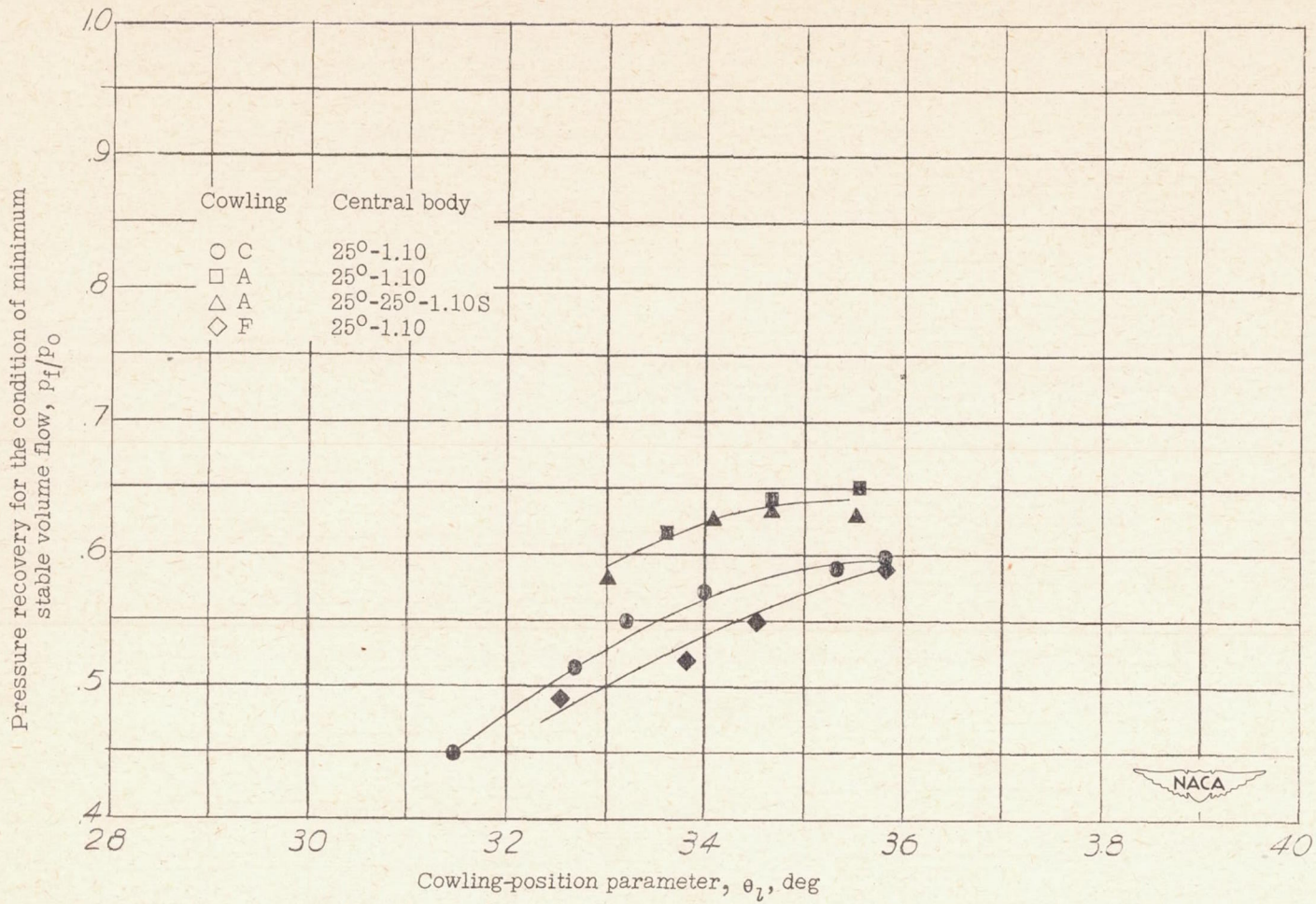

Figure 52.- Pressure recovery of inlets having 25° cone-angle central bodies as a function of the cowling-position parameter at M = 2.70.

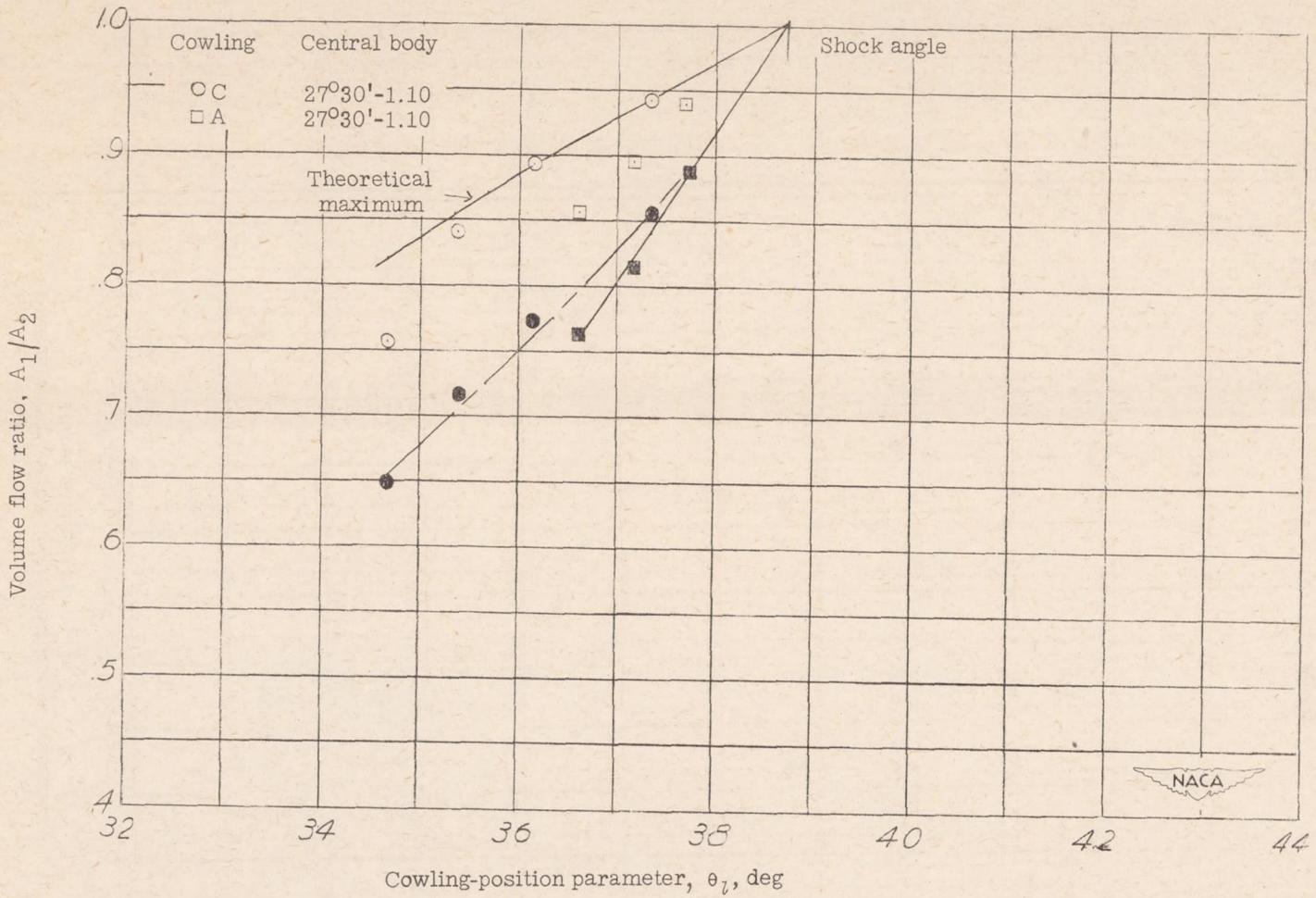

Figure 53.- Volume-flow regulation of inlets having 27°30' cone-angle central bodies as a function of the cowling-position parameter at M = 2.70.

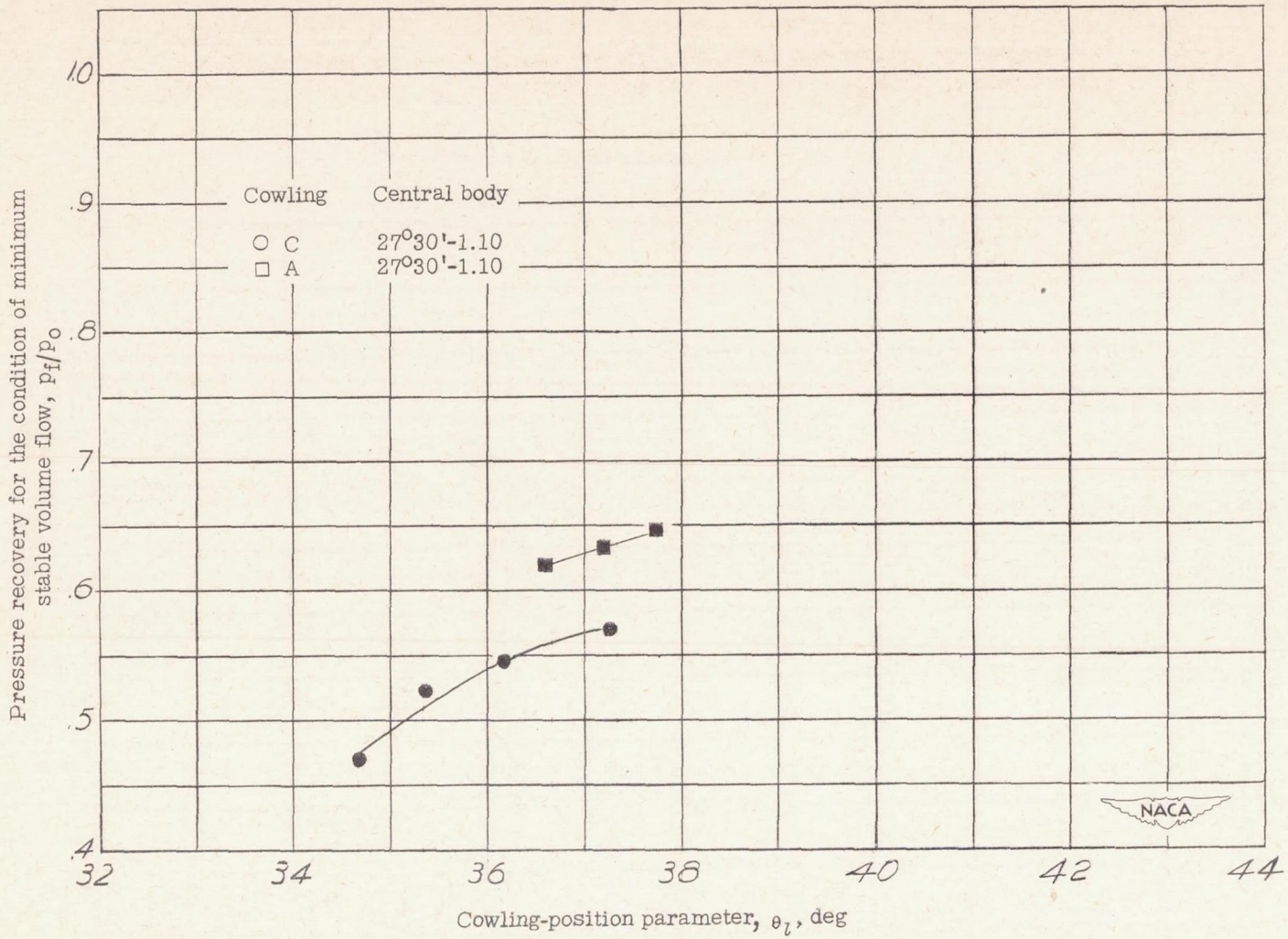

Figure 54.- Pressure recovery of inlets having 27°30' cone-angle central bodies as a function of the cowling-position parameter at M = 2.70.

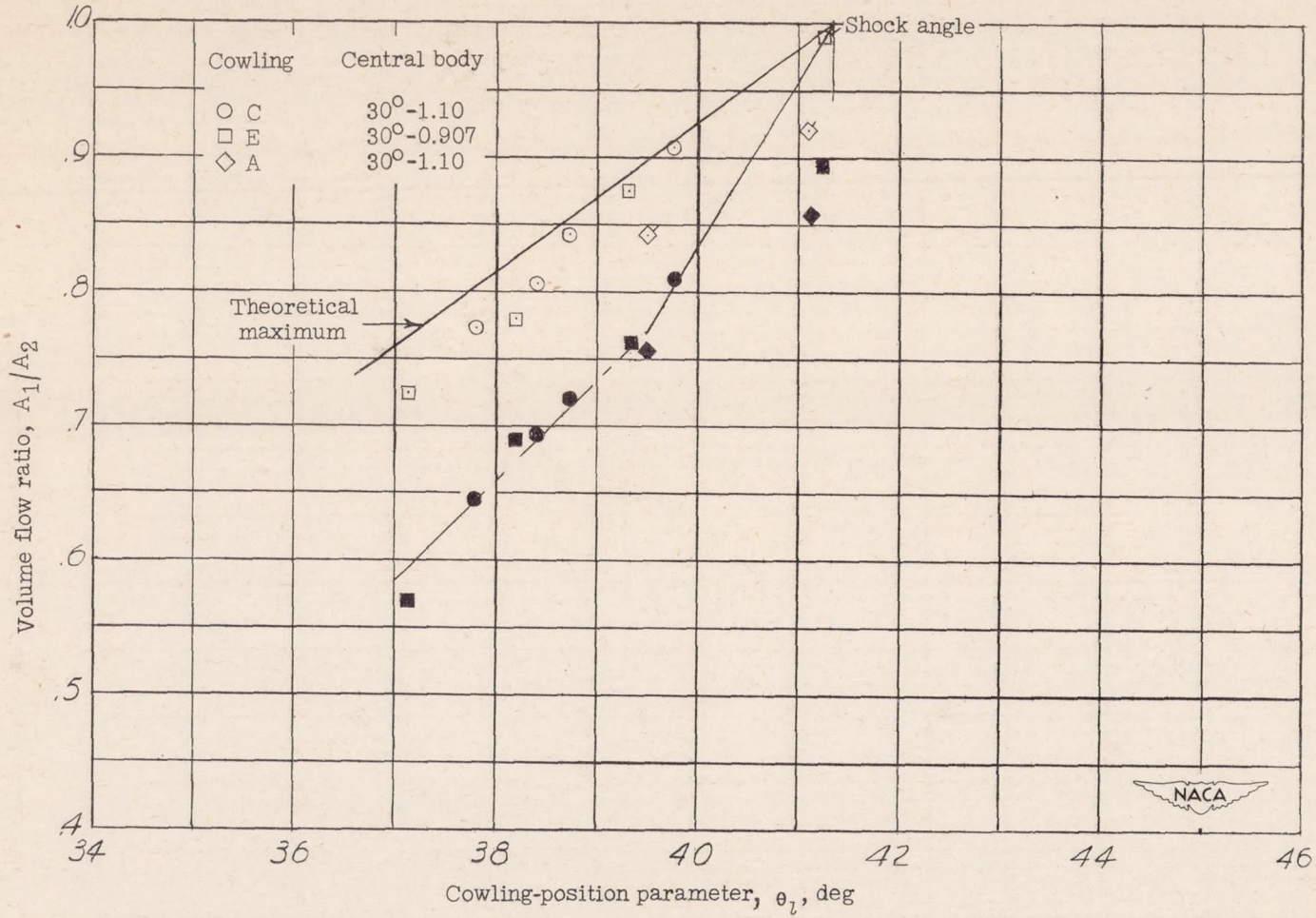

Figure 55.- Volume-flow regulation of inlets having 30° cone-angle central bodies as a function of the cowling-position parameter at M = 2.70.

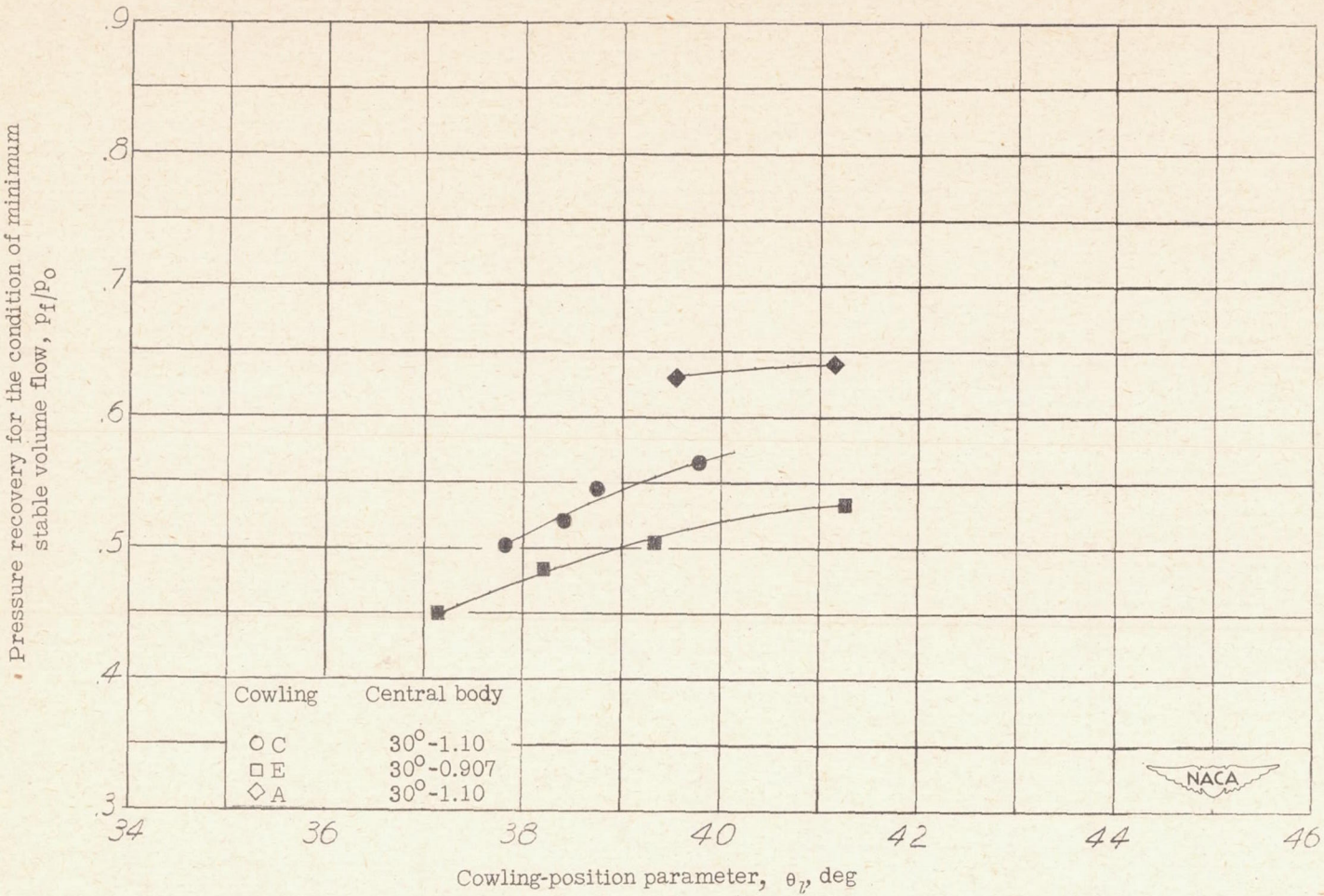

Figure 56.- Pressure recovery of inlets having 30° cone-angle central bodies as a function of the cowling-position parameter at M = 2.70.

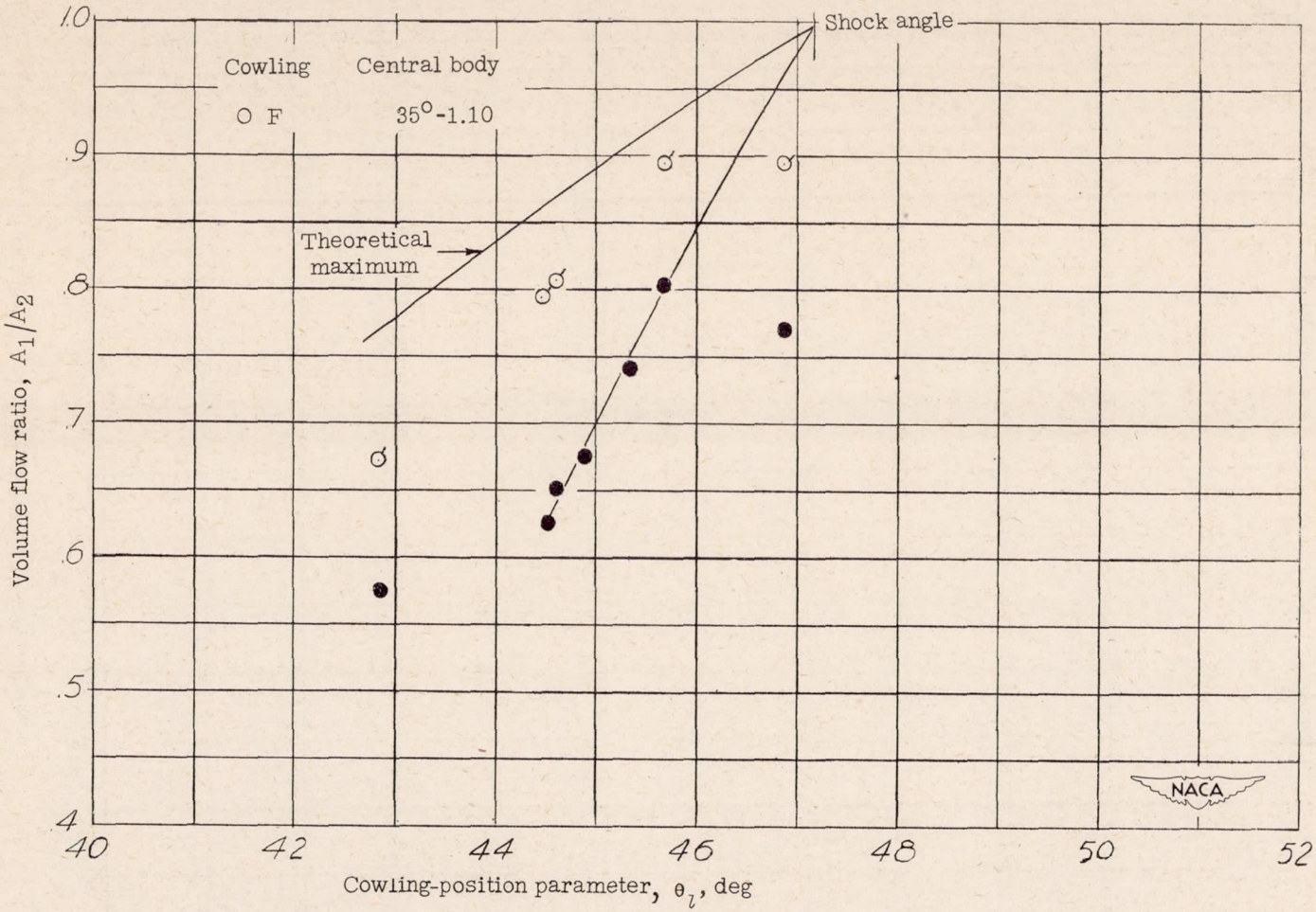

Figure 57.- Volume-flow regulation of inlets having 35° cone-angle central bodies as a function of the cowling-position parameter at M = 2.70.

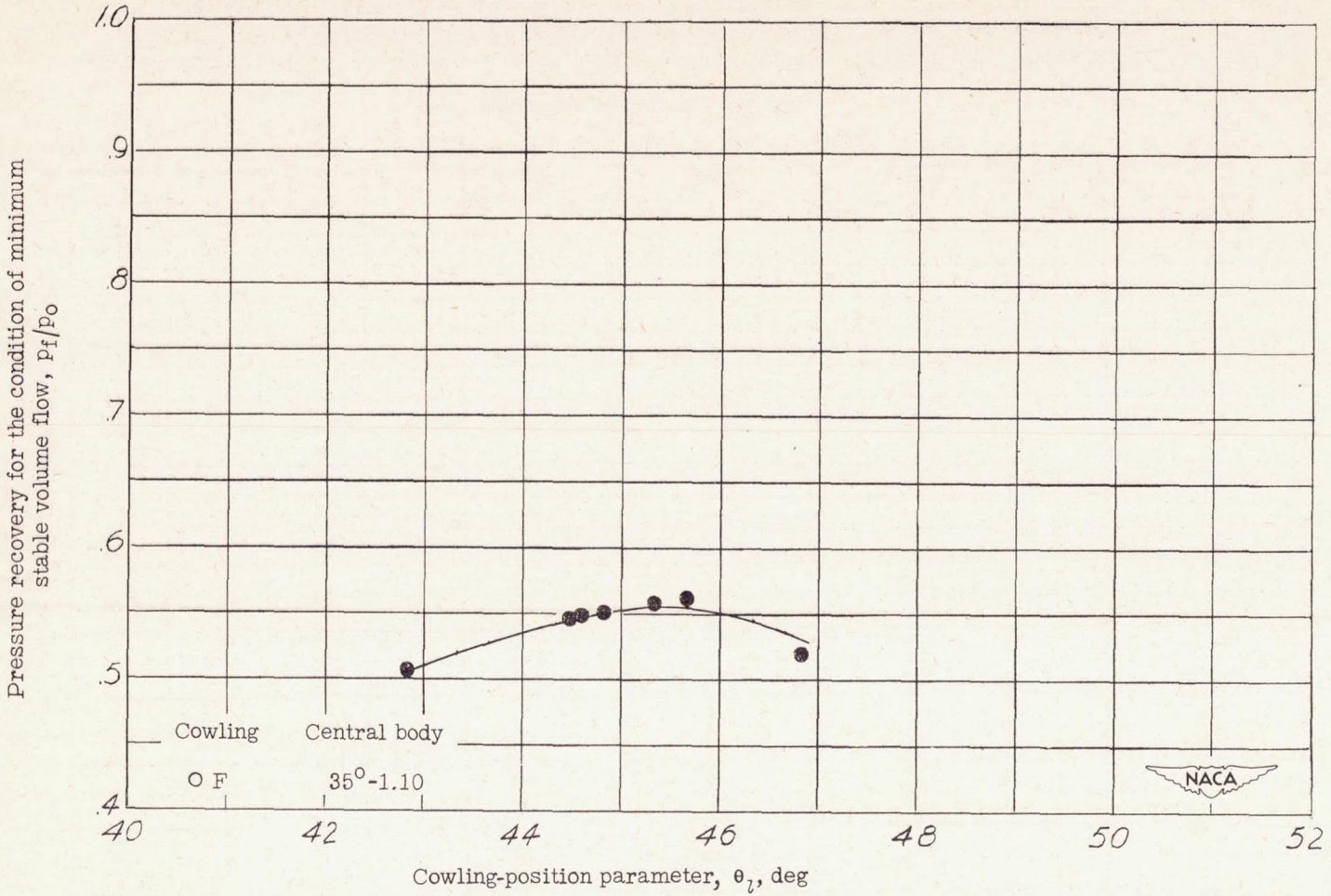

Figure 58.- Pressure recovery of inlets having 35° cone-angle central bodies as a function of the cowling-position parameter at M = 2.70.

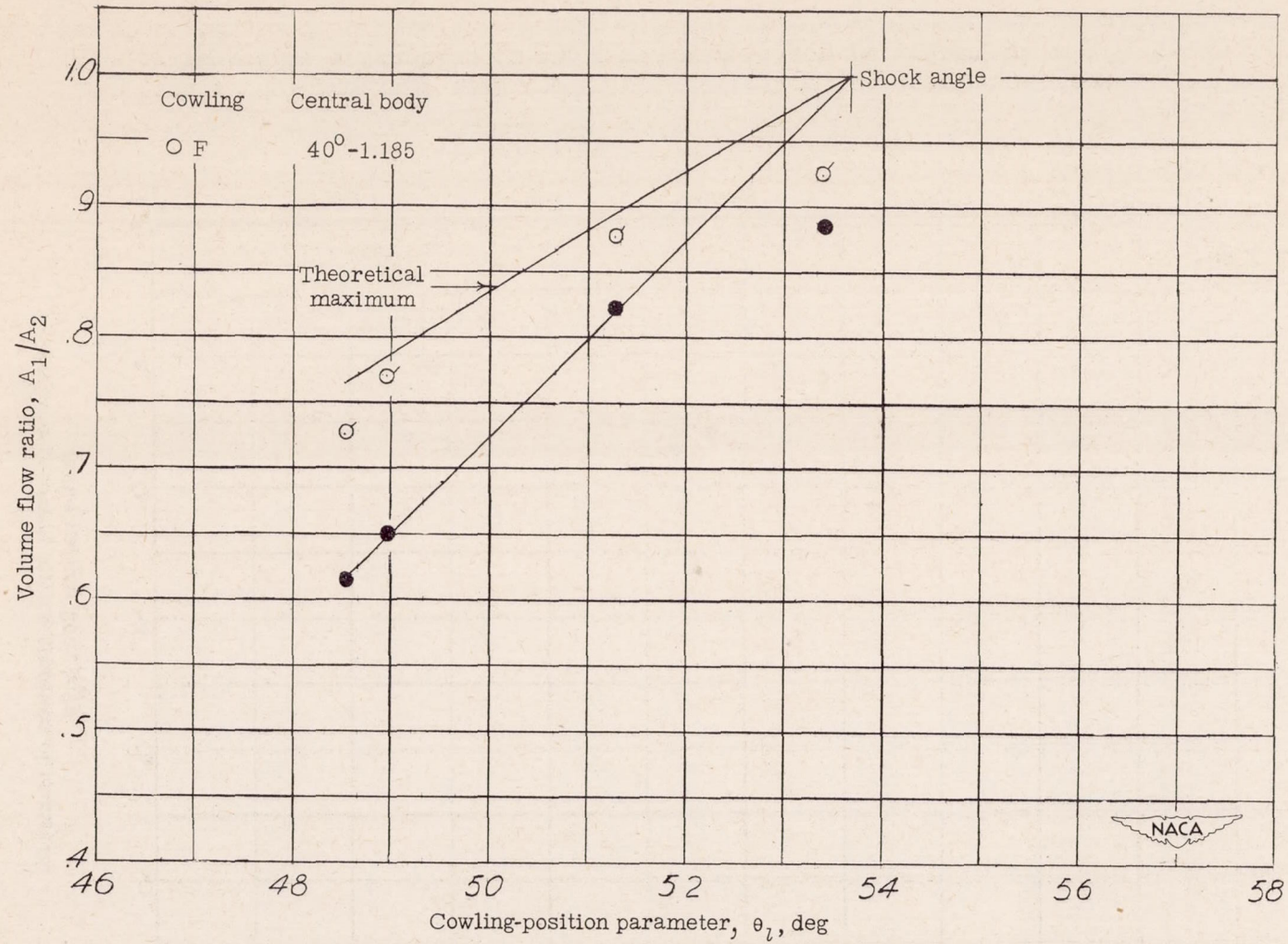

Figure 59.- Volume-flow regulation of inlets having 40° cone-angle central bodies as a function of the cowling-position parameter at M = 2.70.

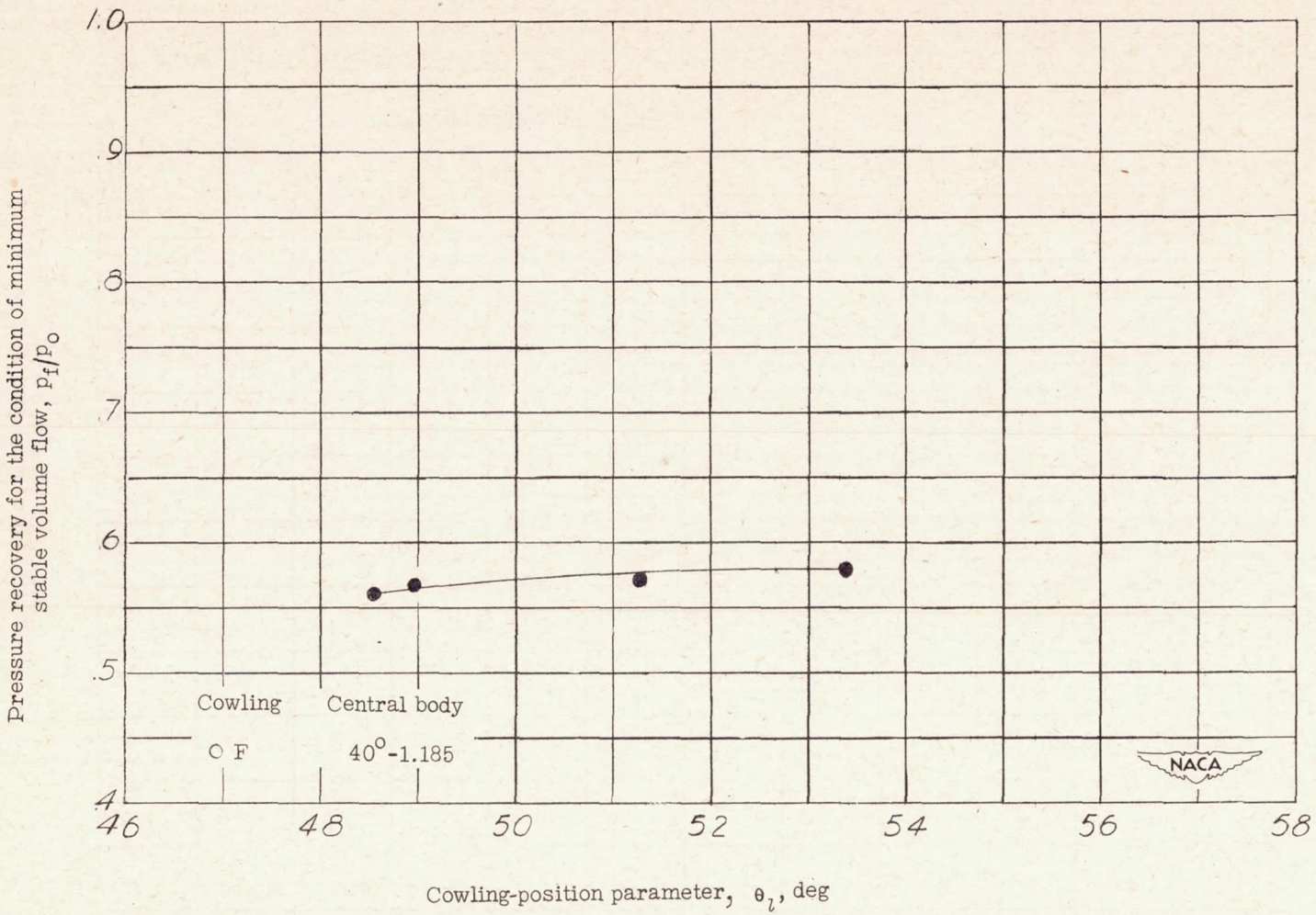

Figure 60.- Pressure recovery of inlets having 40° cone-angle central bodies as a function of the cowling-position parameter at M = 2.70.

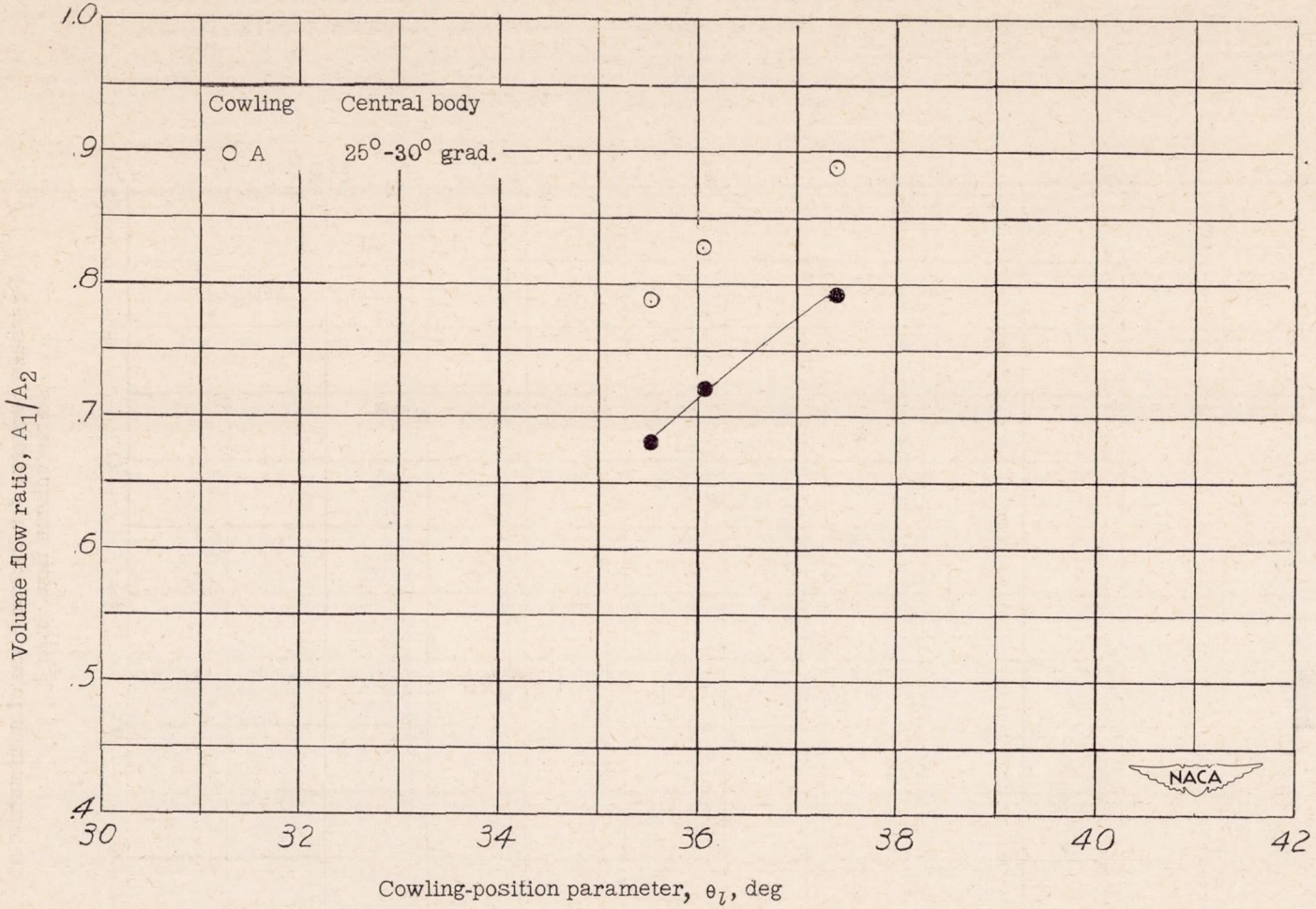

Figure 61.- Volume-flow regulation of inlets having 25°-30°-1.10 body as a function of the cowling-position parameter at M = 2.70.

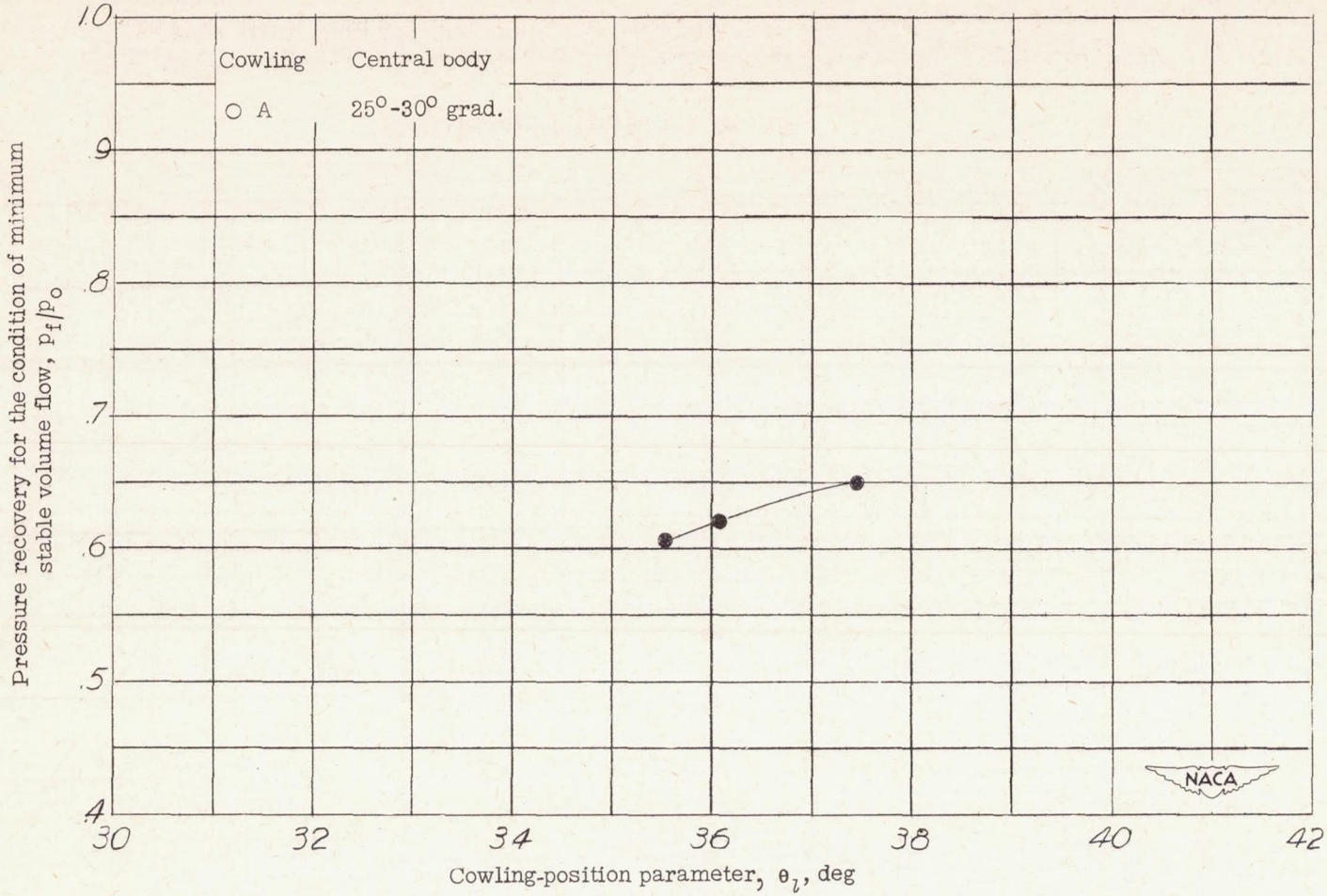

Figure 62.- Pressure recovery of inlets having 25°-30°-1.10 central body as a function of the cowling-position parameter at M = 2.70.

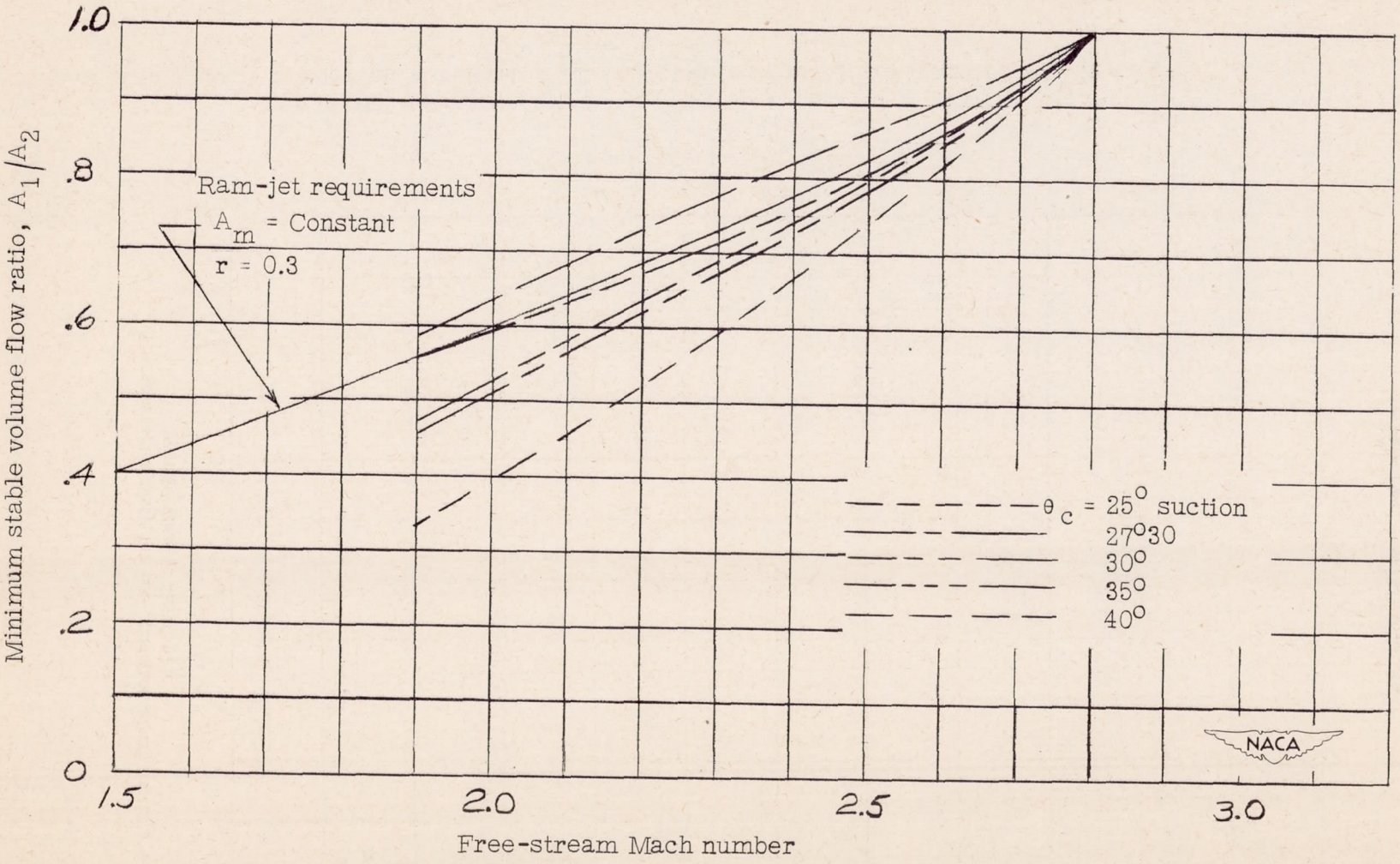

Figure 63.- Minimum stable volume flow for various cone angles for a design Mach number of 2.80 as a function of the free-stream Mach number.